



Norwegian University of  
Science and Technology

# Analysis of a Photovoltaic Power Plant at Evenstad

**Therese Bjørånesset Åsheim**

Master of Energy and Environmental Engineering

Submission date: June 2017

Supervisor: Lars Einar Norum, IEL

Norwegian University of Science and Technology  
Department of Electric Power Engineering



# Abstract

The aim of this master's thesis is to investigate the performance and operation of an existing grid connected PV power plant located at Evenstad in Norway. The PV system has a power rating of 70 kWp and has been operating since November 2013. Measurements of meteorological data and performance data are available for all years of operation. The assessment carried out on this PV plant may be of great significance to the PV industry in Norway. A goal for this thesis is to gain knowledge about performance and operation of PV systems in Norway, which may be of use in the development of the PV industry in Norway.

The first part of this thesis gives an introduction to the theory behind solar energy. This includes the explanation of the solar resource and the PV system with its main components. This is knowledge necessary to understand the content of this thesis. The demands and requirements for grid connected power plants are also presented. To carry out the evaluation of performance and operation of the PV system at Evenstad, a model of the real system is established in the simulation software PVsyst. The next part of the thesis gives an introduction to this simulation software. The simulation model with the implemented settings and parameters is presented, and the reasons why selecting them are justified. Real meteorological data measured on-site is used in simulations to achieve correct comparisons of simulated production and measured production. Variations of the simulation model were used to obtain different studies.

The results of the thesis are divided into four main parts: A discrepancy analysis of the simulation model, simulations and study of one inverter, daily simulations and at last monthly simulations. In the discrepancy analysis the effect of the implemented parameters are analysed, and the results reveal which parameters are important to implement in the model for the system at Evenstad, in order to achieve accurate results compared to real measurements. Correct settings for the module and horizon line in the model proves to give the most impact on the results of the simulations. It is concluded that the relevance of the different parameters varies according to the system analysed. The study of a single inverter in the system provide an overview of the operation and design of the system. Factors like power ratio and power limit for the inverter are proven to be important to implement correctly in the model according to the actual operation of the inverters, to obtain accurate results. Study of the operation of the system implies that the system was installed with too many modules in order to meet the customers demand. Simulations of daily and monthly time frame show that the model give quite accurate results when comparing simulated production to real production. When performing

this comparison for the month of May 2017, the difference becomes as low as 0.3 %. This indicates that the system is performing exactly as anticipated, and that so far there is negligible degradation of the system performance.

# Sammen drag

Målet med denne masteroppgaven er å undersøke ytelsen og driften av et eksisterende nettilkoblet solcelleanlegg lokalisert på Evenstad i Hedmark. Solcelleanlegget har en effekt på 70 kWp og har vært i drift siden november 2013. Målinger av meteorologiske data og produksjonsdata er tilgjengelige for alle årene med drift. Et mål for denne oppgaven er å få mer kunnskap om ytelse og drift av solcelleanlegg i Norge, noe som kan være til stor nytte i utviklingen av og satsingen på solenergi i Norge.

Den første delen av denne oppgaven gir en introduksjon til teorien bak solenergi. Dette inkluderer forklaring av sola som en energikilde i tillegg til oppbyggingen av solcelleanlegg. Dette er kunnskap som er nødvendig for å forstå innholdet i denne oppgaven. Krav til nettilkobling av solcelleanlegg presenteres også. For å gjennomføre evalueringen av ytelsen til solcelleanlegget på Evenstad, etableres en modell av det virkelige systemet i simuleringssystemet PVsyst. Den neste delen av oppgaven gir en introduksjon til dette simuleringssystemet. Simuleringsmodellen med de implementerte innstillingene og parameterne presenteres, og årsakene til de valgte verdiene og innstillingene er begrunnet. Virkelige meteorologiske data målt på Evenstad brukes i simuleringene for å oppnå korrekte sammenligninger av simulert produksjon og målt produksjon.

Resultatene i oppgaven er delt inn i fire hoveddeler: Evaluering av simuleringssystemet, simuleringer av en enkelt vekselretter (inverter), daglige simuleringer og til slutt månedlige simuleringer. I evalueringen av simuleringssystemet analyseres effekten av de implementerte parameterne, og resultatene avdekker hvilke parametere som er viktige å implementere i modellen til anlegget på Evenstad for å oppnå nøyaktige simuleringssystemresultater sammenlignet med virkelige målinger. Korrekte innstillinger for panelet og horisonten i modellen viser seg å ha størst innvirkning på resultatene av simuleringene. Det konkluderes med at relevansen av de forskjellige parameterne varierer i henhold til det analyserte systemet. Analysen av en enkelt vekselretter i anlegget gir oversikt over driften og designet av anlegget. Fordeling av effekt per streng koblet til vekselretterne i tillegg til øverste effektgrense viser seg og være viktige å implementere riktig i modellen i henhold til den faktiske driften av vekselretterne. Det viser seg at det har blitt installert for mange paneler i anlegget i forhold til å møte kundens krav om produksjon på 55 MWh per år. Simuleringer i daglig og månedlig tidsperspektiv viser at modellen gir ganske nøyaktige resultater når man sammenligner simulert produksjon med faktisk produksjon. Simuleringer for mai 2017 gir en forskjell på bare 0,3 %. Dette indikerer at systemet yter som forventet, og at det hittil er ubetydelig degradering av systemytelsen.



# Preface

This master's thesis is part of the final semester and marks the end of a five year master's programme (MSc) in Energy and Environmental Engineering at the Norwegian University of Science and Technology (NTNU). This thesis is a result of an initiative take by Institute for Energy Technology (IFE).

In the thesis a study of the performance and operation of an existing photovoltaic (PV) system has been conducted. The system at Evenstad selected for the study in this thesis, was proposed by Erik Stensrud Marstein at IFE. The reason for selecting this system is the years of available measured performance and meteorological data. This gives exclusive possibilities of analysing system performance.

The motivation for writing this thesis about PV systems, is the confidence that the technology will contribute significantly to the global supply of electricity in the future, also in Norway. The trend in the market is that solar energy is a competitive energy source. The PV industry is still in an early stage, but installed capacity has increased rapidly the last years. Because of this, assessment of system performance and operation is of great use to the industry.

Trondheim, June 16th 2017



Therese Bjøråneset Åsheim





# Acknowledgements

I would firstly like to thank my supervisor at NTNU, Prof. Lars Norum, for his guidance through the work on both the master thesis and the project work completed in the previous semester. He have been of great support to the content of the thesis, and asked some important questions regarding this. Next i wish to thank my co-supervisor at IFE, Prof. Erik Stensrud Marstein, for his huge engagement to my work, and the commitment to the role as a supervisor. His vast knowledge and experience about photovoltaics and the writing of a master thesis have been of great importance and help. I am also very grateful for the detailed feedback on my work. I would also like to thank Thor Christian Tuv, at FUSen, for introducing me to Erik Stensrud Marstein. He is the main reason for the collaboration with IFE. His commitment and enthusiasm to solar energy in Norway has played a major role in my own interest for the technology.

I am also grateful to my parents for always supporting me. They have played a major role in discussions of some important decisions these five years. Their interest and engagement for my work have resulted in some great discussions which have resulted in valuable conclusions. At last I wish to thank my amazing classmates, who have made these five years at NTNU remarkable and unforgettable, especially the last year of writing the master thesis. A special gratitude have to be given to my classmate Per Tore Vatn, for helping me in times of critical need for IT-services.



# Contents

<b>Abstract</b>	<b>i</b>
<b>Sammendrag</b>	<b>iii</b>
<b>Preface</b>	<b>iv</b>
<b>Acknowledgements</b>	<b>vi</b>
<b>Acronyms</b>	<b>xiii</b>
<b>Nomenclature</b>	<b>xv</b>
<b>1 Introduction</b>	<b>1</b>
1.1 Motivation . . . . .	1
1.2 Problem Statement . . . . .	3
1.3 The PV System at Evenstad . . . . .	4
1.4 Limitations . . . . .	5
1.5 Structure of the Thesis . . . . .	5
<b>2 Solar Energy Systems</b>	<b>7</b>
2.1 The Solar Resource . . . . .	7
2.1.1 Blackbody Radiation . . . . .	7
2.1.2 The Components of Sunlight and the Sun's Position . . . . .	8
2.1.3 Measurements and Modelling of Meteorological Data . . . . .	10
2.2 The PV System . . . . .	12
2.2.1 The Electrical Characteristics of a PV Cell . . . . .	13
2.2.2 Temperature and Irradiance Dependence . . . . .	15
2.2.3 Effect of Shading . . . . .	17
2.2.4 PV Cell, PV Module and PV Array . . . . .	19
2.2.5 Module Degradation . . . . .	20
2.2.6 Optimal Tilt Angle of Modules . . . . .	21
2.3 PV System Performance . . . . .	23
2.4 The Inverter . . . . .	24
2.4.1 Inverter Power Rating . . . . .	25
2.4.2 Maximum Power Point Tracker . . . . .	25

2.4.3	Inverter Classifications . . . . .	26
2.4.4	Inverter and Module Wiring Topologies . . . . .	26
2.5	Grid Connection . . . . .	28
2.5.1	Demands and Standards . . . . .	28
<b>3</b>	<b>Experimental Method and Simulation Software</b>	<b>31</b>
3.1	Introduction to Simulation Software: PVsyst . . . . .	31
3.1.1	User Interface . . . . .	31
3.1.2	Project Design . . . . .	33
3.1.3	Detailed Losses . . . . .	35
3.1.4	Meteorological Data in PVsyst . . . . .	37
3.1.5	Simulation Results . . . . .	39
3.1.6	Accuracy of PVsyst . . . . .	39
3.2	Simulating the PV System at Evenstad . . . . .	40
3.2.1	Geographical Location . . . . .	40
3.2.2	PV System Parameters . . . . .	40
3.2.3	PV Array . . . . .	41
3.2.4	Near Shading . . . . .	42
3.2.5	Far Shading . . . . .	43
3.2.6	Incident Angle Modifier . . . . .	44
3.2.7	Module Layout . . . . .	45
3.2.8	Inverters . . . . .	46
3.2.9	Loss Parameters . . . . .	47
3.3	Measured Data for Evenstad . . . . .	48
3.4	Measured Data Management . . . . .	51
3.5	Importing of Meteorological Data . . . . .	51
3.5.1	Generation of Data File for Importing to PVsyst . . . . .	51
3.5.2	Generation of Hourly Values . . . . .	51
3.5.3	Quality Check of Imported Meteorological Data . . . . .	53
3.6	Simulation Variants . . . . .	54
<b>4</b>	<b>Results and Discussion</b>	<b>57</b>
4.1	Discrepancy Analysis of Simulation Model . . . . .	57
4.1.1	Base Scenario . . . . .	59
4.1.2	Modified Tilt Angle . . . . .	59
4.1.3	Detailed Near Shading, 3D Model . . . . .	61
4.1.4	Horizon . . . . .	62
4.1.5	Module Layout . . . . .	63
4.1.6	Modified Module (IAM Losses) . . . . .	64
4.2	Inverter Simulations . . . . .	65
4.2.1	Power Ratio . . . . .	65
4.2.2	Power Output Limit . . . . .	66
4.2.3	Temperature Dependence . . . . .	67

---

4.2.4	Performance of Each Inverter in the System . . . . .	69
4.2.5	Degradation of Inverters . . . . .	71
4.2.6	Soiling Loss Due to Snow . . . . .	72
4.3	Daily Simulations . . . . .	73
4.4	Analysis of Annual Yield and Monthly Simulations . . . . .	75
<b>5</b>	<b>Conclusion</b>	<b>79</b>
<b>6</b>	<b>Further Work</b>	<b>83</b>
	<b>Bibliography</b>	<b>85</b>
	<b>List of Figures</b>	<b>91</b>
	<b>List of Tables</b>	<b>93</b>
	<b>Appendices</b>	<b>95</b>
<b>A</b>	<b>Simulation Data</b>	<b>97</b>
A.1	Simulation Data . . . . .	97
A.2	Inverter Characteristics . . . . .	99
<b>B</b>	<b>Simulation Reports</b>	<b>101</b>
B.1	Report Simulation for Whole system: January 1st to May 23rd 2017 .	102
B.2	Report Simulation for One Inverter: 14-06-2014 . . . . .	109
B.3	Report Simulation for One Inverter: 08-05-2016 . . . . .	116



# Acronyms

**AM** Air Mass.

**BAPV** Building Attached Photovoltaic.

**EHP** Electron-Hole pair.

**IAM** Incident Angle Modifier.

**MPP** Maximum Power Point.

**MPPT** Maximum Power Point Tracker.

**NEC** National Electrical Code.

**NOCT** Nominal Operating Cell Temperature.

**NVE** Norges vassdrags- og energidirektorat.

**PCC** Point of Common Coupling.

**PR** Performance Ratio.

**PV** Photovoltaic.

**STC** Standard Test Conditions.





# Nomenclature

## Greek Letters

$\alpha$	Absorption coefficient
$\beta$	Solar elevation angle ( $^{\circ}$ )
$\delta$	Solar declination ( $^{\circ}$ )
$\phi$	Azimuth angle of module ( $^{\circ}$ )
$\phi_s$	Solar azimuth angle ( $^{\circ}$ )
$\Sigma$	Tilt angle of module ( $^{\circ}$ )
$\theta_z$	Zenith angle ( $^{\circ}$ )

## Roman Letters

$D$	Duty cycle
$G$	Irradiance ( $W/m^2$ )
$H$	Hour angle ( $^{\circ}$ )
$L$	Latitude in angle ( $^{\circ}$ )
$P_{nom}$	Nominal power
$SC$	Solar constant
$T_{amb}$	Ambient temperature ( $^{\circ}C$ )
$T_{cell}$	Cell temperature ( $^{\circ}C$ )
$TC$	Temperature coefficient ( $\%W/K$ )
$U$	Heat loss factor
$U_c$	Constant component of the thermal loss factor ( $W/m^2 \cdot k$ )
$U_v$	Factor proportional of the wind velocity ( $W \cdot s/m^3 \cdot k$ )
$Y_f$	Specific yield/Final system yield ( $kWh/kWp$ )
$Y_r$	Reference yield ( $kWh/m^2$ )



# Chapter 1

## Introduction

### 1.1 Motivation

The growth in installed renewable capacity has been extraordinary the last years, and renewables are finally competitive with fossil fuels in many markets. In 2015 renewables had an increase of 8.7 % in capacity installed, leading to a total of 1.849 GW installed capacity at the end of 2015. Globally, more renewable power capacity is now annually added compared to annually added capacity of all fossil fuels combined. Renewables is estimated to be able to supply 23 % of the global electricity. [1].

The energy source with the biggest potential is solar energy. In only 40 minutes enough energy is hitting the earth to cover the total energy demand of the world [2]. This energy can be collected with Photovoltaic (PV) cells, and used to generate electricity with small amount of greenhouse gas emissions. Compared to coal which has a lifecycle emission of 960 g CO<sub>2</sub>/kWh produced electricity, solar PV only emits 50 g CO<sub>2</sub>/kWh [3].

The tendency is that the use of electricity will replace the use of fossil fuels, and this is expected to continue according to a report from NVE about the future electricity usage from now to 2030 [4]. This is especially the case within the transport sector, with the increase in electrical vehicles. Hence, there is a need for more generated electricity. This, in addition to the big potential, makes solar PV an obvious choice, because it directly produces 100 % renewable electricity after installation.

Figure 1.1 shows the global growth of capacity for different renewable energy sources. Solar PV is the energy source with the biggest growth in installed capacity with a growth of 28 % in 2015. According to IEA's report on trends in PV applications from 2015 [5] and REN21's Global status report from 2016 [1], the global installed solar PV capacity at the end of 2014 was 177 GW. At the end of 2015 this had increased to 228 GW. These growth rates for various renewable energy technologies reflects that the cost of these technologies is falling. It also reflects that the competition for policy support and investment among renewable technologies is increasing. China, Japan and USA is responsible for the majority

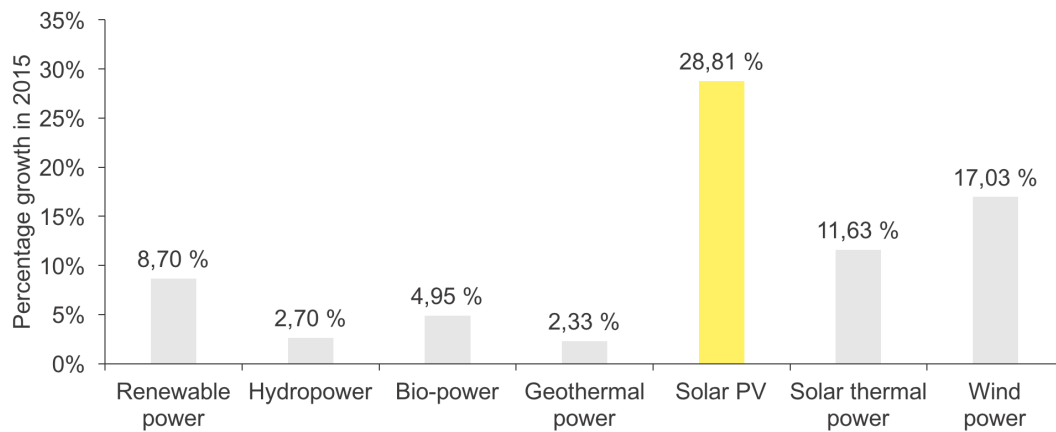


**Figure 1.1:** Average annual growth of renewable energy capacity, 2014 to 2015. Numbers from REN21 Renewables 2016 Global Status Report [1].

of added capacity, but because of the increasing cost-competitiveness of solar PV many countries contributes significantly to the global growth. Approximately 22 countries had enough capacity to cover over 1 % of their electricity demand at the end of 2015. [1]

In Norway the installed PV capacity was 27 MW in 2016. In 2016 over 11 MW PV capacity was installed. This is an increase of 75 % compared to 2015, as can be seen in Figure 1.2. This increase represents a possible turning point for the PV industry in Norway. Of the total capacity the majority is grid connected PV systems, which also stands for most of the increase in capacity. 13.6 MWp is assumed to be grid connected systems. This is anticipated to produce 10 GWh/year, with the expectation that specific production is 750 kWh/kWp in Norway. The annual electricity demand of Norway is approximately 130 TWh [6]. Hence, the solar electricity production is still a small contribution. However, the trend is that solar energy is becoming a more important energy source also in Norway. [7]

Even though installed PV capacity in Norway is increasing, the development of the solar industry is still at the beginning. Weather conditions and the amount of irradiation is different in Norway compared to countries in Central-Europe where the overall irradiation is higher. During winter the PV production is low in Norway due to few days of sun as well as heavy soiling conditions due to snow. Nonetheless, the potential for PV production in cities like Oslo and Kristiansand in Norway is as high as the potential in many cities in Germany, where the installed capacity stands for up to 7 % of the annual electricity production [8]. Even though the amount of irradiance is lower in Norway compared to Germany, factors like low temperatures gives higher system performance.

With a growing PV industry, the ability to give accurate predictions on power production over a systems lifetime, becomes of vital importance. The efficiency with which sunlight is converted to power and how this relationship changes over time, are two key cost drivers for PV systems. The degradation rate quantifies power decline over time. If the degradation rate is known, accurate predictions of production can

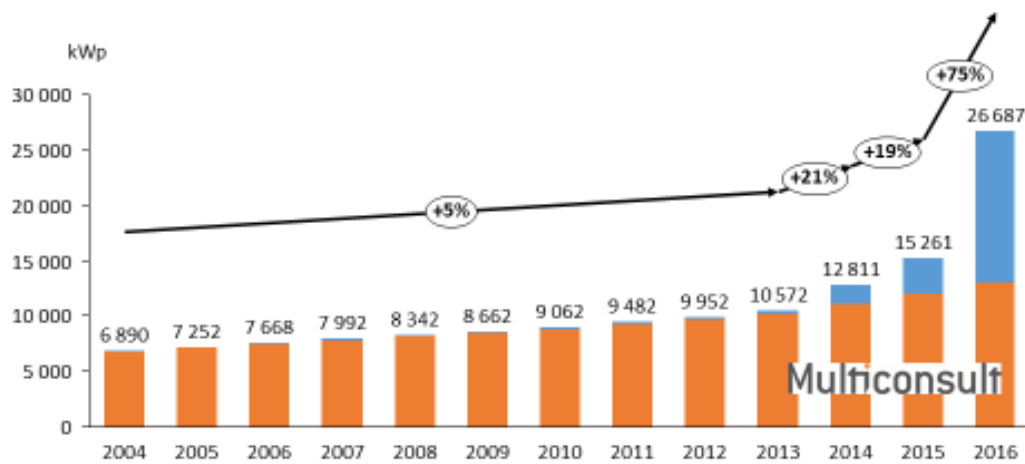


**Figure 1.2:** Accumulated installed PV capacity in Norway from 2004 to 2016. Blue represents grid connected systems and orange represents stand-alone PV systems. [7]

be made. Studies on these aspects will be of great importance to the Norwegian PV industry, and is what this thesis aims to contribute with. [9]

## 1.2 Problem Statement

In this thesis the performance of an existing PV system at Evenstad in Norway will be investigated and analysed. This will be accomplished by establishing a model of the system in the simulation software PVsyst. The model will be used to perform different simulations and comparing the results to the measured data from the system at Evenstad. This will enable the evaluation of the system performance.

One major goal of this thesis is to gain more knowledge about performance and operation of the PV system at Evenstad as an example system in Norway. The assessment of system performance and operation carried out in this thesis may be of great use to the PV industry, and for the development of this industry in Norway.

The other main goal is to consider the model approach itself. Different simulation variants of the model will be compared to see if more complex models give more accurate results compared to the real system. This can establish the importance of the many possible simulation parameters to achieve real results. It will also quantify how accurate a simulation model should be, such that anticipated production is close to real production.

### Research questions investigated:

- How does the PV system at Evenstad perform? Does it perform as anticipated?
- Does the use of more advanced models improve precision of the output results compared to real measured data?
- Can a framework for enabling detection of anomalies be established?



**Figure 1.3:** Geographical location of PV system at Evenstad. Maps by Google.

### 1.3 The PV System at Evenstad

The PV system selected for this study is a Building Attached Photovoltaic (BAPV) system located at Evenstad, Hedmark in Norway (see Figure 1.3). The PV system is installed on a south-faced rooftop with an angle of  $35^\circ$ , on a building which is a part of the University of Hedmark campus Evenstad (see Figure 1.4). It was installed in November 2013 by the Norwegian company FUSen. The PV system consists of 276 modules of type REC 255 PE and 12 Sunny Boy 5000TL-21 inverters of 5 kW rating. There are 23 modules connected to each inverter, distributed over two strings. The installed PV power is 70.380 kWp. [10]



**Figure 1.4:** Picture of the PV system at Evenstad. Provided by Statsbygg.

## 1.4 Limitations

One objective of this thesis is to analyse the performance of the PV plant at Evenstad, through simulations and study of the measured data. The comparison of simulated production and measured production is limited by the available meteorological data. To get accurate comparisons, simulations should be performed by the use of actual measured meteorological data on-site. Irradiance, module temperature and wind speed are available in hourly time unit, for each day of operation, but the downloading of the data in useful form is limited. This issue will be discussed in the content of this thesis.

There are also some limitations to available information and data on parameters that can be implemented to the simulation model. Some assumptions and estimations have been made with regards to this.

## 1.5 Structure of the Thesis

**Chapter 1** This chapter gives an introduction to the thesis including background and motivation for the thesis. The problem statement is described as well as presentation of the PV system at Evenstad which is selected for the study the thesis. At last some limitations to the thesis is addressed.

**Chapter 2** This chapter gives an introduction to the theory behind solar energy and the PV system with it's main components. This chapter is necessary in order to understand the content of the thesis, and can be disregarded by readers with this knowledge. Previous work and studies of relevance are presented. The chapter is to a great extent based on the semester project carried out in the semester in advance on this master thesis, which is not published but can be made available from NTNU on request.

**Chapter 3** In this chapter the simulation software PVsyst is first presented, which is used for simulations in this thesis. Then a presentation of the model built in the simulation software of the PV system at Evenstad is made, with it's parameters and settings. The available measured data for Evenstad is listed as well as the simulation variants used in the study.

**Chapter 4** In this chapter the results of simulations and studies conducted in this thesis are presented and discussed. The chapter is divided into four main sections. The first section covers the discrepancy analysis of the simulation model with six different simulation variants. Next section covers the simulations of one inverter and the analysis of the inverter used in the system at Evenstad. The two last section covers daily and monthly simulations, respectively. The last section consist of simulations using the longest time frame for imported meteorological data and also include study of real annual production data measured on-site.

**Chapter 5** In this chapter a conclusion is made, based on the results and discussions presented in chapter 4.

**Chapter 6** This chapter includes suggestions to further work.



# Chapter 2

## Solar Energy Systems

In this chapter the necessary theory for understanding electricity production from solar energy will be presented. This is knowledge needed to understand how a PV system can work as a electricity generator. The theory is to a great extent based on the semester project written by the author of this thesis [11], which were carried out in the semester in advance of this master thesis. It is not published, but can be made available from NTNU on request.

First the solar resource is looked into. Knowledge about the available sunlight and the solar resource is necessary to be able to design a PV system efficiently. This include the knowledge about the different solar components, calculation of the sun's position during the day and the many angles included in this. By knowing how the sun's position is changing throughout the day can help designing PV systems with optimised electricity generation.

Further insight in the operation of the PV system, with it's main components is needed. First the electrical characteristics of a PV cell is presented. Then the dependence of irradiance and temperature and the effect of shading is explained, and how they affect the IV curve of the PV cell. The configuration of a PV system from cells to full system and the inverter is presented.

### 2.1 The Solar Resource

#### 2.1.1 Blackbody Radiation

The sun can be modelled as a blackbody emitter. A blackbody is defined as a perfect emitter as well as a perfect absorber. The emitted wavelengths is described by *Planck's law*<sup>1</sup>, and is dependent on the temperature of the blackbody. The temperature of the sun's surface is 5800 K, predicted by Planck's law. Figure 2.1 shows the comparison of a 5800 K blackbody and the extraterrestrial solar spectrum, which is the spectrum just outside the earth's atmosphere. 47 % of the sunlight is within the visible light region. [12]

---

<sup>1</sup>See relevant literature for Equation [12]

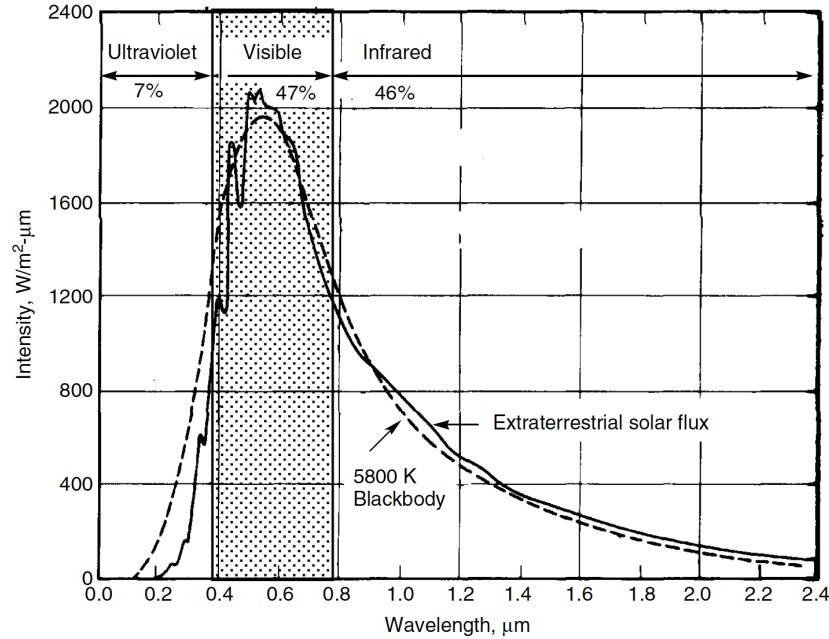


**Figure 2.1:** Extraterrestrial solar spectrum compared to 5800 K blackbody. [12]

*Air Mass (AM)* quantifies the power loss of radiation through the atmosphere. The air mass ratio  $m$  represents the total path length the sunlight has to travel through the atmosphere before it hits the earth's surface. The ratio is calculated using Equation 2.1.  $\theta_z$  is called the *zenith angle* and is measured between the direct beam,  $h_1$ , and the vertical beam,  $h_2$ . Figure 2.2 shows three different definitions of air mass. AM0 is the extraterrestrial solar spectrum right outside of the atmosphere, AM1 where  $m = 1$ , is when the sun is directly overhead, AM1.5 and AM2.0 is when the zenith angle is  $48.2^\circ$  and  $60.1^\circ$ , respectively. At AM0 the irradiance is  $1367 \text{ W/m}^2$ , and is known as the solar constant,  $SC$ . *Irradiance* is quantified as the power density of sunlight. Through the atmosphere the irradiance is reduced by 20-30 % leading to an irradiance of approximately  $1000 \text{ W/m}^2$  at AM1 on a clear day. *Irradiation* is a measure of the amount of irradiance over time and has the unit  $\text{kWh/m}^2$ . [12] [13]

$$m = \frac{h_2}{h_1} = \frac{1}{\cos(\theta_z)}. \quad (2.1)$$

### 2.1.2 The Components of Sunlight and the Sun's Position

The sunlight traveling through the atmosphere can either be absorbed, scattered or it will pass through without being affected by molecules. *Direct radiation*, also called beam radiation, is the sunlight traveling through the atmosphere without being affected. *Albedo radiation* is the reflected sunlight. The sunlight which is scattered by molecules in the atmosphere or clouds is called *diffuse radiation*. Figure 2.3 shows the three components of sunlight. The sum of all the components shown in Equation 2.2, is called the global radiation, GHI, where DHI is the diffuse horizontal

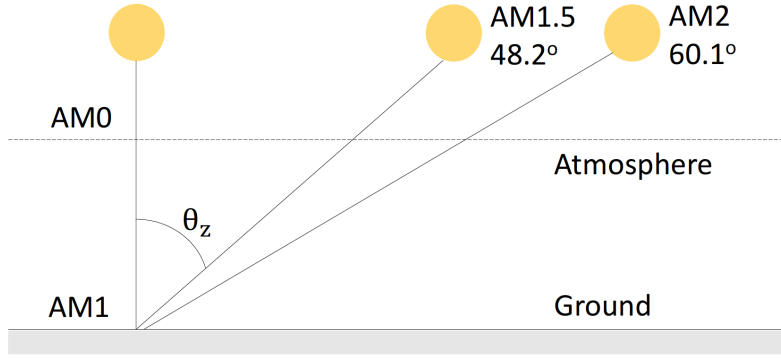


**Figure 2.2:** Definition of Air Mass. AM0 - Right outside atmosphere, AM1 - Zenith angle  $\theta_z = 0$ , AM1.5 -  $\theta_z = 48.2^\circ$ , AM2 -  $\theta_z = 60.1^\circ$ .

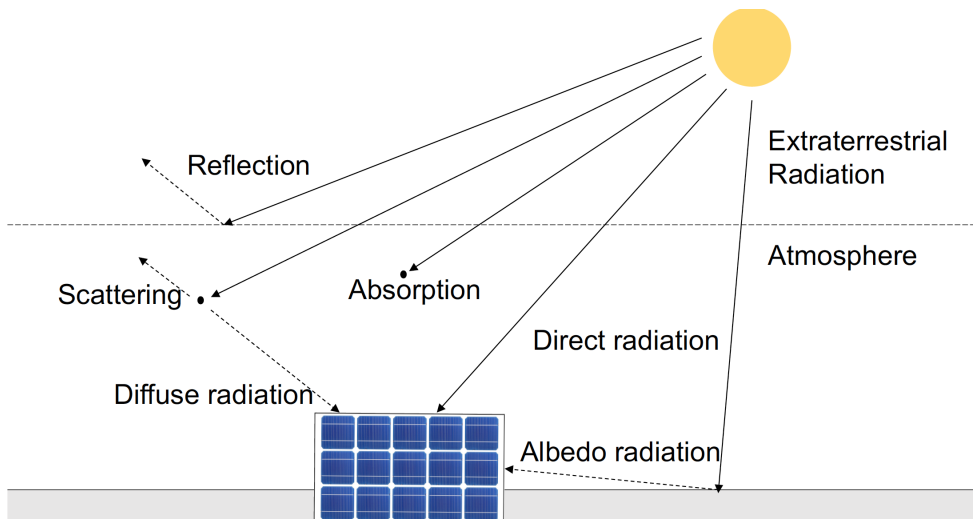


**Figure 2.3:** Components of sunlight.

irradiance and DNI is the direct normal irradiance.

$$GHI = DHI + DNI \quad (2.2)$$

The sun is at its highest at south,  $0^\circ$ . Figure 2.4 shows different angles that are used for radiance and sun position. The sun's altitude,  $\beta$ , is calculated using Equation 2.3. The sun's azimuth angle is calculated using Equation 2.4. The sun's azimuth angle is negative in the morning and positive in the evening, defined by the simulation software used in this thesis.

$$\sin \beta = \cos L \cos \delta \cos H + \sin L \sin \delta \quad (2.3)$$

$$\sin \phi_s = \frac{\cos \delta \sin H}{\cos \beta} \quad (2.4)$$

The declination angle  $\delta$  is the angular distance of a point north or south of the celestial equator.

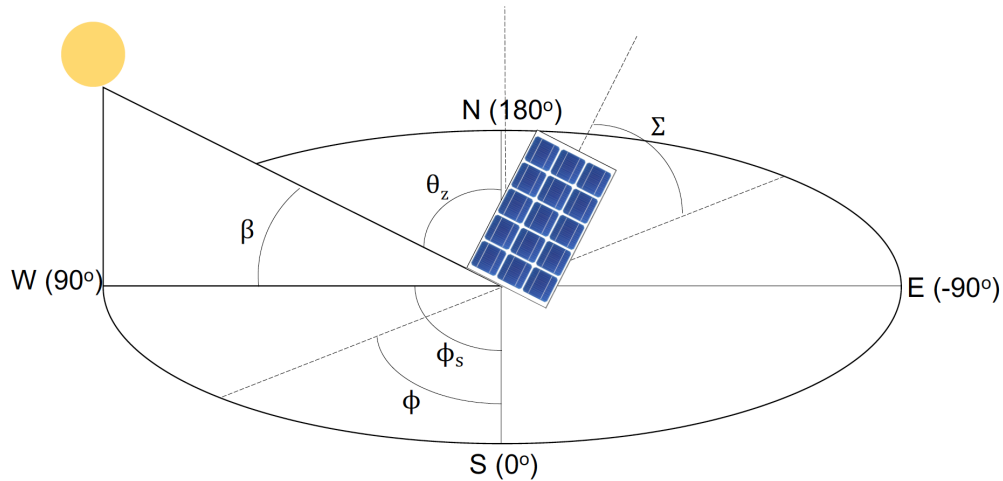


**Figure 2.4:** Definition of solar angles.

**Table 2.1:** Solar Angles

$\delta$	Solar declination	$\phi_s$	Solar azimuth angle
$\beta$	Solar elevation angle	$\phi$	Azimuth angle of module
$L$	Latitude in angle	$H$	Hour angle
$\theta_z$	Zenith angle	$\Sigma$	Tilt angle

The elevation angle,  $\beta$  is the angular height of the sun measured from the horizontal. It equals  $0^\circ$  at sunrise and  $90^\circ$  when the sun is directly overhead. The zenith angle,  $\theta_z$ , mentioned in previous section is similar to the elevation angle but it is measured from the vertical rather than the horizontal, thus *zenith angle* =  $90^\circ - \text{elevation angle}$ , as seen in Figure 2.4.

The hour angle,  $H$ , is the number of degrees the earth must rotate before the sun is directly over the local meridian. The angle is  $0^\circ$  at noon.

### 2.1.3 Measurements and Modelling of Meteorological Data

As the power output of a PV module is directly dependent on irradiance and weather conditions for its location, the input meteorological data (meteo data) for simulations becomes an important factor for accurate simulations. Correct meteo data gives correct simulations for estimate of future energy production. The measurements of irradiance and meteo data is presented in this section.

A variety of data sources with measurements and modelling of solar irradiance are available. The quality of the sources and measured data varies, and which source to use for simulations depends on the geographical location of the system analysed. This section also presents some of the sources available for Evenstad, and their relevance for simulations in this thesis.

## Measurement methods

Solar radiation is an important factor for accurate simulations. Measurements with high quality and over a long period of time is of great value to meteorological databases, and for use in estimations of solar PV potential. The problem is that irradiance is difficult to measure. It requires well calibrated instruments, which is a rare case. Within the stations that measures irradiance the quality and length of the measurements varies. [14]

Sunlight can be measured in either irradiance ( $\text{W}/\text{m}^2$ ) which is the power from the sun hitting the earth, or irradiation ( $\text{kWh}/\text{m}^2 \text{ day}$ ) which is the power over a period of time, hence the energy hitting the earth. Irradiance and irradiation is strongly dependent on location and local weather conditions. They can be measured using a pyranometer, which measures global radiation (GHI), a pyrhelimeter, which measures direct normal radiation (DNI), and/or a pyranometer coupled with a shading disk measuring diffuse horizontal (DHI). The accuracy at 90 % confidence under normal operating conditions are  $\pm 5 \%$  for GHI,  $\pm 3 \%$  for DNI and  $\pm 7 \%$  for DHI. [14, Chapter 5.5]

Quality measurements of DNI enable accurate estimations of PV system performance, because it is the solar component which distributes the most energy for electrical generation systems. If measurements are not available, DNI can be estimated from satellite models or from correlations from GHI. [14, Chapter 5.5]

Irradiance can also be established by using satellite pictures. NASA provides daily irradiance data for the years 1983-2005 [15]. The accuracy of this method has been evaluated by using numerous ground-based measurements. NASA has estimated the monthly data to have an error of 13 - 16 %.

## Meteo databases

The irradiance in Norway is not well mapped, and there exist great uncertainties to the different databases. When estimating performance of large PV systems with high investment costs, it is advised to consider and investigate the different sources available. [16]

If measured data is not available there exist several meteorological sources with irradiation data available. Metonorm and PVGIS, as well as private and public stations are examples of this. Kjeller vindteknikk have done a mapping of the databases in the article *Resource mapping of solar energy* [17].

*Meteonorm*, provided by Meteotest, includes monthly average values from 1961 to 1990, and the database defines about 1100 weather stations which measures irradiance around the world. The data for a specific geographical location is interpolated between the three nearest stations. This is not the case for all regions of the world, where for many locations satellite data is used to complete the information about irradiance. *Meteonorm* uses a synthetification method which combines satellite images and ground measurements. For Norway irradiance is available from Bergen, Bodø and Tromsø in the *Meteonorm* database. Additional stations without irradiance

measurements are also available. [15] [17]

*PVGIS* is an online source where it is possible to estimate the production of PV systems at a specific location. At the *PVGIS* website downloading of solar resource maps as yearly global irradiance on horizontal and optimally inclined surfaces, is possible. In some location it is possible to choose between "Climate-SAF *PVGIS*" and "Classic *PVGIS*", where the first in most cases give more correct answers. [15]

In addition to the mentioned databases as well as others, there exist a network of irradiance measurements stations in Norway and Sweden. Some of these are Bioforsk, Meteorological Institute, stations at different schools and Norwegian Radiation Protection Authority. In addition to these networks, advanced measurement stations operated by research institutes and private stations, exist. [17]

## 2.2 The PV System

PV systems are generally divided into stand-alone and grid-connected systems. Stand-alone systems consist of PV modules, batteries and a load, possibly with a generator back-up. In Norway, they are mostly found in cabins, light houses and antenna stations. Stand-alone systems have the advantage that they can provide power to consumers without the ability of grid connection. In this thesis the study will be on grid-connected PV systems.

Figure 2.5 shows the arrangement of the grid-connected system which will be analysed in this thesis. The PV array produces dc-energy which flows to the inverter as  $E_{array}$ . The amount of energy depends first of all on the sunlight hitting the array, and on number of PV modules, their power ratings and how they are connected to each other. The inverter transforms the dc-energy to ac-energy at inverter output,  $E_{out\ inv}$ , which is fed into the main grid or directly to the user. Usually the energy produced is directly fed to the user to cover the total demand. The excess energy

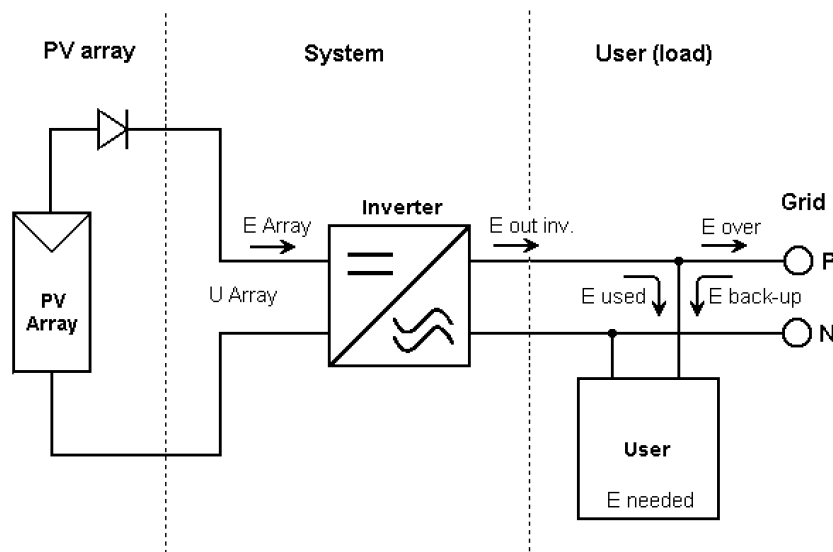


**Figure 2.5:** Flow diagram of a grid connected system.

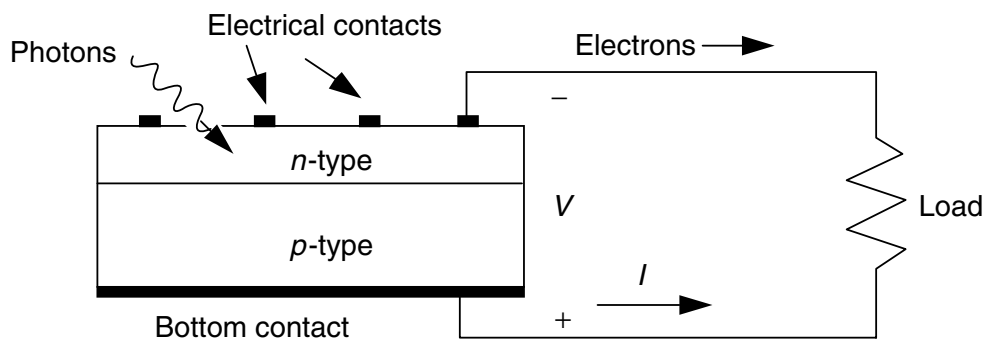
which is not used will be fed to the grid. If the system can not produce enough energy to meet the users demand, energy will be drawn from the grid. It is important that the transformed ac-power meet the utility power quality requirements, e.g. having the same frequency and voltage amplitude. More about grid connection in Section 2.5. [18] [12]

### 2.2.1 The Electrical Characteristics of a PV Cell

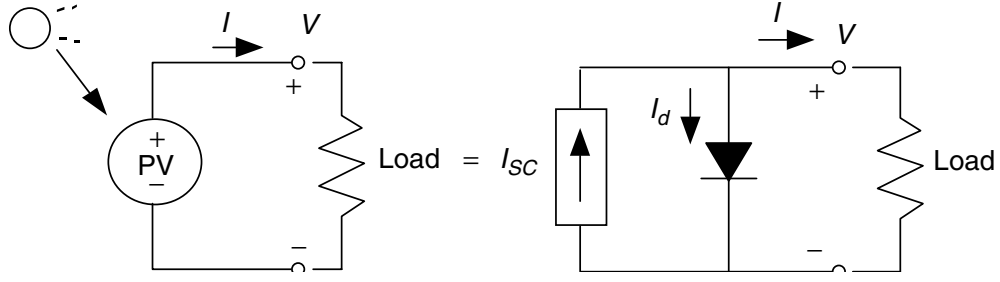
A PV cell can be characterised as a special pn-junction behaving like a diode. A pn-junction consist of a n-doped and a p-doped semiconductor material joined together. More about pn-junction, doping and semiconductor materials can be found in [11, p. 7-12].

Figure 2.6 shows a PV cell with the pn-junction getting hit by photons from the light. For the photons to be absorbed the energy of the photons have to be equal or larger than the band gap energy,  $E_g$ , of the semiconductor material used in the PV cell. For silicon the band gap energy is 1.12 eV. Photons that are absorbed in the PV cell generates Electron-Hole pair (EHP). The free electrons are collected by electrical contacts in the PV cell, and will flow from the n-side to a connected wire, through the load and back to the bottom contact of the PV cell where they recombine with free holes at the p-side. Current is flowing in the opposite direction of the electron flow, by convention. [12]

Figure 2.7 shows a simple equivalent circuit for a PV cell. The PV cell consist of a real diode in parallel with a ideal current source, which is delivering current in proportion to the solar flux the cell is exposed to. Two interesting conditions are: (1) the short-circuit current,  $I_{SC}$ , flowing when the terminals are short circuited, and (2) the open circuit voltage,  $V_{OC}$ , over the terminals when they are open circuited. At short-circuit condition the diode voltage  $V_d = 0$ . This means that all the current from the ideal current source are going through the shorted terminals. Hence the current proportional to the sunlight hitting is almost identical to the short-circuit current,  $I_l = I_{SC}$ .



**Figure 2.6:** PV cell when hit by photons that are absorbed, and connected to a load. The result is electron flow through the wire from n-side to p-side. [12, p. 268]



**Figure 2.7:** Simple equivalent circuit for an irradiated PV cell. [12, p. 277]

According to *Kirchhoff's current law* the current delivered to the load is:

$$I = I_{SC} - I_d. \quad (2.5)$$

By substituting the diode Equation into this Equation the IV-characteristic Equation (also called IV-curve) for a PV cell is obtained:

$$I = I_{SC} - I_s \left( e^{\frac{qV}{kT}} - 1 \right), \quad (2.6)$$

where  $I_s$  is the saturation current,  $V$  is the cell voltage,  $q = 1.6 \times 10^{-19}$  C,  $k = 1.38 \times 10^{-23}$  J/K and  $T$  is the temperature.

Figure 2.8 shows the IV-curve of a PV cell. The output power is also plotted. At Maximum Power Point (MPP) the product of cell current,  $I_R$ , and voltage  $V_R$  are at it's maximum and the PV cell has it's maximum power output ( $P_{max} = I_R \cdot V_R$ ).  $FF$  is the fill factor and is often used to quantify the cell performance, and is defined in Equation 2.7. Other key parameters which are identified in the figure are short-circuit current,  $I_{SC}$ , and the open circuit voltage,  $V_{OC}$ . The open circuit voltage is given by Equation 2.8.

$$\text{Fill factor (FF)} = \frac{P_{max}}{I_{SC} \cdot V_{OC}} = \frac{I_R \cdot V_R}{I_{SC} \cdot V_{OC}} \quad (2.7)$$

$$V_{OC} = \frac{kT}{q} \ln \left( \frac{I_{SC}}{I_s} + 1 \right). \quad (2.8)$$

To get a more accurate equivalent circuit of the PV cell, a parallel leakage resistance,  $R_p$ , and a series resistance,  $R_s$ , are introduced, as shown in Figure 2.9.  $R_p$  represents the voltage drop when charge carriers drift from the semiconductor to the electrical contacts.  $R_s$  represents the ohmic losses in the wire connection between cells. The IV-curve then becomes:

$$I = I_{SC} - I_s \cdot \left( e^{\frac{q(V+I \cdot R_s)}{kT}} - 1 \right) - \frac{V + I \cdot R_s}{R_p}. \quad (2.9)$$



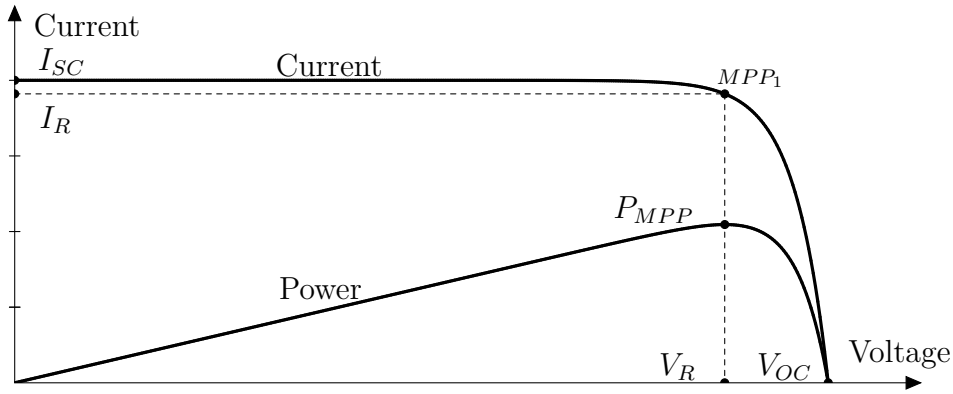


**Figure 2.8:** IV-characteristics and power output of a PV cell. MPP is the point where the PV cell delivers the most power.

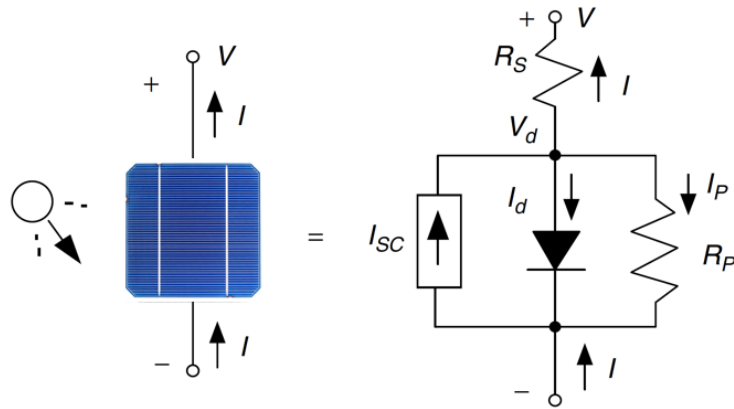


**Figure 2.9:** A more complex and accurate circuit equivalent of a PV cell, including  $R_p$  and  $R_s$ . [12, p. 283]

### 2.2.2 Temperature and Irradiance Dependence

The efficiency of a solar cell is given by the Equation

$$\eta = \frac{P_{max}}{P_{in}} = \frac{FF \cdot I_{SC} \cdot V_{OC}}{P_{in}}, \quad (2.10)$$

which describes how much of the incident power,  $P_{in}$  is generated to output electricity. The efficiency of a solar cell is dependent of the material and type of solar cell. A typical efficiency for a silicon solar cell is between 15 and 22 %. [19]

When testing PV modules, Standard Test Conditions (STC) are used. This means:

**Table 2.2:** Standard Test Conditions (STC).

Irradiance:	1000 W/m <sup>2</sup>
Air mass:	AM1.5
Cell temperature:	25°C

Solar cells rarely operate under STC. The IV-curve of a PV cell is directly dependent on irradiance and temperature. In a day the irradiance may vary more than the temperature. When the irradiance is reduced by half, the resulting power output also is reduced by half.

The open circuit voltage and efficiency of a solar cell is temperature dependent as can be seen from Equations 2.8 and 2.10. Seemingly, from Equation 2.8,  $V_{OC}$  increases with temperature. However, the reverse saturation current,  $I_s$ , is increasing with temperature, and the effect is that  $V_{OC}$  decreases with increased temperature. Hence, increasing temperature leads to decreasing open circuit voltage and resulting in decreasing efficiency. PV cells thus perform better in cold than warm conditions, given the same irradiance. [12]

When a solar cell is being illuminated, only about 10 to 20 % of the solar irradiance is absorbed by the solar cell. Some of the additional irradiance will be converted to heat resulting in heating of the solar cell. According to [19] the open circuit voltage decreases by 2.3 mV per Kelvin for a silicon solar cell. This corresponds to a temperature coefficient of  $-0.4\%/K$ .

Since not all of the energy hitting the solar cell is converted to electricity, solar cells are heated up when irradiated. The temperature of a cell is estimated by formula 2.11 where  $G$  is irradiance ( $kW/m^2$ ),  $T_{cell}$  and  $T_{amb}$  are cell and ambient temperatures ( $^{\circ}C$ ), respectively. Nominal Operating Cell Temperature (NOCT) is the expected cell temperature at  $20^{\circ}C$  with irradiance of  $800 W/m^2$  and a wind speed of 1 m/s. This is a parameter supplied by the PV module manufacturer. Power output of a module is dependent on temperature according to Equation 2.12, where  $TC$  is the temperature coefficient ( $\%/K$ ) which defines how much the maximum power of the module is reduced for each degree over  $25^{\circ}C$ . When the cell temperature is increasing the power output of a module is decreasing. Power loss due to high temperatures may be a big problem in warm climates. This is why the efficiency of a PV system usually is better in cold climates and northern countries.

$$T_{cell} = T_{amb} + \frac{NOCT - 20^{\circ}C}{0.8} \cdot G \quad (2.11)$$

$$P_{out} = P_{rated} \cdot (1 - TC(T_{cell} - T_{amb})) \quad (2.12)$$

Because the solar cell is temperature dependent, the IV-characteristic changes with varying cell temperature. This is also the case for different illumination levels, since the current produced by the solar cell is proportional to the irradiance. More irradiance means more generated current leading to higher power output.

This effect can easily be seen in graphs of IV and PV curves. The effect is illustrated in Figures 2.10a and 2.10b which shows plots of irradiance dependence, and in Figures 2.10c and 2.10d which shows plots temperature dependence. All these plots are based on PVsyst models performed by the author of this thesis, and are for a REC 255 Wp module, which will be used for simulations explained later in this thesis. Plots are simulated and extracted from the simulation software PVsyst. MPP is represented by the white circles in the Figures, where it can be seen how

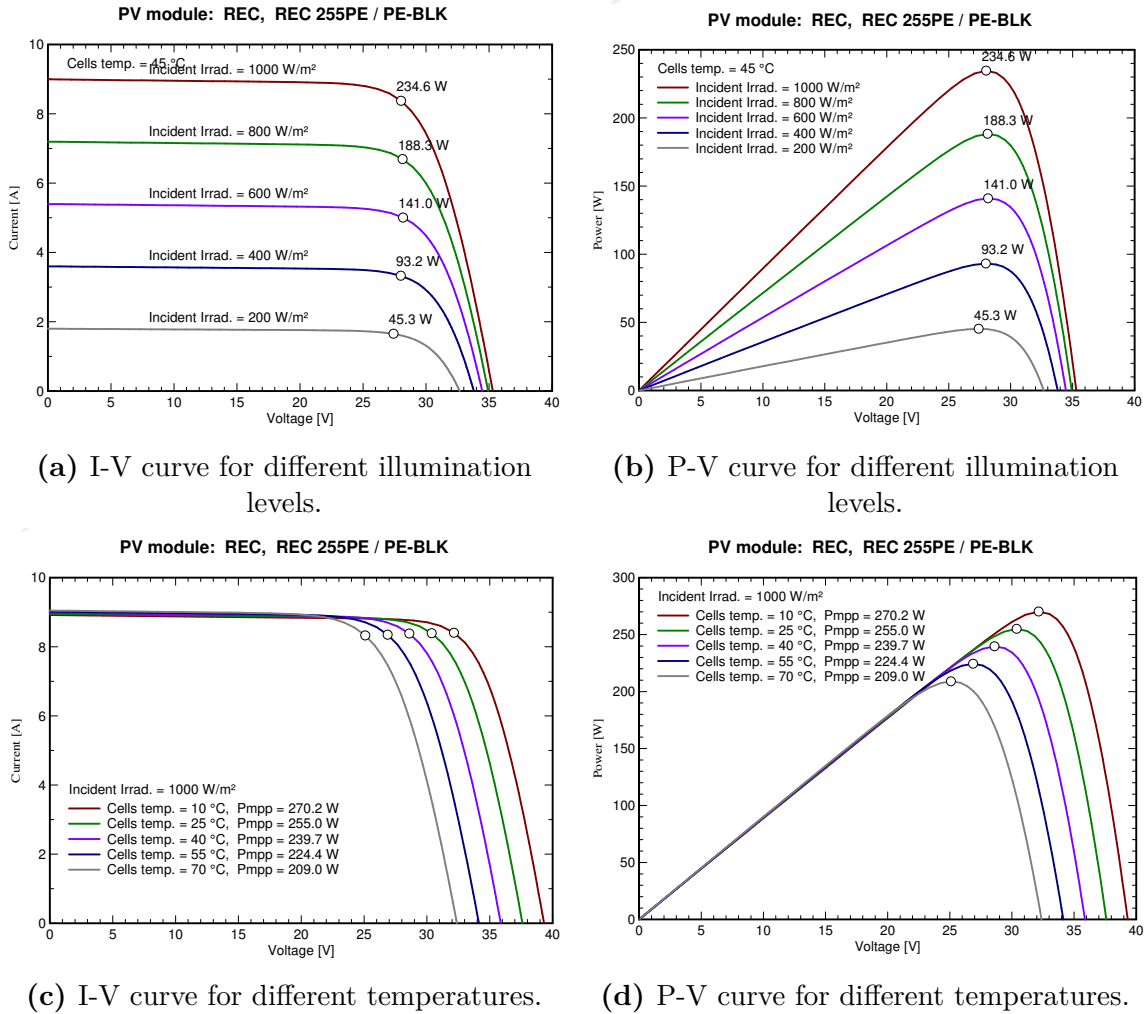


**Figure 2.10:** I-V and P-V characteristics for a REC 255 W PV module. Taken from PV Syst.

MPP decreases with increased temperature and decreased irradiance. [20] [18]

### 2.2.3 Effect of Shading

Cells in a module may become shaded or damaged, making them unable to generate the same current as the other cells. This leads to cell mismatching. When one cell in a string is shaded the current generated by this cell limits the possible current output of the module. Since the current in the cells that are not shaded are larger than the current output, the diode in the cells circuit (See Figure 2.9) becomes forward biased and a diode current is flowing. In short circuit condition the diode in the shaded cell must be reversed biased in magnitude equal to the forward biased diode, to ensure voltage balance. This will change the shaded cell from a power generator to a current dissipater, which can generate heat. The result can be a hot spot which can damage the cell. [21]

Mismatches of cells will also decrease the open circuit voltage,  $V_{OC}$ , but for a

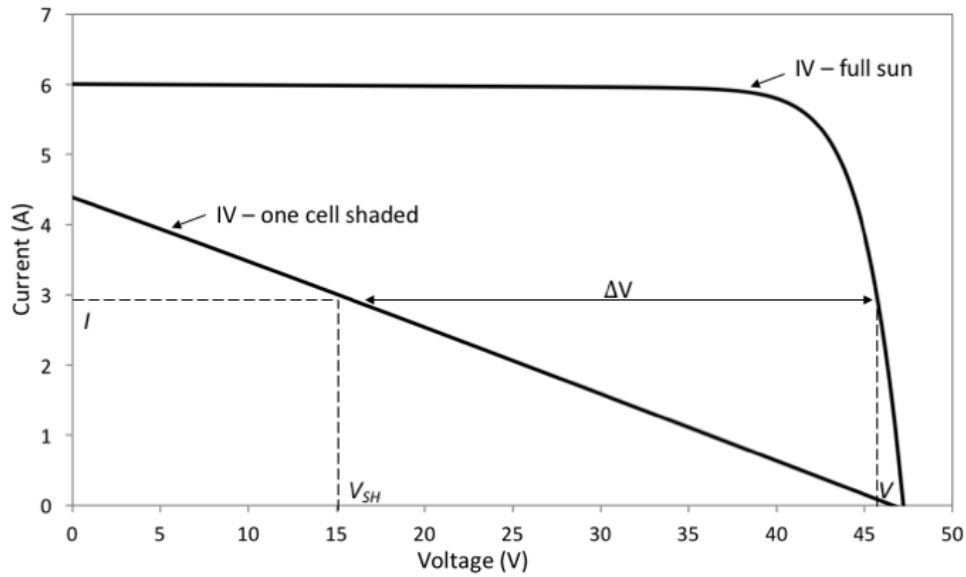


**Figure 2.11:** Effect of shading of one cell in a module of  $n$  cells.

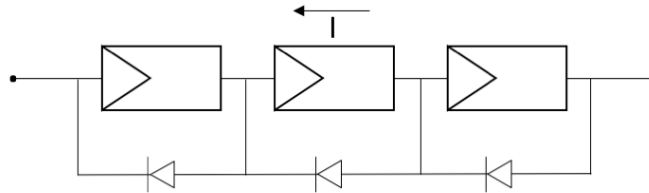


**Figure 2.12:** Three bypass diodes, each covering one third of the cells.

module consisting of a large string of cells (typically 36-60 cells), the  $V_{OC}$  is only slightly decreased. The limiting of the output current is what will reduce the power output for a module.

The effect of one fully shaded cell in a module of  $n$  cells is shown in Figure 2.11. When the one cell is fully shaded, the current in the module flows through  $R_p$  and  $R_s$  in the shaded cell, resulting in a voltage drop. At any give current the voltage drops by  $\Delta V$ , given by the Equation

$$\Delta V = \frac{V}{n} + I \cdot (R_p + R_s) \cong \frac{V}{n} + I \cdot R_p, \quad (2.13)$$

where  $R_p$  is assumed to be many times grater in magnitude than  $R_s$ . Full deriving of this Equation can be found in [12, p. 295]

To prevent reduction of power output and hot spots bypass diodes can be used. Figure 2.12 shows three bypass diodes connected in parallel to the cells in the string. During shading, the bypass diode in the part of the string with shaded cells becomes forward biased. Bypass diodes can be provided for each cell in a module, but the more common approach is that the manufacturer of a module provides a few diodes, each covering a certain number of cells. Bypass diodes makes the current go around a shaded or damaged cell within a module, or around a module within a string. This will improve the system performance compared to the case where no bypass diodes are used, and prevent hot spots.

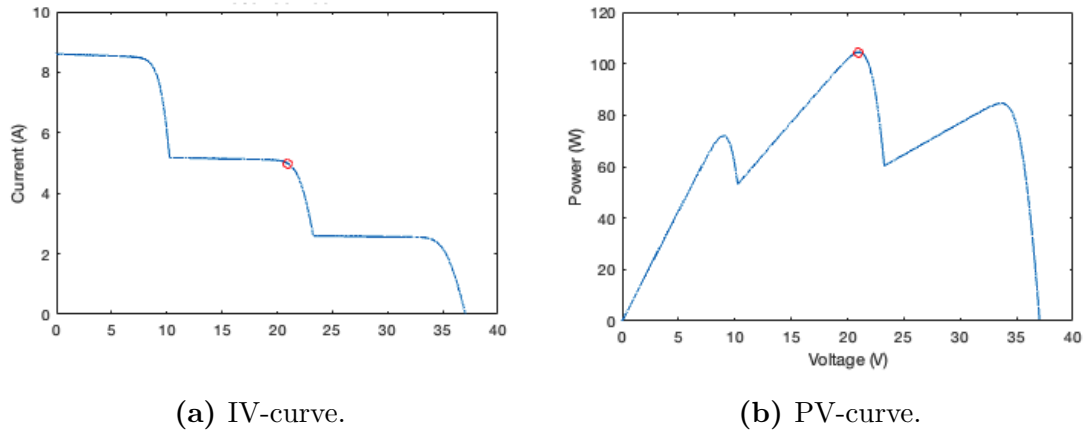


**Figure 2.13:** Shaded PV module with three bypass-diodes. [22]

An example from MathWorks [22] shows the effect of bypass diodes when shading of cells. The system consist of three strings of 20 series connected cells, where bypass diodes are connected in parallel, which is connected to a variable dc voltage source. This can present a module of 60-cells, with three bypass diodes. The first string has an applied irradiance of  $1000 \text{ W/m}^2$ . The irradiance of string 2 and 3 are  $300 \text{ W/m}^2$  and  $600 \text{ W/m}^2$ , respectively, as a result of partial shading. At the end of the simulation I-V and P-V characteristics are plotted which is showed in Figures 2.13a and 2.13b. When modules are partially shaded the I-V and P-V curves get several MPPs with different qualities, local and global MPPs. The power of local MPPs are lower in value than the power of global MPPs. In the Figures 2.13a and 2.13b the red circle indicates the global MPP at 104 W. It can be seen that the curves have in total three MPPs.

## 2.2.4 PV Cell, PV Module and PV Array

The *PV cell* is the part of the PV system which is generating electricity when sunlight is hitting. One single PV cell produces approximately 5 W at a voltage of 0.5 V for a Silicon PV cell [12, p. 284]. The voltage over an individual cell becomes

$$V_{cell} = V_d - IR_s. \quad (2.14)$$

For PV applications cells are connected in series which forms a *PV module*. The cells carry the same current, and at any given current, the voltages of each cell in series adds up. The voltage of a module then becomes as shown in Equation 2.15, where  $n$  is number of cells in a module. [12]

$$V_{module} = nV_{cell} = n(V_d - IR_s) \quad (2.15)$$

Modules are connected in series to increase the output voltage and power of the PV system. This is called a PV string. The number of modules connected in series is determined by the desired output voltage. To obtain the desired current, strings

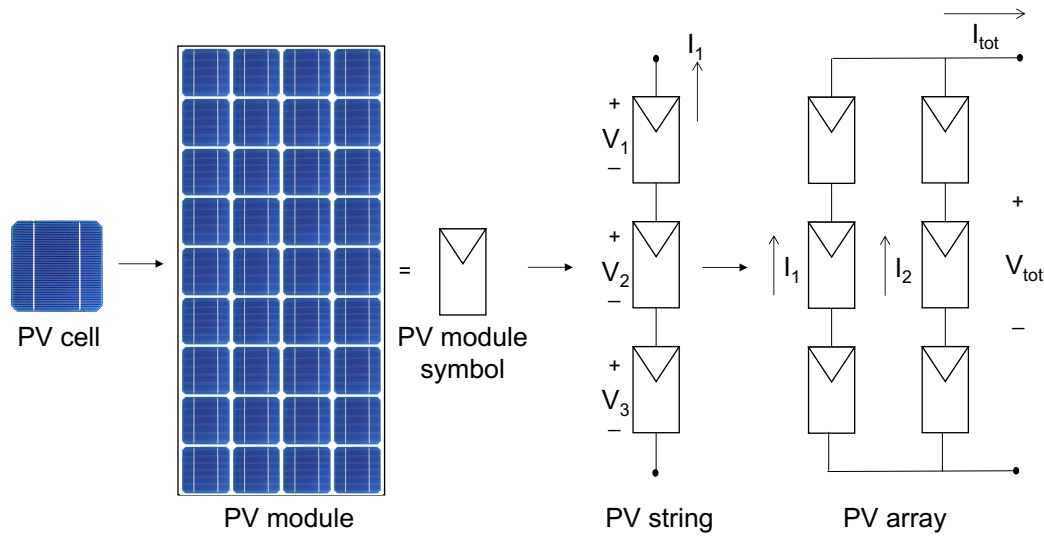


**Figure 2.14:** PV cell, PV module, PV string and PV array. Array output current:  $I_{tot} = I_1 + I_2$ . Array output voltage:  $V_{tot} = V_1 + V_2 + V_3$ .

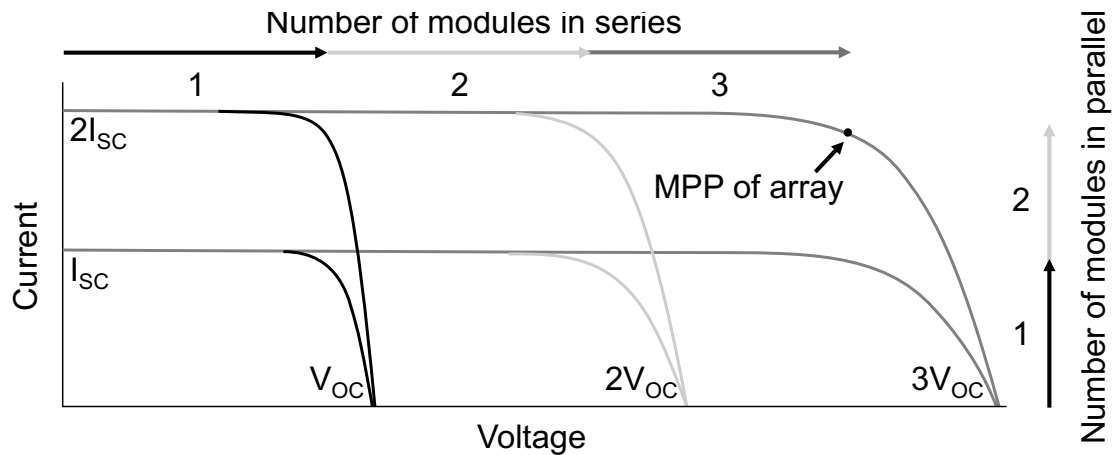
are connected in parallel. When connecting strings in parallel the output current will become the sum of the currents from each individually string. The product of which is power. Combinations of series and parallel connected PV modules are referred to as a *PV array*. [18] [12]

Figure 2.14 shows a PV cell, a PV module with 36 cells in series, a PV string of three modules in series and a PV array with two strings in parallel. The output voltage of the array,  $V_{tot}$ , becomes the sum of the voltages over each module in series. The output current of the array,  $I_{tot}$ , becomes the sum on the currents through each string. The current within a string is decided by the most shaded module, and the current within a module is decided by the most shaded cell. Figure 2.15 shows how the IV curve changes when modules are connected in series and parallel. The MPP is for the PV array in Figure 2.14.

## 2.2.5 Module Degradation

In most electrical generating systems the major source of reliability issues is moving parts. PV generators have no moving objects, so the operating lifetime depends on the panel material and on stability and resistance to corrosion of the materials. When buying a module, the manufacturer guarantees up to 25 years performance warranty [23]. Nevertheless, modules may have reduced power output or failure due to several failure modes and degradation mechanisms. These mechanisms are mostly related to water ingress or temperature stress. [13]

Knowledge about the degradation rate of PV modules used in systems, may give accurate predictions of power production for the systems lifetime. The degradation rate is also important financially, because high degradation rates gives less power production and increased cost for operation and maintenance, which leads to reduced future cash flow. [9]



**Figure 2.15:** IV characteristics of a PV array with three modules in series and two strings in parallel.

All modules will degrade in performance over time, but the degradation rate varies between different modules, and it is preferable to select modules with low degradation rate. After selecting a module there are a few minor things that can be done to protect against degradation and ensure maximum performance. Modules have to be carefully handled under installation, and damage on the modules has to be avoided. Mishandling can lead to increased and accelerated degradation. Regular cleaning and maintenance is also important. In Norway, the weather conditions usually ensure regularly rainy periods, which will clean the modules from dust. Soiling may still lead to the need for cleaning to prevent partial shading, in some cases. [24]

## 2.2.6 Optimal Tilt Angle of Modules

When designing and installing a PV array, the method of mounting has to be decided, and several considerations have to be taken into account. The easiest method is to mount the array horizontally on the ground, or on a flat roof. This gives a tilt angle,  $\Sigma$ , of  $0^\circ$ , and does not optimise the collection. This is because the beam radiation collected is proportional to the cosine of the angle  $\gamma$  between the incident beam (DNI) and the normal to the plane of the collector, as seen in Figure 2.16. Since the DNI is the solar component which contributes the most to electricity generation, it is important to consider it in the decision of tilt angle. [18, Chapter 2.5]

The solar zenith angle,  $\theta_z$ , is equal to  $L - \delta$  at solar noon, where the sun is at it's highest. This is when the sunlight travels at the minimum path through the atmosphere and correspond to the lowest AM for the day. Because of this the optimal tilt angle will be equal to  $L - \delta$ . Beyond solar noon, the sunlight intensity will decrease because the AM will increase, and the angle between the normal of the collector and the incident sunlight will increase (if the collector is at it's optimum). Hence, the maximum performance of a PV system is obtained by having a tilt angle equal the optimum for the location. [18, Chapter 2.5]

In Norway this the optimal tilt angle varies according to the time of the year, since the height of the sun at solar noon varies with the time of the year. On-site [25], the solar angle, and hence the optimal tilt angle, can be calculated according to month of the year. The result for optimal tilt angle for Oslo, Norway is listed in Table 2.3. If the system has fixed tilt angle, the optimal tilt angle can be found by looking at which angle gives the annual highest energy output. The tilt angle can be optimised according to several factors. Two cases can be either highest overall energy output or energy output at a specific time of the year, e.g. summer.

**Table 2.3:** Optimum tilt angle of solar modules by month for Oslo, Norway [25].

Jan	Feb	Mar	Apr	May	Jun	Jul	Aug	Sep	Oct	Nov	Dec
14°	22°	30°	38°	46°	54°	46°	38°	30°	22°	14°	6°

Modules can be mounted with tracking systems, such that the tilt angle and/or azimuth angle of the collector changes during the day according to the sun's position. The tracking can either be two-axis trackers, changing the tilt and azimuth angle, or single-axis tracker, changing only one of them. This function can increase the total irradiance collected by the module, but the tracking requires energy, so the economic and total output have to be studied in order to see if it is useful. [12]

Often other parameters also have to be considered when deciding the tilt angle of the array in addition to the total energy output. If the system is mounted on an already tilted roof top, additional mounting systems to achieve another tilt angle adds expenses. The increased performance has to be good enough to make up for the additional expenses, which is often not the case. In many cases the aesthetic of a building plays a role for the tilt angle of the PV array. For a flat roof, the desire is that the PV array is not visible when looking at the building. The tilt angle most likely can not then be at optimal angle. Some PV arrays are now also mounted on the facade of a building. In this case all the areas of a building which is faced either east, south or west can be used for energy generation. The tilt angle of the modules mounted on the facade are then 90° degrees, which decreases the performance even more. Because not only engineers are a part of the design of a PV system, especially for building integrated systems, and because cost plays an important role in the design, the optimal tilt angle is not always chosen.

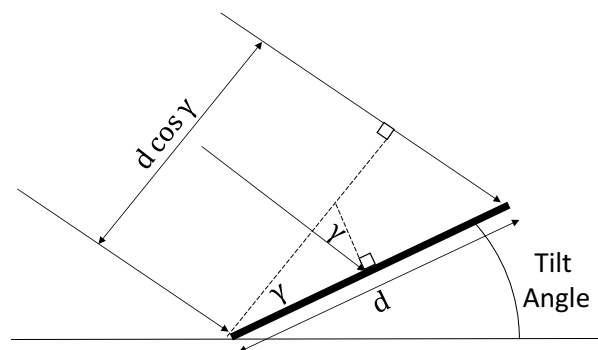


**Figure 2.16:** Illustration of effect of module tilt angle on effective area presented to beam component of radiation.



## 2.3 PV System Performance

### Main performance terms:

The main parameters used for evaluating system performance [26] and some important terms related to PV system performance are:

**Power rating [kWp]** - Peak power of the total PV array at STC (See Table 2.2) represents the maximum power that can be produced under ideal conditions. For a PV system it represents the size of the system, hence the power rating,  $P_{rated}$ . The power rating is independent of geographic situation and field orientation. [15]

**Specific yield [kWh/kWp]** - Specific yield (or final system yield,  $Y_f$ ) represents the array output energy,  $E$ , with respect to the nominal peak power of the system,  $P_{rated}$ . This term can be used for comparison of system quality between PV installations with different locations and orientations. The term refers to the potential of electricity production over a specified period for a specific location.

$$Y_f = \frac{E}{P_{rated}} \quad (2.16)$$

**Performance Ratio (PR)** - Represents the ratio of the produced energy, with respect to the reference yield,  $Y_r$  ( $kWh/m^2$ ). The reference yield is the theoretical energy produced by the system under perfect operation conditions at STC. PR is a measure of the quality of the system, and is independent of location and often described as a quality factor. This factor normalises the performance of the system with respect to irradiance and orientation of system, and is dimensionless. PR includes array losses as well as system losses, and provides information the total effect of losses. The parameter is used to evaluate long term performance of systems.

$$PR = \frac{Y_f}{Y_r} \quad (2.17)$$

### Main performance factors:

There are several factors affecting the system performance. These can be summarised as [27]:

1. **Temperature:** As explained in Section 2.2.2, the power output of the modules is dependent on the module temperature, thus affecting the performance of the system.
2. **Partial Shading:** Even small amount of shade can cause large effects on the system performance, and the effect of partial shading on the power output is non-linear.
3. **Soiling:** Reduction in incoming radiation due to soiling in form of dust or snow will negatively affect the potential of power generation. The amount

of soiling is heavily dependent on the local climate on-site. In Norway snow greatly reduces the system performance in winter.

4. **Degradation:** As explained in Section 2.2.5 the output of the modules will drop with the ageing of the modules once the initial break-in period has elapsed.

## 2.4 The Inverter

The inverter represents a very important component for grid connected PV systems. It has three main tasks ([28]):

1. **Power conversion:** Converts the generated dc power to ac power before fed into the main grid or to the ac system of the user. The conversion efficiency of the inverter is the most important characteristics. High efficiency is desired to ensure that most of the generated power from the PV plant is used and not lost. The inverter efficiency indicates the proportion of input direct current (dc) that comes out as alternating current (ac) that is delivered to the grid. Inverters used today usually have high efficiency, and can operate at 98 % efficiency.
2. **Power optimisation:** To ensure maximum power operation. The IV curve of the PV module changes with temperature and irradiance, and during a day can vary a lot and fast. The inverter has to find and track the maximum power point of the PV plant continuously to ensure optimal operation. This will secure that the PV generator produces maximum power output. It's essential that each inverter has this function which is called a Maximum Power Point Tracker (MPPT).
3. **Power quality:** The power injected to the grid must meet the power quality requirements which is specified in several standards. This includes the right voltage amplitude and frequency of the transformed ac power, as well as other power quality aspects.

The inverter should be monitoring yield of the PV plant as well as monitoring the grid, and signal problems and disconnects from the grid if any problems occur to ensure safety of both PV plant and main grid. To ensure maximum energy conversion, it is essential for the inverter to precisely identify change parameters, such as grid current and PV voltage.

Because of the large number of different inverters available, some design characteristics have to be considered when selecting the right inverter for a PV system. This includes things like power rating, circuit topology, module wiring topologies.

### 2.4.1 Inverter Power Rating

First the right power rating of the inverter have to be selected. The inverter size can range from 5 kW for residential rooftop systems to 800 kW for PV power stations. The inverter is sized depending on the peak power, which is the maximum power the inverter can supply, and the typical operating power, which is the power the inverter usually must supply. [28] [29]

### 2.4.2 Maximum Power Point Tracker

The IV curve of PV modules are constantly shifting due to changing solar irradiance, temperature and shading conditions. It is always preferable to operate the PV system at it's optimum point so that no the PV system operates at maximum potential. This is done by including a Maximum power point tracking (MPPT) in the system. Power optimisers are dc-dc converters which aim to maximise the operation of PV arrays with the use of MPPT. Modules are usually connected in strings to obtain higher voltages, and the string output current is consequently limited by the current of the most shaded module. If a module in a string is partially shaded the current output of this module can be drastically reduced, leading to the output current of the hole string to be reduced. This change causes the MPPT system to change the operating point, moving the rest of the modules away from their best performance. [12] [15]

The benefit from including power optimisers to the system is the recovery of electrical mismatch losses, which may either be current differences or partial shadings. Current differences take into account that real modules cannot be exactly identical, and there may be a difference expressed by a tolerance range within a given string. This is especially the case for current. The mismatches between modules is not homogeneous and can increase significantly along the years. The mismatch is characterised by a derate factor in simulations. Other factors like difference in soiling and orientation within a string cause current differences. When modules are partially shaded and have several MPPs, the inverter should find the global MPP and operate at this point. This is to ensure highest possible energy yield of the array, even when it is shaded. [12]

A way to ensure maximum power point operation is to convert the dc voltage from one level to another. This can be done by using a buck-boost converter. Boost-mode is used to step up the voltage, and buck-mode is used to step down the voltage. The output voltage is decided by a duty cycle defined by the controller which tells the tracker how to adjust the duty cycle. Several algorithms can be used to find the MPP. Two types are the *perturb-and-observe* approach and the *incremental conductance* method. Further detail about these methods can be found in the literature, and are not further explained in this thesis.

### 2.4.3 Inverter Classifications

Inverters can be one-phase or three-phase, and they can be with or without transformers. Transformers provide galvanic isolation which is required in some countries. The size of the power plant as well as classification of and requirements from the power grid, decides what kind of inverter that should be used. Another way to classify inverters is with regards to power processing stages. This includes single-stage or multi-stage inverters. Single-stage inverters only include one dc-ac converting stage, and handles all task including MPPT, voltage amplification (if necessary) and grid current control. They can provide low cost, reduced weight, easy module integration, high reliability and performance. Multi-stage inverters have two or more power processing stages, having separate dc-dc conversion and dc-ac conversion stages. They are expected to be more expensive and less efficient than single-stage inverters. The advantage is the possibility of separate and better MPPT to reduce module mismatching.

Inverters used in PV systems can be classified as either line commutated or self commutated inverters [30]. Line commutated inverters are switched on and off by thyristors once per period and the output voltage needs to be compensated with a filter. These inverters are cheap, robust and efficient but have large current harmonics. Today self commutated inverters are more used, containing high frequency switches like MOSFETs, IGBT's and BJT's. These inverters have reduced reactive power consumption and current harmonics.[31]

### 2.4.4 Inverter and Module Wiring Topologies

There are several ways to connect modules to the inverter. Different module wiring topologies are presented in Figure 2.17. Which inverter option to choose depends on the power rating of the system and the decision on the amount of PV modules connected to one inverter [32].

#### Central Inverter

For central inverters (Figure 2.17a) PV strings, generating large enough voltage so there is no need for amplification, are connected in parallel in a generator connection box and then connected to an inverter feeding the generated power to the grid [19]. This is an inverter topology used a lot in the past. Disadvantages and limitations related to central inverters are high-voltage dc cables between modules and inverter, losses in string diodes, mismatch losses between modules because of shading and power losses due to centralised MPPT. Advantages of the system is the need for only one inverter. Most centralised inverters used are line commutated with PWM switching at high frequencies larger than 16 Hz [33]. Large current harmonics and low power quality due to line commutated inverters are reasons for new and better inverter topologies. [34]

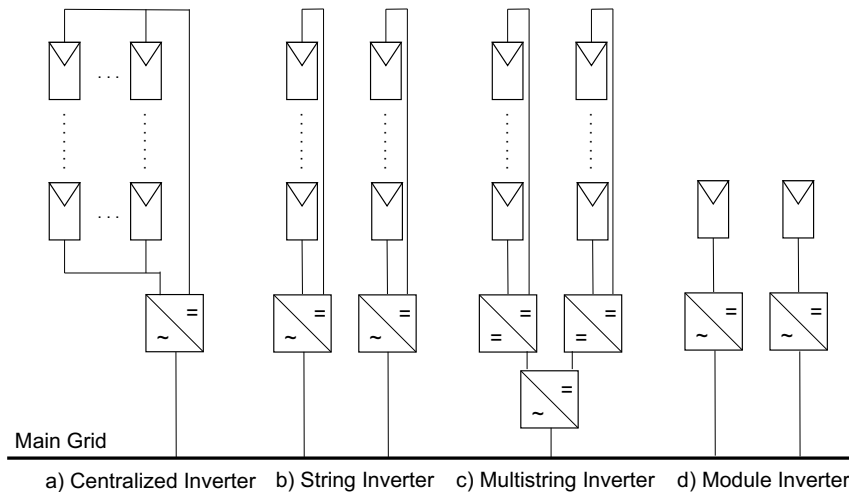


**Figure 2.17:** Module wiring topologies. For the inverter: (=) indicated direct current, (~) indicated alternating current.

### String Inverter

A reduced version of the central inverter is the string inverter (Figure 2.17b) where one string is connected to each inverter. By connecting the right amount of modules in series it is possible to obtain large enough output voltage that there is no need for voltage amplification. Controlling the output voltage magnitude can also be done by connecting a dc-dc converter to the string before the inverter. Separate MPPT is also possible which makes the system easy to monitor. [34]

### Multi String Inverter

Multi string inverters combine the advantage of high energy yield of string inverters, and low cost and simplicity of centralised inverters. This is a further development of the string inverter, and is considered to be the present and future of inverter topologies due to its advantages. In this topology each string has its own dc-dc converter with MPPT of each string. The strings are then connected to one common inverter. Figure 2.17c shows the multi string inverter topology. Multi string inverters are preferred over centralised inverters due to the possibility of individually control of strings. Enlargement of systems are also easily achieved by connecting new strings with dc-dc converters to existing power plant. [34]

### Module Inverter

Module inverters is the concept of integrating the PV module and the inverter in one component. Figure 2.17d shows how module and inverter are connected together in one component. Advantages of this concept is that it removes mismatch losses between modules. Each module has MPPT and can be individually monitored. The price per watt may be high due to complex circuit topologies, and the need for high-voltage amplification, which can reduce the efficiency. Enlargement of systems

is easy and this topology provides a flexible system, but replacement due to faults may also be difficult and expensive. Systems that use module integrated inverters usually have a power rating of less than 500 W, and consist of one or a few modules connected [35]. The voltage level of these kinds of systems are usually low due to few PV modules, and when grid-connected, voltage boosting is needed. [34]

## 2.5 Grid Connection

### 2.5.1 Demands and Standards

There are several technical difficulties when it comes to grid connected PV systems, and the power injected to the grid must meet utility power quality requirements [36]. To ensure power quality of the injected power as well as safety, efficiency and reliability of the electrical system, different standards have been developed. The two most common codes are the National Electrical Code (NEC) and IEEE Standard 929 which is reflected in IEEE 1547-2003. Additional to these electrical standards, mechanical standards and requirements also apply for PV systems because of the mechanical components. [18]

NEC consists of articles regarding electrical safety and efficient utilisation for electrical systems, like grounding, wiring methods and motor circuits. Which components to be used, including fuses, switches and wires, and where they should be placed in the system, are specified. The voltage drop in feeder and branch circuits are required in NEC to be less than 5 % of, whereas for PV systems the feeder circuit is considered to be the inverter output circuits that connect to the utility grid, and the branch circuit is considered to be the circuit connecting the PV array to the power conditioning equipment (the equipment converting dc voltage to ac voltage [37]). [18]

IEEE Standard 929 covers demands regarding power quality and disconnection of PV systems in case of faults. In 2003, IEEE Standard 1547 was developed focusing of the technical specifications and testing of electrical systems. It provides requirements for performance of the system, testing, operation, safety considerations and maintenance of equipment. Requirements on power quality and island operation is also provided. Island operation is the continued operation of the inverter after the grid has been disconnected in case of faults. The inverter is then just providing power to local loads. The inverter must monitor the frequency for 5 minutes in case of shut down due to voltage or frequency disturbance. If the frequency remains unchanged the inverter can restart. [38]

The requirements provided in IEEE Standard 1547-2003 shall be met at the Point of Common Coupling (PCC). Some general requirements provided includes that the electrical system shall not change the voltage at the PCC and voltage fluctuation at PCC shall not be greater than  $\pm 5$  % of the voltage level resulting in synchronisation with grid. Integration with grid grounding, distributed secondary spot network, monitoring provisions, isolation between the electrical system and grid shall also be obtained. In regards to power quality requirements, injected dc current

---

to the grid shall not be more than 0.5 % of rated output current and flicker shall not be created. When the electrical system is providing power to balanced loads harmonic current injection shall not exceed 4 % for harmonics in order less than 11, and the total demand distortion shall not exceed 5 % of the current. [39]





# Chapter 3

## Experimental Method and Simulation Software

In this chapter the simulation program PVsyst which was used in this thesis is presented. The parameters and settings for the simulation model of the PV system at Evenstad is discussed. The available measured data for Evenstad is presented as well as the accuracy of the measurements. In the last section the different variants of simulations performed in PVsyst are listed.

In this thesis simulations of an existing PV system have been carried out. This is a big grid connected PV plant on a tilted rooftop at Evenstad in Hedmark, Norway. The system consist of 276 PV modules and 12 inverters with a rated power of 70.38 kWp.

### 3.1 Introduction to Simulation Software: PVsyst

There exist several different simulation software packages suitable for PV system analysis. Some examples are SAM - The System Advisor Model, PVsyst, PV\*SOL, Polysun, Helioscope and PVGIS.

The simulation software selected for this thesis is PVsyst. For the thesis version 6.62 is used. This is one of the most used simulation tools used in the PV industry today. In this section an introduction to the simulation tool is given, and is based on a PVsyst user manual [40]. Additional information about the software that may be of interest, can be found on PVsyst online help [15].

#### 3.1.1 User Interface

The user interface of PVsyst is shown in Figure 3.1 and consists of four sections:

**Preliminary design:** In this section a quick evaluation of a project can be made with it's potentials and possible constraints. The accuracy of this tool is limited and is not used for customer reports. It can be a useful

tool for pre-sizing of stand-alone systems, but for grid-connected systems it's just a tool used to get a quick evaluation of the PV potential of a building.

**Project design:** This section is the main part of the software. It is used to give a complete study of a PV system project. It includes selection of meteorological data, system design, detailed shading studies, determination of losses as well as economic evaluation. The output is a complete report with many additional results of a full year in hourly steps. This is the tool used for the study and simulation in this thesis.

**Databases:** Climatic data management is done in this section, which includes monthly and hourly data, synthetic generation of hourly values and importing of external data. The databases also contains the definitions of all the components involved in the PV installations like modules, inverters, batteries, etc.

**Tools:** Estimation and visualization of solar installation behavior can be given by using additional tools provided in this section. Tools for importing measured data of existing solar installations for close comparison to the simulation is also included in the section.

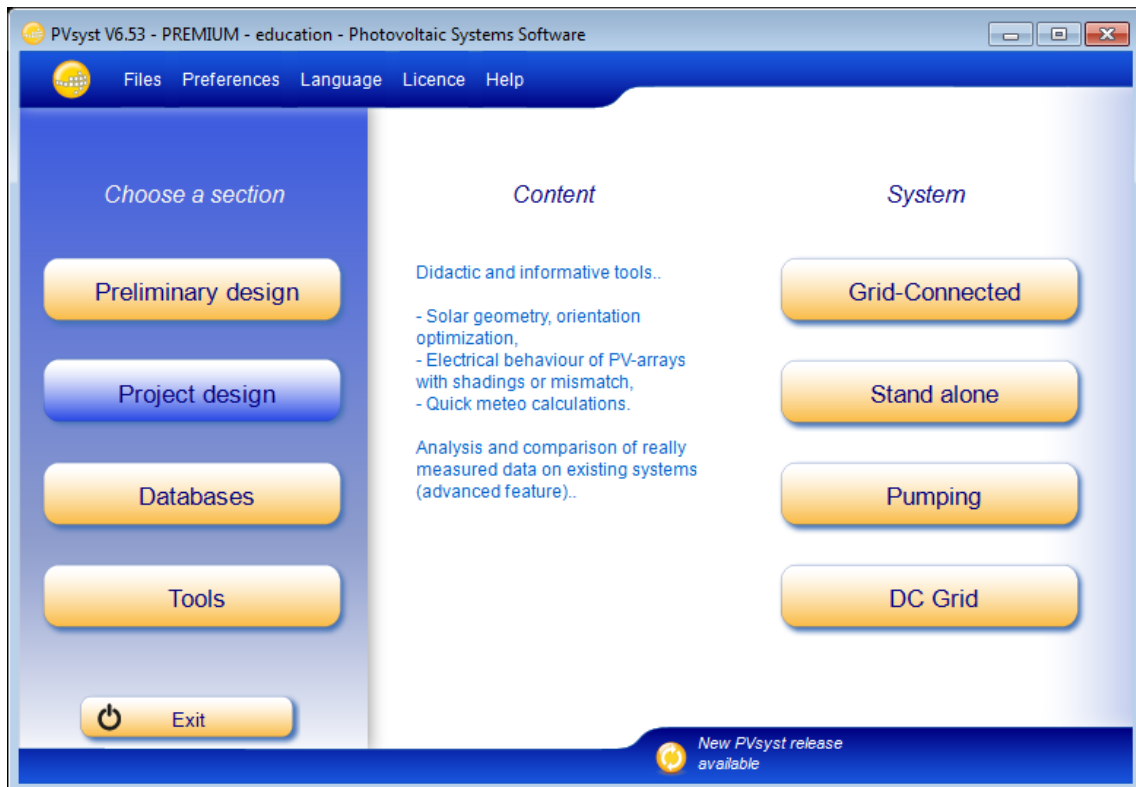


**Figure 3.1:** Screen shot of user interface in PVsyst. [40]

### 3.1.2 Project Design

For the simulation in this thesis the *Project design* section is used. This part aims to perform a thorough design and performance analysis using detailed hourly simulations. Optimisation and parameter analysis can be performed through different simulations runs, also called simulation variants.

In *Project design* the selection between four different system types is possible, as can be seen in Figure 3.1. This includes grid-connected, stand-alone, pumping and DC Grid systems. For the system in analysed in this thesis grid-connected is selected.

In the screen dialog the project specifications are defined. After selecting the project name, under the tab *Site and meteo* the project geographical location by coordinates with associated meteo data can be defined. As explained in section 2.1.3, meteo data can be defined from several sources. In the *Site and meteo* tab, the desired meteo file can be selected. This makes it possible to perform simulations using different meteo data sources.

In the *Albedo - Settings* tab access to monthly albedo values, design conditions and design limitations are available. Albedo values are usually not modified, and the standard value of 0.2 is used in most cases. Nevertheless, if the project is located at a place with specific albedo values, they can be changed under the *Albedo* tab. Under the tab *Design considerations* the value for *Lower temperature for Absolute Voltage limit* is an important site-dependent value. It is related to the safety of

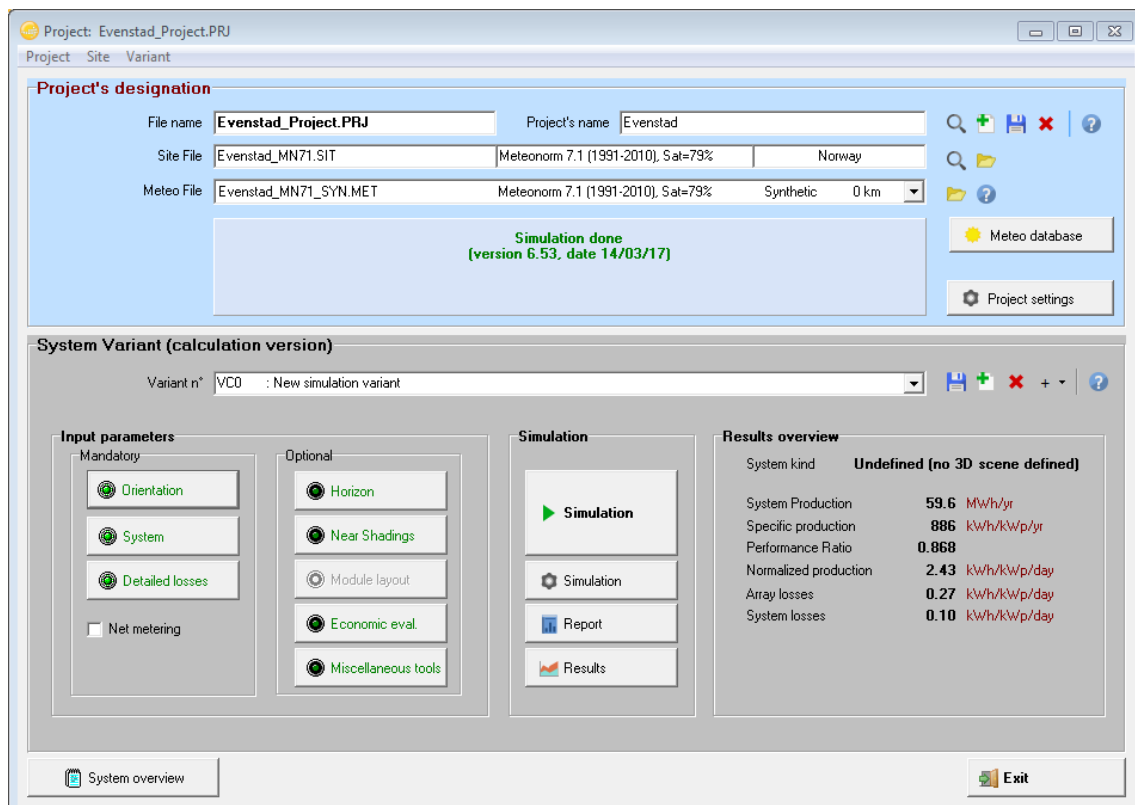


Figure 3.2: Screen dialog of Project design. [40]

the system, and it should ideally be the lowest temperature ever measured on-site during daylight.

Before doing any simulations, the project must be saved. After this the next step is to define the system. For input parameters there are some mandatory and some optional.

### **Mandatory:**

The two tabs *Orientation* and *System* are marked red and will define the PV system. In *Orientation*, module tilt and azimuth angle is defined as well as field type. PVsyst also proposes optimal angles with respect to the geographical location. The optimisation can be with respect to yearly yield, summer or winter.

In *System* tab the components of the PV system are selected, including type of modules and inverter, number of sub-arrays and strings as well as design of the system. By defining several sub-arrays, strings with different number of modules connected in series can be defined. Different modules and inverters can also be selected for the different sub-arrays. Many inverters and modules are implemented in the database of PVsyst, and some parameters can also be changed. PVsyst guides with messages through the different steps of definition and execution of a simulation. This ensures that parameters are realistic and selected correctly.

### **Optional:**

The optional input parameters can make the simulation more accurate. This include horizon, near shading objects, module layout, economic evaluation and other tools.

The *Horizon* tab describes far shading objects and is defined as the horizon line. This is objects that are sufficiently far away and act on the PV array in a global way. The distance to these objects should typically be ten times larger than the PV array size. An accurate way to define the horizon is to importing it from tools like the Solmetric SUNeye which gives professional site evaluation [41]. The horizon can also be defined manually. To gather information about a azimuth angle and height in degrees for the horizon, tools like the application Theodolite Droid can be used [42]. Theodolite is a multi-function viewfinder that combines compass, two-axis inclinometer, GPS, map and tracker, among other things.

*Near shadings* is defined as the objects close to the PV array which directly draws visible shades on the array. This is implemented in the simulation by making a 3D model of the PV Array and its surroundings. This could be trees, buildings and other objects. The 3D model can't be imported from other other software packages like Autocad and SketchUp, but needs to be manually drawn in PVsyst.

For the beam component of the near shading, two losses have to be considered:

1. **Irradiance losses:** these are the linear shading losses and correspond to the deficit of irradiance on the cells, and represent a lower limit to the shading effect.

2. **Electrical losses:** this is the upper limit to the shading effect and covers the effect of mismatch of electrical response between modules in series and strings in parallel. When a cell is shaded the current in the whole string is affected by the current in the most shaded cell.

The *Module layout* tab lets the user specify the geometrical arrangement of modules in the 3D scene defined in the near shading tab. The module interconnections can be defined. These specifications help with accurate calculation of the electrical effects of partial shading of near objects for Si- crystalline modules. This is the last step for development of a model for PV system study.

### 3.1.3 Detailed Losses

Under the tab *Detailed losses* several parameters are set to default values for early simulations. These loss parameters can be changed to more reasonable values according to system specifications. In this section a short description will be given of each parameter.

#### Thermal Parameters

At each simulation step the thermal behavior of the array is calculated by a thermal balance shown in Equation 3.1, where  $\alpha$  is the absorption coefficient of solar radiation and  $\eta$  is the cell efficiency. In PVSyst the default value of  $\alpha$  is 0.9, but can be changed if desired. The efficiency of the cells are calculated according to the operational conditions if possible. 10 % efficiency is used if calculations is not possible.

$$U \cdot (T_{cell} - T_{amb}) = \alpha \cdot G \cdot (1 - \eta) \quad (3.1)$$

The thermal balance is characterised by the *Heat loss factor* given by the U-value which is shown in Equation 3.2, and establishes the instantaneous operating temperature, to be used by the PV modules modelling.  $U_c$  is a constant component of the thermal loss factor and  $U_v$  is a factor proportional to the wind speed  $\nu$ . The value of these factors depends on the mounting of the modules. The mounting method used determines how well the array is ventilated, which will increase the cooling of the system and reduce the thermal losses.

$$U = U_c + U_v \cdot \nu \quad (3.2)$$

If module temperature measurements are available they can be imported to PVSyst and used as thermal parameters. An option to use measured array temperature becomes available for selection when module temperatures are imported via meteo files.

#### Ohmic Losses

The ohmic losses determine the power losses in the wiring module interconnections and inverter connection cables. These losses can be specified by average length

(m/circuit) and cross section ( $\text{mm}^2$ ) for string module connections and inverter connections. It is also possible to define the ohmic losses by a global wiring resistance, if details about cross sections and lengths are not known. The ohmic losses are calculated by PVsyst using Equation 3.3 where  $R$  is the global wiring resistance.

$$P_{loss} = I^2 \cdot R \quad (3.3)$$

### Module Quality – LID – Mismatch

Module quality loss is a parameter which reflects the users confidence that the module's set performance implemented in the simulations, is matching the manufacture's specifications. It can be set to any desired value, and will under simulation induce a loss on the array  $P_{mpp}$  production, constant in percentage over all operating conditions.

LID (Light Induced Degradation) is for crystalline modules a loss of performance arising in the first hours of exposition to sun. It may affect the real performance by respect to the final factory flash tests data delivered by some PV module providers.

Mismatching losses is due to the fact that the current within a string is limited by the lowest current of a module. Modules used in installation of systems are in reality not identical.

### Soiling Loss

Soiling losses include everything that covers PV modules and reduces the transmission through the front glass. The result is an efficiency drop over time. Soiling losses can either cause soft or hard shading. Soiling that causes soft shading includes thin layers of snow or ice, dust, sand, pollen and condensed water that leaves stains on the PV modules. Hard shading can be caused by soiling like thick layers of snow, bird dropping and leaves. The effect of partially shading on IV-curves have been described in Section 2.2.3. [43]

Soiling losses become an important loss factor in Nordic climates, like Norway, because of snow covering panels during winter. In Norway 1/3 of the rain comes as snow. There can be months where the soiling losses due to snow are up to 80 % due to many days with snow (see simulation in Section 4.4). Hard shading due to snow, can give zero PV production, even for clear days with no clouds and good irradiance conditions. For simulations of PV systems in Nordic countries snow conditions, implementing soiling losses becomes an important factor for accurate simulations.

Soiling losses also include dust and particles that cover the panels and reduce the irradiance that reach the PV cell. This is usually a negligible factor, except for industrial environments or desert climates, where the factor can be significant. In Norway it rains regularly. This is a factor that reduces the soiling losses due to dust and particles, because rain cleans the PV panels.

In PVsyst soiling losses can be specified as a percentage for each month or as a

yearly factor. When implemented to PVsyst, periodical cleaning and rainy periods needs to be taken into account.

### **IAM Losses**

Incident Angle Modifier (IAM) is a term for the incident effect that corresponds to the decrease of irradiance which really is reaching the PV cell surface due to increase in reflection with incidence angle, as a reference to irradiance under normal conditions. It is the variance in output performance as the sun's angle changes with respect to the PV cells surface. IAM accounts for the expected rates of reflection when compared to incident at the normal plane (i.e.  $90^\circ$ ). The IAM value identifies the expected impact on the performance with the varying angle of the sun through the day and the year, with respect to the collector plane.

In PVsyst IAM losses is sufficiently well defined by parameters proposed by "Ashrae" (US standards office), but it is also possible to define points for a costume curve according to module manufacture's specifications. More about this modification will be presented in section 3.2.6.

### **Unavailability**

Sometimes the system stops working due to a fault. This unavailability parameter can be specified as a fraction of time, or as number of days. This is usually unpredictable and periods can be created randomly. If there exist knowledge about specific periods of unavailability, they can be defined.

#### **3.1.4 Meteorological Data in PVsyst**

Importing of meteorological data in several ways is available in section Databases in PVsyst. The built-in database for meteorological data is given as an object including geographical coordinates and associated monthly meteo data, and are stored as \*.SIT files. If a new geographical site is defined PVsyst generates as a default monthly data from Metenorm. An alternative is to use satellite data for monthly values from NASA-SEE, which is available for any point on earth. Furthermore, PVsyst gives access to other public data sources where it distinguishes between monthly and hourly data.

The built-in database Metenorm was presented in Section 2.1.3. All the measured stations available in the Metenorm database are available in PVsyst for Europe. In PVsyst the year 1990 is considered as a convention to label all data which don't correspond to real measured data at a given time. This is often, the case for synthetic hourly generated data. This is used because recent data is scarce in public published data. The measurements of real meteo data is considered as a very complex job. As explained later, real measured meteo data is available for the location Evenstad. [40]

Since the simulation in PVsyst operated at hourly values, hourly meteo data have

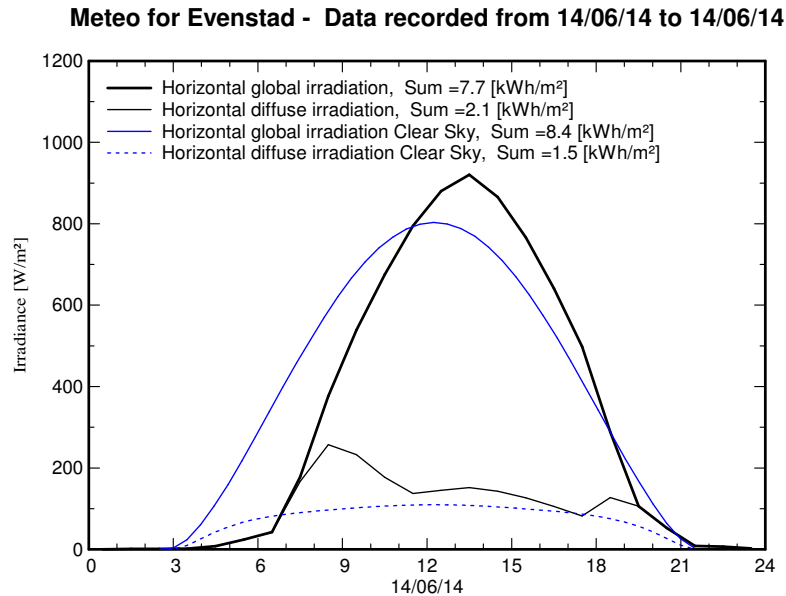


**Figure 3.3:** PVsyst excerpt of best clear day quality check of imported meteo data with time shift of 59 minutes for date 14-05-14

to be constructed from the monthly values if measured hourly data isn't available. Synthetic hourly data will be stored in \*.MET files. The synthetic hourly generation from monthly averages is performed by using stochastic models for the irradiance. The models used were developed by the Collares-Pereira team in the 1980's. It uses Markov transition matrices to first generate daily values, then 24 hourly values per day. These matrices have been established such as to produce an hourly sequence, with distributions and statistical properties analogous to real hourly meteo data measured on more than 30 sites all around the world. The generation of hourly values of temperature as a function of irradiance, have no available models. This is because the temperature is not only dependent on irradiance, but mostly on atmospheric circulations. Hourly generated temperature values are thus mostly random. Although, the temperature profile within a day is well correlated to the irradiance, as can be seen in Figure 3.13. This gives a sinusoidal looking shape of the temperature over 24 hours, with an amplitude proportional to the daily irradiation and with a phase shift of about 3 hours with respect to the highest solar angle. This is based on the fact that the warmest hours are around 3:00 solar time. [40]

PVsyst also offers tools for importing meteo data from other predefined sources. A semi-automated importing of data is possible for a set of external sources. Both sources with monthly and hourly data is available. For the sources only containing monthly data synthetic hourly data has to be generated.

In some cases none of the predefined sources offers satisfactory meteo data. If a better data source is available, like a local weather station or sensors on-site, this data can be imported from ASCII files. The ASCII file is assumed to hold one line per time step, and each time step should be in hours or fraction of hours. When importing unit conversion can be performed to match PVsyst internal standard formats (MJ, MJ/m<sup>2</sup>, °C, m/s).



It's important that the imported data is quality checked. PVsyst proposes four ways to do this evaluation under the *Check data quality* tab. The first way is to check the time shift of monthly best days with respect to the clear day model. An example of time shift after importing of data is presented in Figure 3.3. For this case the best clear day is shifted with 59 minutes with respect to the clear day model represented by the blue line in the Figure. A consequence of the imported date not being correctly shifted with respect to the clear day model, is that the irradiance will be cut. Analysis of this quality check will be further investigated in Section 3.5.3.

Other ways to quality check the imported meteo data is to look at the cloud of hourly  $K_t$  in the morning and evening, where the points shall have even distribution for a hole year. This check only makes sense for data imported for longer periods than one day, where it only exist one point for evening and one for morning. Clearness index with respect to the clear day model and the ranking of days according to their clearness index can also be used for quality check.

### 3.1.5 Simulation Results

The results of the simulations in PVsyst are generally represented in a report including simulation parameters, horizon definition, near shading definition, main results and loss diagram. An example of such a report is represented in appendix B with an explanation. A description will not be given here, for the sake of brevity.

### 3.1.6 Accuracy of PVsyst

The accuracy of simulations in PVsyst, according to [44], depends strongly on the input meteorological data and simulation parameters decided by the user. The method for validation the model is to compare simulated results to measured data. Obtaining high quality measured data is often difficult. Data from existing systems are often proprietary and difficult to get access to. The validation of a model comes down to the two components: measurement and modelling accuracy.

As explained in Section 2.1.3 the measurements of irradiance and irradiation is very important for accurate simulations, but difficult to measure. Irradiation is measured over a specific time period, usually a day, and is commonly used for simple PV system design, while irradiance is used for more complex simulations which calculates performance at each point of the day [13].

Measurements of electrical data is usually easier to get more accurate. Malfunctions of the system are however often not documented well. This may effect the measurements. [44]

The module performance represents the main uncertainty for modelling accuracy. It is based on STC values provided by the manufacturer, temperature coefficients,  $R_{shunt}$  and  $R_{series}$ , which may be default values or established by low-light irradiance performance data, Light Induced Degradation (LID), Potential Induced Degradation (PID) and degradation ratio.

In the article [45], the calculative accuracy of several simulation software, including PVsyst, were examined. The main results was that the software packages tend to overestimate the global irradiation received by the modules and at the same time underestimate the electrical energy generated by the system significantly. The main source of error in estimation of generated power is in the PV cell model the simulation packages uses.

## 3.2 Simulating the PV System at Evenstad

In this section the main parameters and settings for the simulation model of the PV system at Evenstad, are presented. This includes description of geographical location for the system, PV system components and their specifications, shading analysis, module specifications, module layout and loss parameters.

### 3.2.1 Geographical Location

The geographical location of the PV system at Evenstad is listed in Table 3.1. It is located in a valley in the east part of Norway, in Hedmark. The system is located far away from marine environment and the weather conditions can be considered not so rough.

**Table 3.1:** The geographical location of the PV system at Evenstad

Latitude:	61.4242892	Altitude:	259 m a.s.l
Longitude:	11.078757	Time zone:	+1

### 3.2.2 PV System Parameters

Selected parameters for tilt and azimuth angle for the system at Evenstad is listed in Table 3.2. The parameters are selected with respect to actual values of the existing system. Figure 3.4 shows the optimization of plane tilt and orientation implemented in PVsyst.

The azimuth angle of  $-10^\circ$  was found by using Google Earth, and is an estimation of the actual azimuth angle of the PV array and building. South is  $0^\circ$  according to Figure 2.4, which is the definition of the azimuth angles in PVsyst. A comparison of selected parameters to the optimum is also provided, as seen in the Figure. Loss by respect to optimum is  $-1.7\%$  with the selected values.

**Table 3.2:** Orientation parameters selected in PVsyst for Evenstad.

Tilt angle:	$35^\circ$
Azimuth angle:	$-10^\circ$
Field type:	Fixed tilted plane

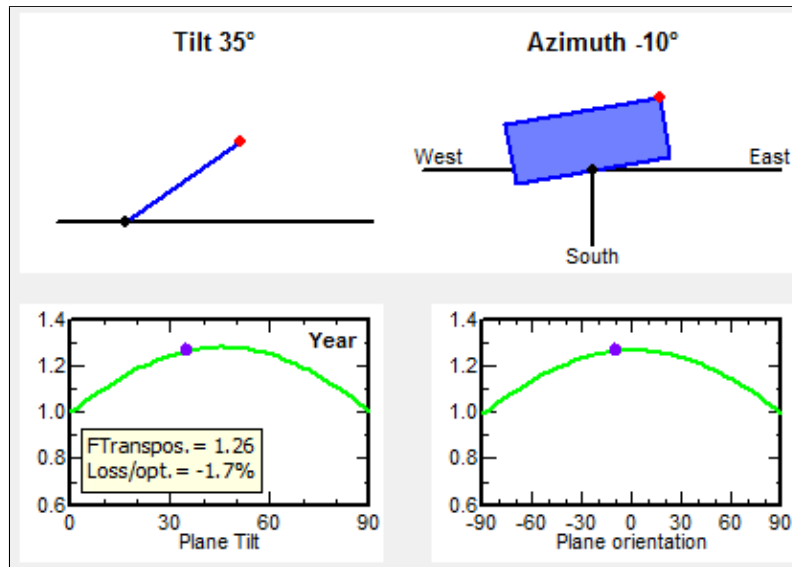


**Figure 3.4:** Tilt and azimuth angle selection in PV Syst, with comparison to the optimal angle.

Some additional settings for the project include albedo settings and reference temperatures for the design of the PV array. Albedo coefficient is the fraction of global irradiation reflected by the ground to the titled plane. The albedo value increases with tilt angle, and is zero for a array with  $0^\circ$  as tilt angle. Albedo values can be set for each month, and NASA provides global albedo values [46]. The overall albedo value for the model is though set to default value of 0.2, which can be considered a reasonable value for Evenstad when considering the surroundings.

As mentioned in Section 3.1.2 the value for lower temperature for absolute voltage limit is an important site-dependent value. It is set to  $-33.4^\circ\text{C}$  and is based on data collected from the meteorological site Yr [47]. This is the lowest temperature measured since 2001, and was measured on 03-02-2012.

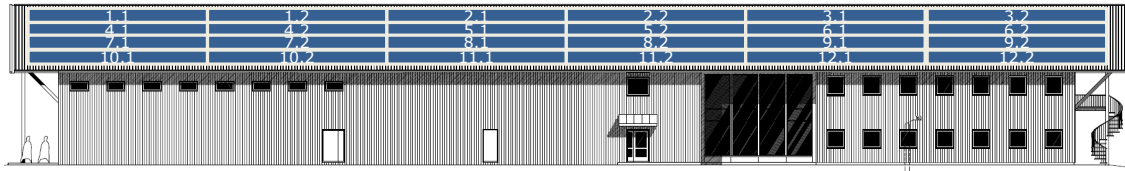
### 3.2.3 PV Array

The PV system selected for this study is a BAPV system located in Evenstad, Norway. The PV system is installed on a south-faced rooftop located near the University of Hedmark campus Evenstad and was installed in November 2013 by the Norwegian company FUSen. The PV system consist of 276 REC 255 PE PV modules and 12 Sunny Boy 5000TL-21 inverters. There are 23 modules connected to each inverter. The total installed PV power is 70.380 kWp. Two strings are connected to each inverter, where one string consist of 12 modules and the other string consist of 11 modules. The inverter includes two MPPT, one for the 12 modules string and one for the 11 modules string. The inverter is explained in detail in Section 3.2.8.

Figure 3.5 shows a sketch of the PV plant at Evenstad. Numbers in the annotation define string and inverter arrangements as they are presented in Table 3.4. The first number specifies which inverter, and the second number specifies which module

**Table 3.3:** PV Array characteristics.

<b>Total PV system power:</b>	70.380 kWp	
<b>Modules:</b>		
PV module	REC 255PE BLK	×276, modules
PV module manufacturer	REC Solar AS	
Unit nominal power	255 W	
Module/Cell area	455 m <sup>2</sup> /403 m <sup>2</sup>	
<b>Inverters:</b>		
Inverter	Sunny Boy 5000TL-21	×12, inverters
Inverter manufacturer	SMA	
Operating voltage	175 – 500 V	
Total/Unit nom. power	55 kWac/4.60 kWac	

**Figure 3.5:** Sketch of the PV plant at Evenstad. Numbers in the annotation define string and inverter arrangements. Picture provided by FUSen.

string, where 1 indicates a 11 module string and 2 indicates a 12 module string. Such that (8,2) presents a string with 12 modules which is connected to inverter number 8.

In PVsyst the strings are divided into two sub-arrays. One sub-array representing the strings containing 11 modules in series, and one sub-array representing the strings containing 12 modules in series. Each sub-array consists of 12 strings.

**Table 3.4:** Technical data of sub-arrays.

	String	Number of modules	Total power	$U_{MPP}$	$I_{MPP}$
Sub-array #1	1.1; ... 12.1	11 modules	33.7 kWp	302 V	100 A
Sub-array #2	1.2; ... 12.2	12 modules	36.7 kWp	329 V	100 A

### 3.2.4 Near Shading

Figure 3.6 shows the 3D model of the PV system and its surroundings for near shading analysis in PVsyst. The dimensions used for the 3D model are included in Table A.4 in Appendix A.1. Information about azimuth angle of buildings and PV array as well as dimensions of shading objects have been found using Google Earth. Height and placement of shading objects are therefore not accurate, and only an estimation.

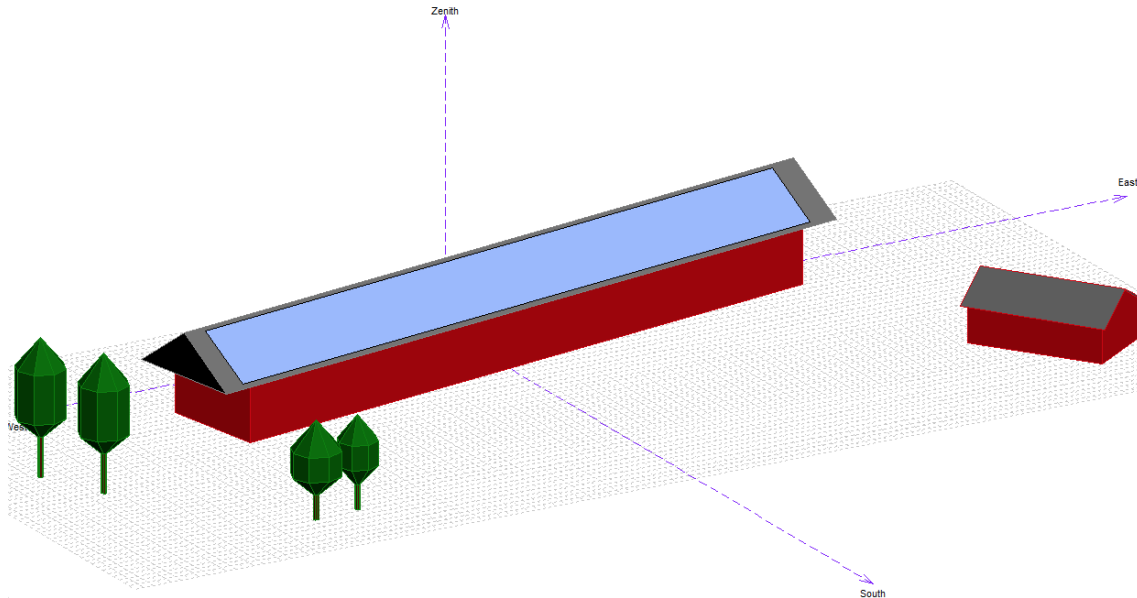


**Figure 3.6:** 3D model of PV array and its surroundings for near shading analysis. The blue field represents the PV array.

The blue field in the Figure represents the area of the PV array at Evenstad. This area has a width of 69.76 m and a height of 7.24 m, which is sized with respect to the 276 modules in the system, as well as space between the modules and snow guards. There are two snow guards placed under in the middle of the array and at the bottom of the array. The modules are placed in portrait position, and have four modules in height and 69 modules in width. The size of one module being  $1,66 \times 0,99$  m.

### 3.2.5 Far Shading

Far shading is, as mentioned before, defined as the horizon line. There are several ways to define the horizon in azimuth angle and height degrees. One way is to be on-site with tools like Solmetric SUNeye or apps like Theodolite Droid.

For this thesis an alternative way was used. A panorama picture of the horizon on-site was created using Google Earth, and can be seen in Figure 3.7. This picture was imported to Meteonorm software which produces horizon profiles that can be imported to PVsyst. In this software a horizon profile can be manually drawn according to a panorama picture of the horizon. When saved as a \*.hor file, it can be imported directly to PVsyst. Points with azimuth angle and height degree are implemented to PVsyst from the horizon file.

Figure 3.8 shows the sun path diagram of Evenstad. The grey field in the picture defines the horizon profile imported from the Meteonorm horizon file.



**Figure 3.7:** Snapshot of the horizon at Evenstad. Made from using Google Earth.

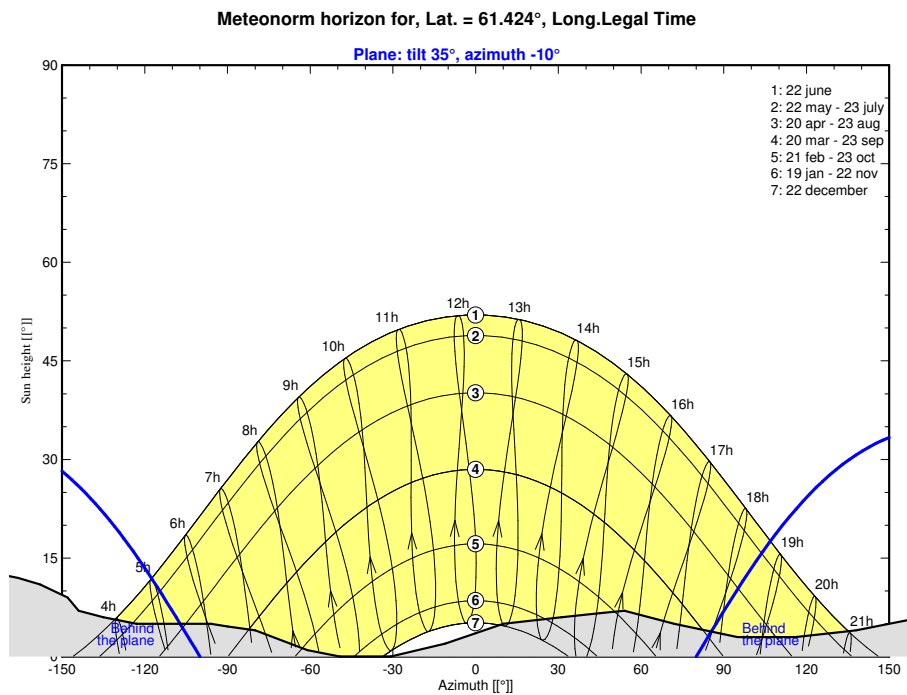


**Figure 3.8:** Sun path diagram and horizon profile (grey field) for Evenstad.

### 3.2.6 Incident Angle Modifier

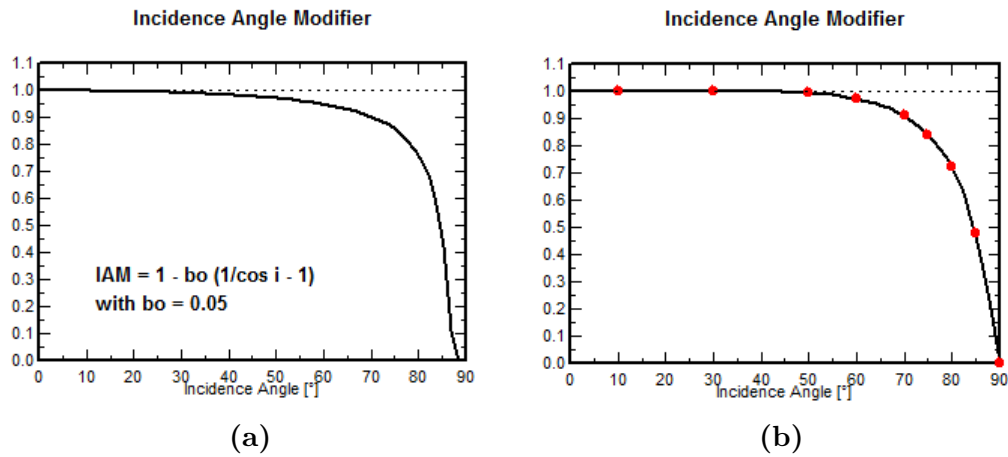
The module used for the PV system is a REC 255PE by REC Solar AS. This module exists in the PVsyst database and can be directly selected. The article [48] contains a study done by REC Solar about assessing reflection for REC Peak Energy Series modules. The main result is that the modules are operating better than the module in the database in PVsyst are in simulations. As mentioned in Section 3.1.6 the main reason for the underestimation of generated power in PVsyst is the PV cell models used in the simulation software. By implementing correct values for IAM losses, this error is reduced.

The modules have a AR glass treatment which reduces the reflectance of the modules. The treatment ensures that the reflection is only significant affected after a 60° tilt angle of the modules. By implementing new values for IAM into the simulation in PVsyst, will enable accurate predictions of system performance.

Table 3.5 shows the IAM values that were implemented in PVsyst. Figure 3.9 shows the corresponding graphs for IAM with regards to incident angle, Figure 3.9a

**Table 3.5:** IAM values for non-treated and AR treated glass for REC modules. [48]

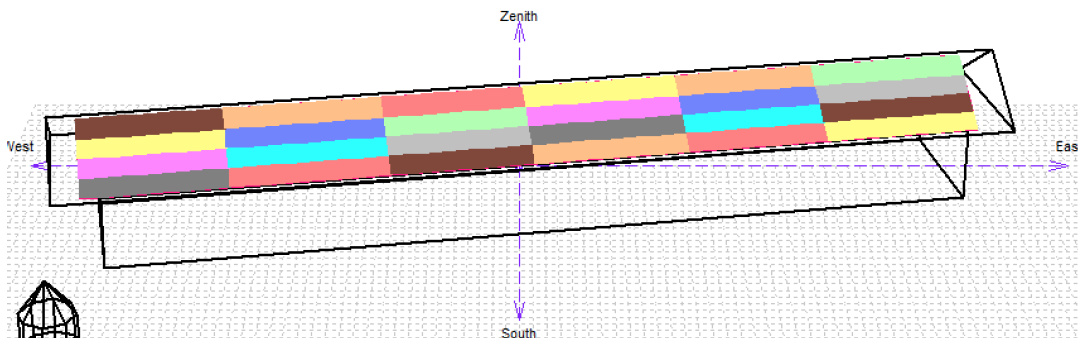
Angle	10°	30°	50°	60°	70°	75°	80°
IAM non-treated glass (%)	100.0	99.9	98.5	95.3	87.0	79.0	67.7
IAM AR treated glass (%)	100.0	100.1	99.4	97.4	91.1	84.1	72.2

**Figure 3.9:** Graph for Incident angle modifier. (a) Module implemented in PVsyst database, (b) Modified module according to values in [48].

for modules with non-treated glass and Figure 3.9b for AR treated glass.

### 3.2.7 Module Layout

Figure 3.10 shows the arrangement of the 276 modules representing the PV system at Evenstad. The module layout is defined with respect to the PV area defined in the 3D model described in Section 3.2.4. The different colours represent the different strings. For this system this means 24 strings, as can be seen in the Figure. Each string, consisting of either 11 or 12 modules, was manually placed within the area. The module spacing in Y- and X-direction was set to 0.2 m. Each module consist of three strings of 20 cells, each string with one by-pass diode. This gives 3 by-pass diodes per module [48].

**Figure 3.10:** Module layout for PV System at Evenstad.

### 3.2.8 Inverters

The system include 12 SMA SunnyBoy 5000 TL inverters. It's characteristics are included in Appendix A.2. The nominal ac power of the inverter is 4.6 kW<sub>ac</sub> and the maximum ac power is 5.0 kW<sub>ac</sub> as the name indicates. Maximum efficiency is 96.2 % at a voltage level of 175 V. The maximum efficiency is set to be 97.5 % according to European efficiency, which is average operating efficiency over a yearly power distribution corresponding to middle-Europe climate. The efficiency curve of the inverter is shown in Figure 3.11. Figure 3.14a shows one aspect of the demanding conditions the inverter have to operate under, with fast fluctuating input power. The inverter topology is transformerless and has multi-string technology. It uses convection as cooling method. Inverter night consumption of 1.0 W was added to the Sunny Boy 5000 TL inverter found in PVsyst's database.

The inverter has two MPPT inputs which makes it possible to connect strings with different number of panels to one inverter. As mentioned in Section 3.2.2 the strings in the systems consist of either 11 or 12 modules, which are connected to one inverter. The nominal power of the two strings connected to the inverter is 4.6 kW<sub>ac</sub> which fits well with the inverter's nominal power.

The default setting in PVsyst is that the limit of the inverter power is set to nominal power. The effect of changing this limit to maximum power instead, will be discussed in Chapter 4. The selected power ratio for the different sub-arrays will also be discussed in this Chapter.

The MPPT is handled by a OptiTrac operation control in the SunnyBoy inverter, and ensures maximum energy yield. The OptiTrac global peak has an additional function so that the controller can temporarily operate the PV array at a great distance from the known operation point. This function gives the inverter the possibility to always find the operating point with highest performance. Though this procedure leads to losses being unavoidable, the losses are kept at a maximum

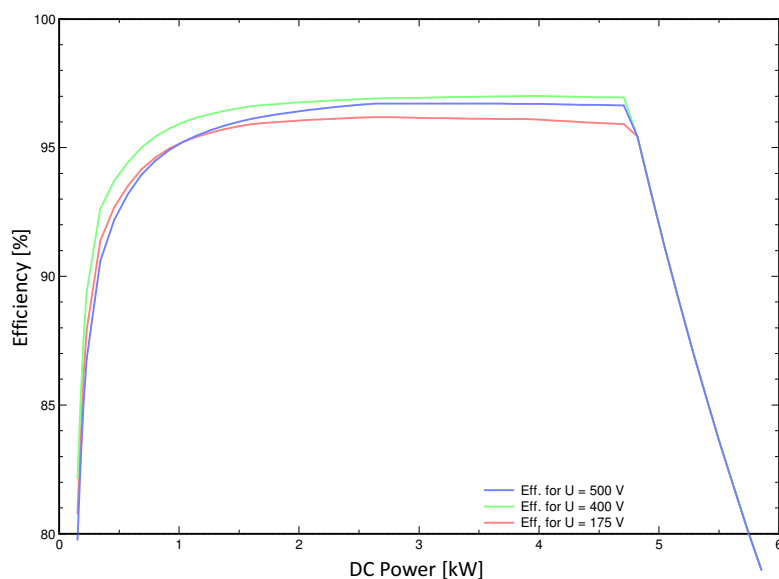


**Figure 3.11:** Inverter efficiency vs. DC input power. Excerpt from PVsyst.



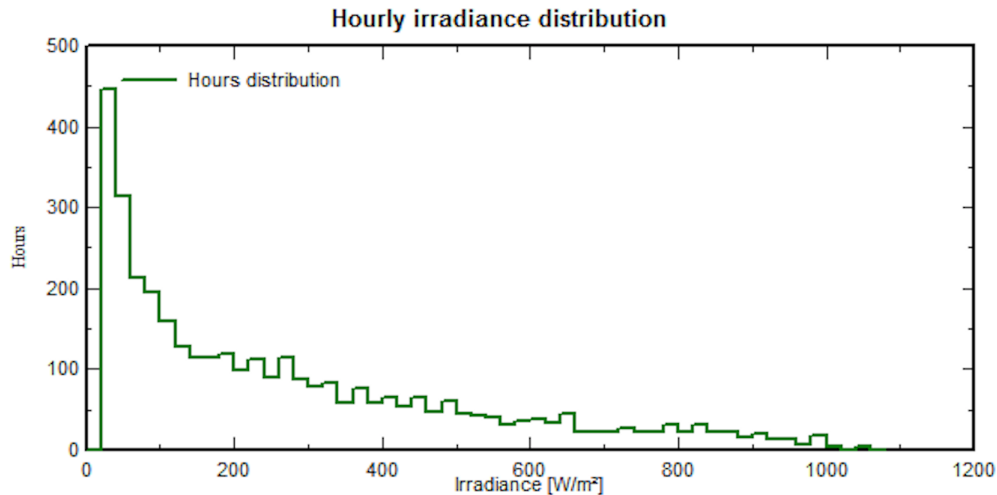


**Figure 3.12:** Number of hours of total irradiation for different irradiance values for Evenstad. Figure excerpt from PVsyst 6.62 with meteo from Metenorm 7.1 database.

of 0.2 %. The inverter’s MPP operation range is 175 V - 500 V.

The produced energy at each inverter are measured and presented at the SunnyPortal site for Evenstad [10]. The measuring devices at each inverter are there to ensure proper system management and to take precise energy measurements. According to tests conducted by SMA of SunnyBoy inverters [49], the inverter’s measuring channels may have a tolerance of up to  $\pm 3\%$  compared to the calibrated feed-in counter and based on the respective final value of the measurement range under nominal conditions. The relative deviation may therefore be large when input power is low. In Figure 3.12 it can be seen that a big portion of the irradiance is of low level at Evenstad. The low efficiency of the inverter for low input dc power, makes the operation performance of the inverters at Evenstad interesting to investigate.

### 3.2.9 Loss Parameters

Most of the loss parameter settings are kept at default values due to lack of details and information about them. The known loss parameters which are implemented to the model include IAM-losses, which was explained in section 3.2.6, and thermal losses.

On the Sunny Portal site for Evenstad [10], data about module temperature is available. Under the *Thermal parameter* tab, it’s possible to decide that the model shall use measured module temperatures in the simulations.

The result of using module temperature for thermal losses rather than default values for thermal loss factor explained in Section 3.1.3, is a more accurate value for the energy output. This was observed by simulation for the two possible settings, for a clear sky day, and comparing the results.

Ohmic losses were calculated in PVsyst by knowing the cross section and lengths of the wires used. The cross section of the wires connecting the modules in strings is

4 mm<sup>2</sup> [23], and the cross section of the wires connecting the strings to the inverter is 6 mm<sup>2</sup> [50]. Since accurate knowledge about wire lengths was not known, these values were estimated by looking at the array layout. In PVsyst the average lengths of the wires were implemented. It was known that all the wires from the strings to inverter goes through a common hole in the middle of the roof.

The approximations were that the length of string module connections were 35 m for sub-array #1 and 39 m for sub-array #2. For the length of main box to inverter wires the approximations were 35 m for sub-array #1 and 35 m for sub-array #2. This gave a global wiring resistance of 22.8 mOhm for sub array #1, and 24.4 mOhm for sub array #2. These values give ohmic losses of 1.1 %, calculated by PVsyst using Equation 3.3. Compared to the default values which gave losses of 1.4 %, the approximations done can be expected to not give big errors in simulations.

### 3.3 Measured Data for Evenstad

There are five measured quantities available from Evenstad which are used in this thesis. These are:

- AC power at inverter output
- Global irradiance on tilted plane
- Cell temperature
- Wind speed
- Ambient temperature

#### Sunny WebBox

The Sunny WebBox is a communication hub for medium- to large-scale PV plants. It includes system monitoring, remote diagnosis, data storage and visualization, and collects data continuously from the inverters of the system side. The WebBox is able to inform about errors in the system, which can be a valuable feature. By including a GSM modem, the data collected by the WebBox can be transmitted to Sunny Portal. It measures the ac power at inverter output. [51]

#### Sunny Sensorbox

The Sunny Sensorbox is a pyranometer which measures irradiance in W/m<sup>2</sup> as well as module temperature in °C with a thermometer. It is mounted onto the modules at Evenstad, and in combination with a Sunny WebBox and Sunny Portal, the measured data is available for analysis. It is possible to include additional sensors, which is done for Evenstad were a sensor measuring wind speed in m/s is also included. [52]

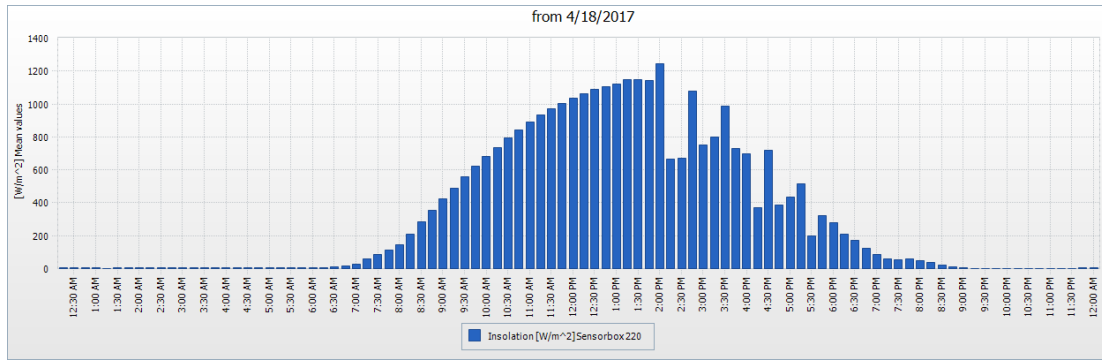
By logging into Sunny Portal, the measured data can be downloaded and analysed. The access to Sunny Portal was provided by Tarald Eng-Øvermo at Statsbygg. Some data is also publicly available at the site [10]. At Sunny Portal daily, monthly and yearly graphs and data sheets are available, from the first day of operation in November 2013 until today. The time unit can be in either in 15 minute, hour, day, month or year unit. The two first are only possible for daily graphs. One big drawback is that yearly graphs are not available in hourly time unit. If this had been the case, collection of data which would be used in simulations in PVsyst, would be simple. This is because simulations are proceeds in hourly steps.

Irradiance in units like kWh/day or  $W/m^2 \cdot day$ , are not a possible choice at Sunny Portal. Only mean, maximum and minimum values are available, and makes yearly graphs with the lowest time unit (days), not useful for simulations in this thesis. This is also the case for module temperature and wind speed, which is then also only available in hourly steps for daily graphs. The only way of collecting meteorological data in hourly units from Sunny Portal is to download one \*.csv file for irradiance and one \*.csv file for module temperature and wind speed. This gives two \*.csv files per day, which makes the downloading of data for a whole year quite time consuming. Because of this simulations of a full year with measured meteo data were not possible in this thesis.

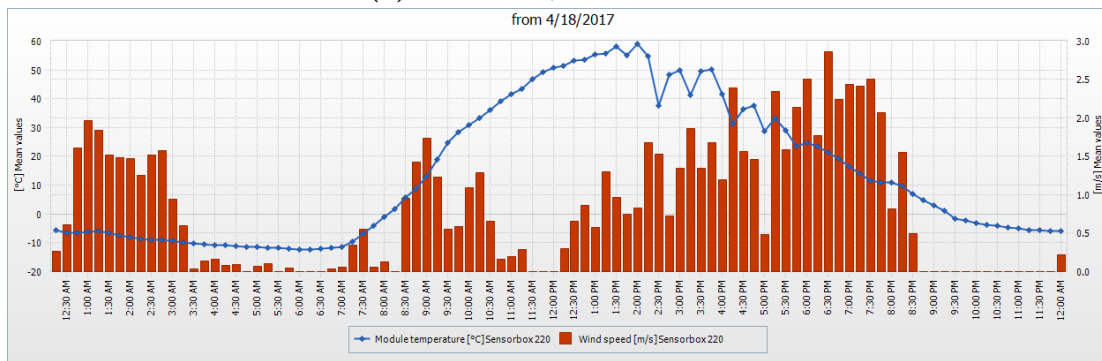
Figure 3.13 shows the meteo data from Sunny Portal for the date 18-04-2017. The data is in this case represented in daily graphs with 15 min time unit for Figures 3.13a and 3.13b, and with hourly time unit for Figures 3.13c and 3.13d. The change of the graphs at Sunny Portal can only by conducted by people with administrative access to Sunny Portal, e.g. Tarald Eng-Øvermo at Statsbygg. Because of this the access of desired graphs can be inconvenient and difficult.

### Other Measurements

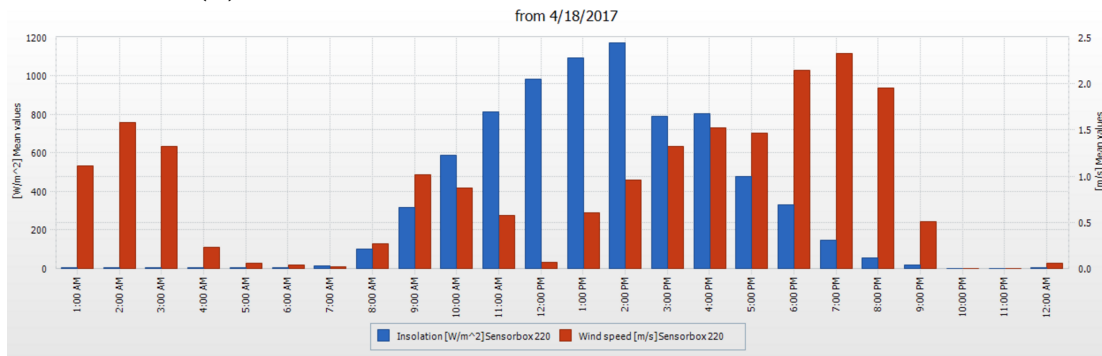
For simulations, two components for imported meteo data is required: irradiance, represented by either horizontal global irradiance or global irradiance on tilted plane, and ambient temperature. All other parameters are not mandatory, but can bring more accurate meteorological conditions to the simulation. The ambient temperature is not measured by the sensorbox, though this is a possible additional feature. Ambient temperature is collected from local weather stations near by. This data is downloaded by using a matlab script provided by IFE.



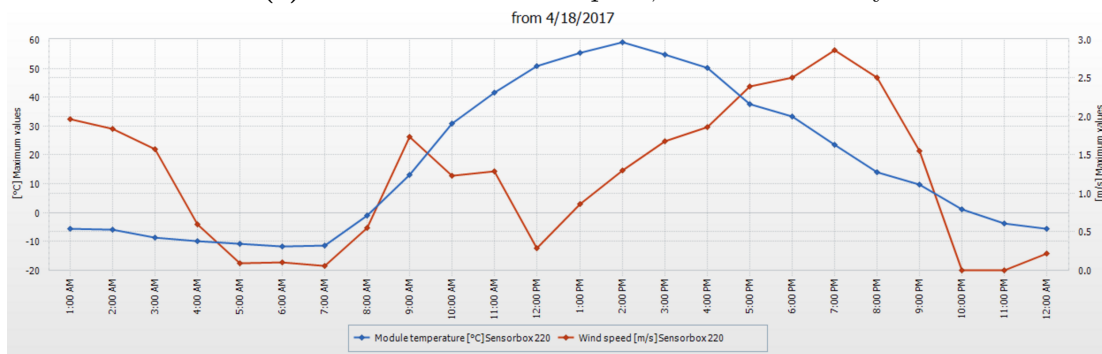
(a) Irradiance, time unit: 15min



(b) Module temperature and wind speed, time unit: 15min



(c) Irradiance and wind speed, time unit: hourly



(d) Module temperature and wind speed, time unit: hourly

**Figure 3.13:** Meteorological conditions at Evenstad for date 18-04-2017 with 15 min time unit [(a) + (b)] and hourly time unit [(c) + (d)]. [10]

## 3.4 Measured Data Management

The system of data measurement, including Sunny Sensorbox and WebBox, can be set up correctly for easily collecting of data. A variety of processing options for data management is provided. The challenge when installing and setting up a system for data monitoring and measurement for a new PV plant, is to be aware of in what form the data shall be collected and stored. Often this is not analysed well enough, and when the system performance is to be studied after some years of operation, collecting of data in the correct structure is at best time consuming, sometimes even impossible. This has been the case for Evenstad.

The ideal case would be if the data of irradiance, module temperature and wind speed is collected in one \*.csv file, in hourly time unit for each year. These are data which may not be representing logical information in graphs, but for simulations this is exactly the data required. Because the irradiance and temperature is varying continuously during the day as well as during the year, data in time steps is necessary for analysis of system performance.

A note for future installation of PV systems, is to set up a monitoring system which collects valuable data in a correct structure. The performance of a PV system varies a lot from location to location, because it is directly dependent on weather conditions on-site. This is why a study of several years of data for operating systems can give many important answer to future installation of systems. For Norway good performance data is mostly lacking.

## 3.5 Importing of Meteorological Data

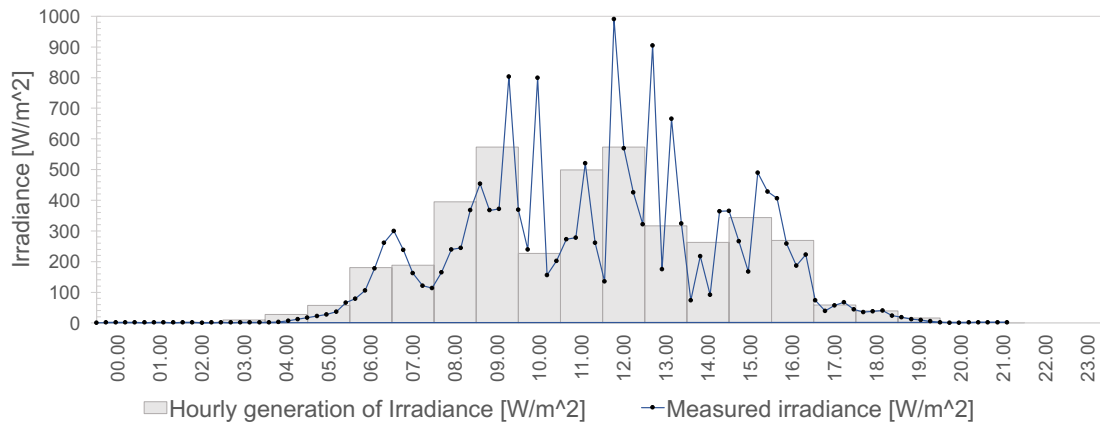
### 3.5.1 Generation of Data File for Importing to PVsyst

A meteo file for the specific time period is prepared as a \*.csv file so that it can be imported to PVsyst as a ASCII-file. Meteo data about irradiance, wind speed and module temperature is collected from the local measurements available on a Sunny Portal [10]. Data about ambient temperature is collected using a matlab-script provided by IFE. This matlab-script downloads meteo data from the local weather station Evenstad (skogskolen), which is located close to the PV system. It measures ambient temperature and wind speed, and was created in 2001. Only ambient temperature data is used.

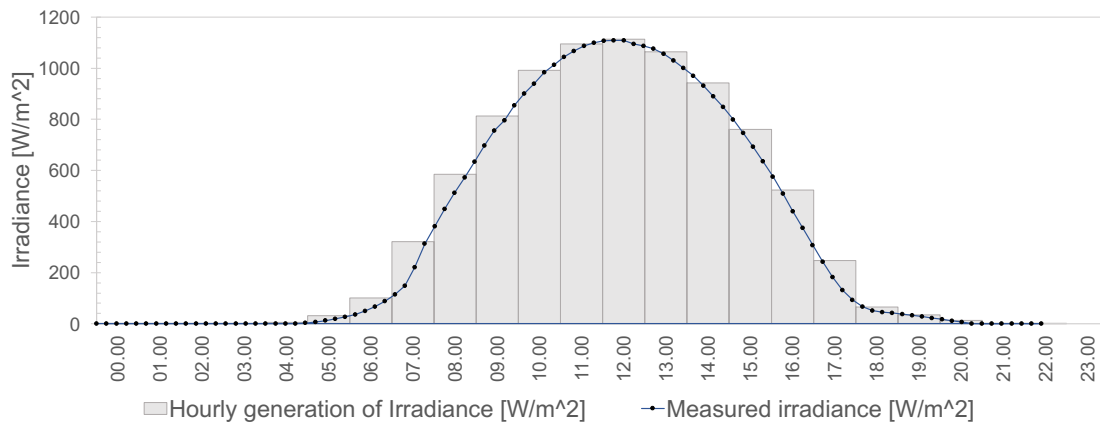
### 3.5.2 Generation of Hourly Values

PVsyst performs simulation in hourly steps. For the meteo data measured in 15 minute steps generation of hourly values have to be performed. The comparison of actual measured points for irradiance (measured every 15 min) and hourly generated values for irradiance is represented in Figure 3.14a and Figure 3.14b.

Figure 3.14a is from the date 14-05-16, which was a cloudy day with varying



(a) The cloudy day 14-05-2016.

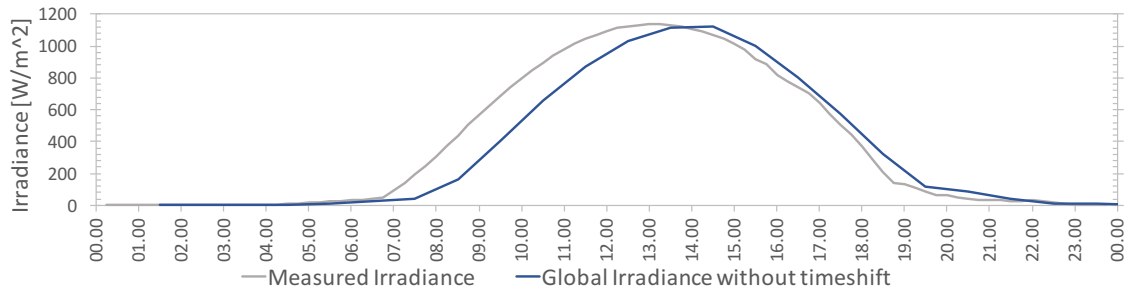


(b) The clear sky day 08-05-2016.

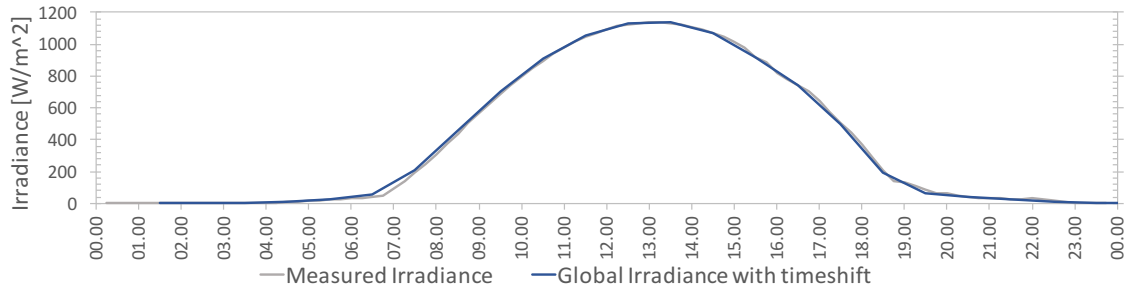
**Figure 3.14:** Instantaneous (measured) values of irradiance (blue line) and hourly values generated by PVsyst.

irradiance from high to low values. The maximum irradiance on that day was  $990 \text{ W/m}^2$ , at time 11:15. The measured values are collected from Sunny Portal [10]. From this Figure it can be observed that the maximum irradiance for the hourly generated values is  $572 \text{ W/m}^2$ , and 40 % lower than the actual maximum irradiance on that day. During a day like this where the irradiance fluctuates frequently, the inverter is constantly under different power loads. The inverter's efficiency is dependent on the instantaneous power input to the device according to Figure 3.11. If the load is smaller, caused by low irradiance at the PV array, the efficiency is lower.

Figure 3.14b is from the date 08-05-16, which was a clear sky day. This Figure shows how the hourly generated values for irradiance is quite well generated compared to the actual irradiance on that day.



(a) Without timeshift.



(b) With 15 min timeshift and summertime.

**Figure 3.15:** Simulated global irradiance compared to measured irradiance for date 14-06-2014.

### 3.5.3 Quality Check of Imported Meteorological Data

When importing meteorological data it is essential to check the quality of the measured data to achieve relevant simulation results, as explained in section 2.1.3. Figure 3.15 represents imported meteo data without any time shift (Figure 3.15a) and imported meteo data with time shift as well as summertime (Figure 3.15b).

Comparisons like this can be done in PVsyst when meteo data is imported under *Check data quality*, and is comparison of time shift of monthly best days with respect to the clear day model. Time shift can either be to the left or to the right and implies that the sun goes up earlier or goes down later than the clear sky model. PVsyst performs simulations starting from the horizontal irradiance. This is because the models used for estimating diffuse irradiance only is available from horizontal plane. The measured irradiance is from the plane of irradiance (POA). Starting from this a retro-transposition is required to get the horizontal global and diffuse irradiances. Time shift may often be the case when starting from POA, and can lead to errors in simulations especially in the morning or evening when the sun is low on the horizon. This will give high erroneous horizontal global irradiance, which will be limited by the clear day model. If a time shift from the clear day model is present, a time shift has to be implemented when the meteo data is imported to PVsyst. For the imported meteo data with time shift, summertime is also implemented, which gives a more exact meteo file import.

The energy output of simulations when using these two meteo files, gives different results. The meteo file which doesn't fit the clear sky model has an energy output of

475.5 kWh, and has according to PVsyst a time shift of 59 minutes compared to the clear sky model. The meteo file which does fit the clear sky model has implemented a 15 minute time shift as well as summertime. This gives a model close to the clear sky model and an energy output of 527.1 kWh, which is very close to the actual energy output of the system on 14-06-2014 which is measured to be 527.64 kWh [10]. When importing the meteo files it is also possible to decide if the values are measured at the beginning or at the end of the interval. When choosing the end of the interval, a 15 min time shift is not necessary.

The conclusion is that when importing the meteo the following settings needs to be implemented:

1. Summertime
2. Data measured at interval end
3. No time shift

## 3.6 Simulation Variants

Simulations of the PV system is carried out in order to check the performance, by comparing anticipated and actual production. At the Sunny Portal site, energy at inverter output (ac energy) is available both for the whole system and for each inverter separately. The comparison will not be satisfactory by using average meteorological data for the location. To get an reasonable comparison, actual measured meteorological parameters is needed. Fortunately, this is available at the Sunny Portal site.

In PVsyst simulations with different variations to the model were implemented to see the discrepancy evolution for the simulation model. The different variations were:

1. Base scenario, with only the mandatory inputs: system, orientation, meteo data and default losses.
2. Optimal tilt angle of the system.
3. Scenario (1) + detailed near shading 3D model.
4. Scenario (2) + horizon.
5. Scenario (3) + module layout.
6. Scenario (4) + modified module (IAM losses).
7. Scenario (5) + modified inverter (Power limit, power ratio).

Scenario one acts as a default model, including the most basic and necessary parameters for a simulation model. Scenario two allows one to quantify the loss caused by compliance to architecture. Scenario 3-7 gives each a more precise model. The effect off implementing more details for the model, can be investigated from these simulation variants.

Other simulations which were carried out:

- Simulations on only one inverter, to investigate the performance of the inverters in the system.



- Daily simulations of selected days, to analyse the accuracy of the model, and compare the simulated results to measured values.
- Monthly simulations.

Real measurements of meteo data were used for daily and monthly simulations. In addition to the simulations performed, the available measurements of the production data for the PV system is studied. Because of the issue addressed in Section 3.3 about downloading meteo data for a full year in hourly steps, yearly simulations with real meteo data were not carried out in this thesis. The simulations performed for a full year use data from Meteonorm which uses a reference year and not real measured meteo data for the site.



# Chapter 4

## Results and Discussion

In this chapter results of simulations and studies conducted in this thesis are presented and discussed. The chapter is divided into four main sections. The first section covers the discrepancy analysis of the simulation model with six different simulation variants. Next section covers the simulations of one inverter and the analysis of the inverter used in the system at Evenstad. The two last section covers daily and monthly simulations, respectively, where the last section consist of simulations using the longest time frame for imported meteorological data and also include study of real annual production data measured on-site.

### 4.1 Discrepancy Analysis of Simulation Model

In PVsyst several parameters and settings can be implemented to achieve an accurate model compared to the real system. To obtain simulation results close to the real measurements, the desire is to have a model which is very similar to the real system with respect to design of the system, loss factors and other parameters. Not all simulation parameters give big impact on the result. By comparing the results before and after implementing selected parameters, the impact and importance of them can be analysed. In many cases information about parameters are lacking, such that the knowledge of the importance of them in simulations can be of great interest. If some settings can be excluded because of their low impact on the output, this can make simulations easier in some cases. This study is done for the model of the system at Evenstad. The results and conclusions can be used for simulations of other systems in different locations in Norway, similar to Evenstad.

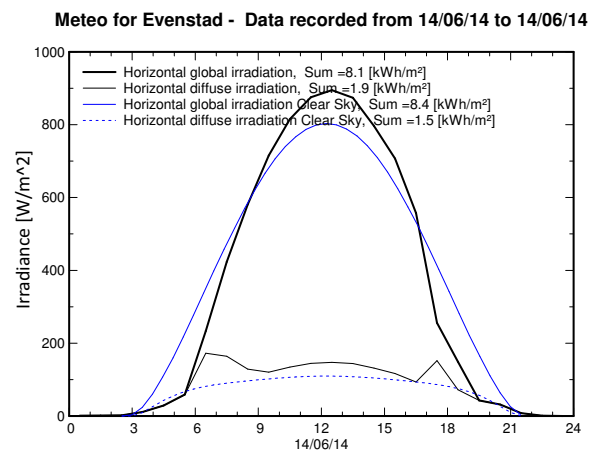
A discrepancy analysis of the different simulation variants listed in Section 3.6, was carried out to see the effect of the numerous simulation settings. The results of interest for these simulations where total yield, performance ratio and specific yield. Each of the following sections contains one parameter added to the model. To see if the result from the simulations improve or not, the results are compared to the previous simulation variant, e.g. the result from simulation of adding horizon line is compared to the result of the previous simulation variant containing base scenario and near shading 3D model. See the list in Section 3.6 for summary of the variants.

The variant listed as number 7 in this list is included in Section 4.2.

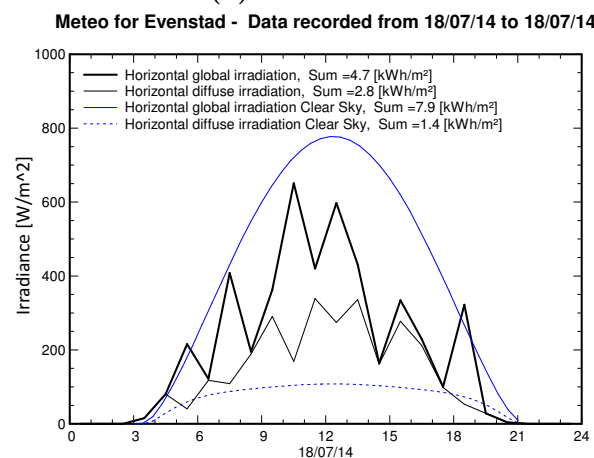
Since meteorological data from the operating years was difficult and time consuming to download, Meteonorm was used as a database for meteo data for simulations over a year. To get simulations with the actual meteo data, some selected dates were used. The availability of the meteorological data is explained in Section 3.3. The dates chosen are one perfectly clear sky day: 14-06-2014, and one day with varying irradiance: 18-07-2014. 2014 as year was chosen to avoid as much degradation of system as possible, as this is the first operating year. The imported irradiance compared to PVsyst's clear sky model is showed in Figure 4.1 for the two dates.

Hence, the three meteo files used in simulations are:

1. 1 year with Meteonorm data
2. Clear sky day: 14-06-2014
3. Cloudy day: 18-07-2014



(a) 14-06-2014



(b) 18-07-2014

**Figure 4.1:** Imported meteorological data for daily simulations.

### 4.1.1 Base Scenario

The base scenario include the settings which were mentioned as mandatory in Section 3.1.2. This include the parameters listed in Table 4.1. Details of the parameters included in the base scenario can be found in Section 3.2.1, 3.2.2 and 3.2.3.

**Table 4.1:** System overview: base scenario.

---

<b>Orientation parameters:</b>	
Field type:	Fixed Tilted Plane
Plane tilt/azimuth =	35° / -10°
<b>Compatibility between System defintions:</b>	
Full system orientation:	tilt/azimuth = 35° / -10°
2 sub-arrays	PNom = 70 kWp, modules area = 455 m <sup>2</sup>
<b>System parameters:</b>	
2 sub-arrays defined	Total 267 modules, and 12 inverters
Sub-array #1:	
PV modules:	12 strings of 11 modules in series, 132 total
Pnom = 255 Wp	Pnom array = 34 kWp, Area = 218 m <sup>2</sup>
Inverters (4.60 kWac)	12 MPPT inputs, Total 28 kW
Sub-array #2:	
PV modules:	12 strings of 12 modules in series, 144 total
Pnom = 255 Wp	Pnom array = 37 kWp, Area = 238 m <sup>2</sup>
Inverters (4.60 kWac)	12 MPPT inputs, Total 28 kW
<b>Shading scene parameters:</b>	
No shading scene defined	

---

### The results

The results of the simulations for a year as well as the dates 14-06-2014 and 18-07-2014 are listed in Table 4.2.

**Table 4.2:** Simulation results: Base scenario.

---

	Year	14-06-2014	18-07-2014
Total yield	61.97 MWh/year	504.1 kWh/day	278.5 kWh/day
Specific yield	880 kWh/kWp	7 kWh/kWp	4 kWh/kWp
PR	0.867	0.775	0.836

---

### 4.1.2 Modified Tilt Angle

The rooftop of Evenstad, where the PV array is mounted, is already a tilted rooftop with an angle of 35°. In this case additional mounting system to achieve another

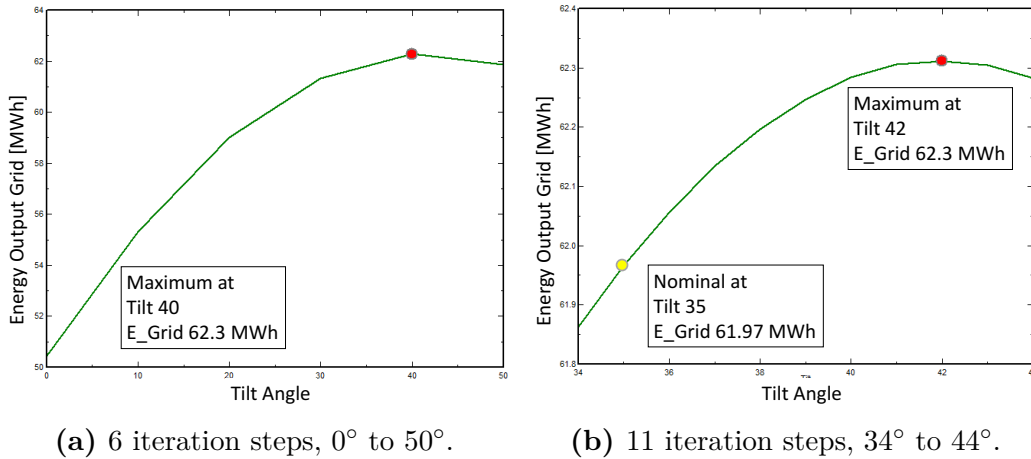


**Figure 4.2:** Optimisation of tilt angle for Evenstad.

tilt angle, which may increase the performance of the array, will add extra expenses. The increased performance has to be good enough to make up for the additional expenses, which may not be the case. A tilt angle of 35° is already a good angle for achieving high performance of the collectors.

Simulations for Evenstad can be done to see the effect of different tilt angles. In PVsyst the optimal tilt angle for the system at the selected location can be found. Under the *Simulation* tab, an optimisation tool can easily find the optimal values for tilt angle and azimuth angle. It performs a set of simulations, where the parameters are systematically varied according to the selected range, with as many iterations as specified. The iterations are then plotted in a graph which shows the optimal value.

This method was used to find the optimal tilt and azimuth angle. The number of iteration steps were first set to 6, with the range in tilt angle from minimum of 0° to maximum of 50°, as seen in Figure 4.3. The nominal tilt angle of the system is 35° as mentioned earlier. Because the iterations may take some time, it is divided into two steps. First for the range in Figure 4.3, then for a smaller range close to the first optimal angle. The results of the two steps are presented in Figure 4.2. The first sets of simulations gave an optimal angle of 40° as seen in Figure 4.2a. This gives an energy output of 62.3 MWh. By narrowing the iteration range down to a minimum of 34° and to a maximum of 44°, optimal tilt angle down to the degree can be found, with number of iterations of 11 steps. This gave an optimal angle of 42°. The energy output with this tilt angle is 62.3 MWh, hence there is no significant energy difference between 40° and 42°.

In Figure 4.2a the yellow circle represents the nominal tilt angle of 35° for the system with an energy output of 61.97 MWh as simulated in the base scenario. The difference in yield between the actual tilt angle of the system and the optimal is 330 kWh/year, which is not much. The additional cost for mounting the modules at a tilt angle of 42°, with the low increase in total yield, does not make it a desired choice. In addition, if the modules are tilted more than the tilt of the roof, the strings of will shade each other more with the set spacing. The area available has no extra space to ensure that this doesn't happen. To keep the tilt at 35° is therefore a good choice.

For the optimal azimuth angle the result was  $0^\circ$  with an Energy output of 61.8 MWh with a tilt angle of  $40^\circ$ . This was the case for tilt angles in the range from  $10^\circ$  to  $50^\circ$ . Only at a tilt angle of  $0^\circ$ , the optimal azimuth angle was not  $0^\circ$ , but  $45^\circ$ . For this the energy output was as low as 50.7 MWh, and does not make for a desired design of the system. PV modules should be orientated to the true south in the northern hemisphere (Azimuth angle =  $0^\circ$ ), which is the obvious conclusion.

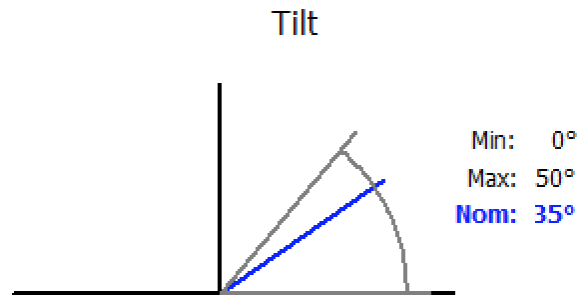


**Figure 4.3:** Tilt angle range for iterations.  
Figure from PVsyst.

### 4.1.3 Detailed Near Shading, 3D Model

To ensure that the near shading 3D model is not too far from reality, comparison of irradiance and production on specific days can be done. The approach is to find a clear day with ideal irradiance, and compare it to the production that day. If the production doesn't match with the irradiance, near objects draw shades on the modules reducing the production.

By doing this for selected days the 3D model can be ensured to be correct. The conclusion of doing this evaluation is that the close objects that may shade the array, do not have great impact on the energy output and do not shade the array that much. This is also the case for simulation with the 3D model, so the model can be concluded to be accurate to reality, with respect to the shading effect.

Figure 4.4 shows the shading factor diagram for Evenstad with the implemented 3D model shown in Figure 3.6. The dashed lines are representing shading losses of different factors (1 %, 5 %, ...). It can be seen in the Figure that the objects which are shading, don't give that big shading effect. Some shading happens in the evening, and is because of the trees west for the array.

When performing simulations with the three meteo data inputs, the results become as listed in Table 4.3. The near shading objects may either have impact on the amount of irradiance hitting the array, or an impact on the electrical performance of the modules due to shading which leads to module mismatching. After including the near shading, either the incident on collector plane or electrical yield change much from the base scenario for all three meteo cases. This builds up under the conclusion that the near shading objects have small shading effect on the array. The simulated near shading losses is set to 0.1 %, which is a small contribution to the total losses. It has to be noted that this can be very different depending on the PV system. In some cases near shading objects may have large impact on the yield. Study of the near shading scene may therefore be an important aspect.

The system efficiency and system losses is changing insignificantly with near shading implemented, because it affects the irradiance which is hitting the modules,

rather than the performance of the system.

**Table 4.3:** Simulation results: near shading.

	Year	14-06-2014	18-07-2014
Total yield	61.86 MWh/year	504.0 kWh/day	278.3 kWh/day
Specific yield	879 kWh/kWp	7 kWh/kWp	4 kWh/kWp
PR	0.857	0.774	0.835

#### 4.1.4 Horizon

The results of the simulations with horizon profile is listed in Table 4.4. When included in simulations this horizon profile gives an annual far shading loss of 1.8 %. For the daily simulations the loss becomes 0.7 % for 14-06-2014 and 1.6 % for 18-07-2014. The far shading losses have biggest effect when the sun rises in the morning and sets in the evening. For date 18-07-2014 a bigger part of the total irradiance is in the morning and evening, compared to 14-06-2014, where a large part of the total irradiance is in the middle of the day. This can be seen in Figures 4.1. This may be the reason for more far shading loss at 18-07-2014 than for 14-06-2014.

The daily simulations are for months June and July where the sun rises earlier and sets later compared to the winter months. So for days during winter the far shading losses is expected to be bigger. The yearly simulation both include winter

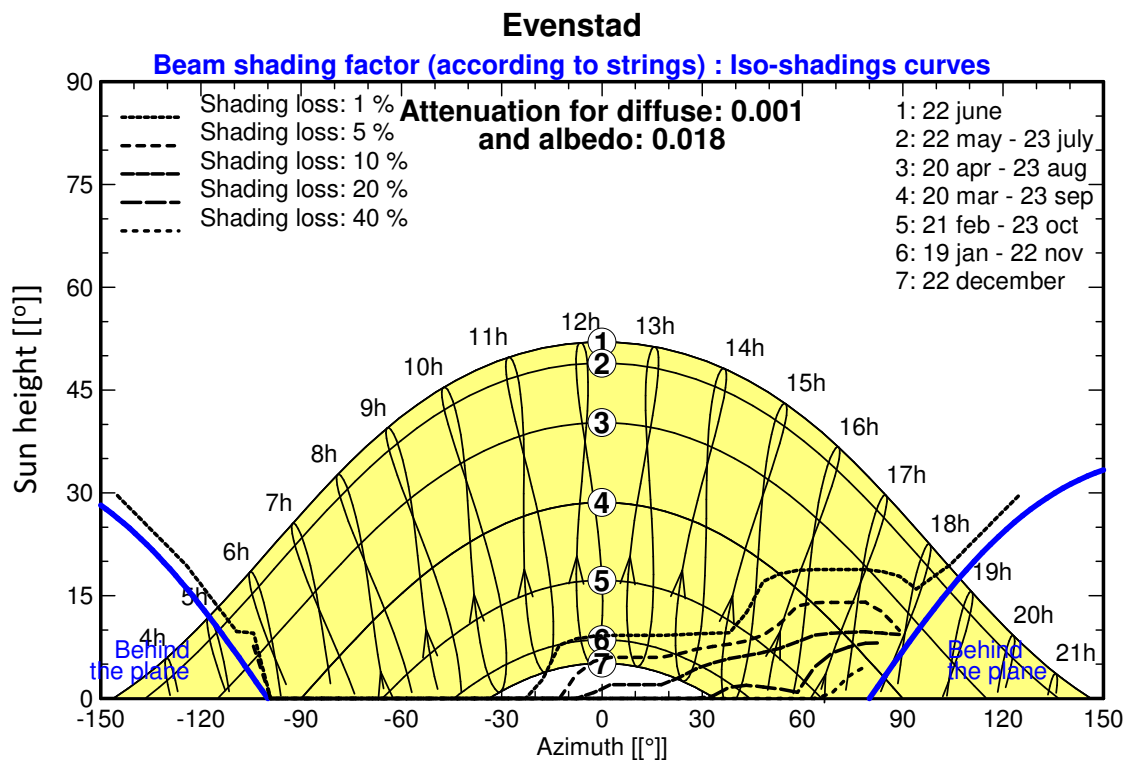


**Figure 4.4:** Shading factor diagram of Evenstad.



**Table 4.4:** Simulation results: Far shading.

	Year	14-06-2014	18-07-2014
Total yield	60.79 MWh/year	501.7 kWh/day	273.9 kWh/day
Specific yield	864 kWh/kWp	7 kWh/kWp	4 kWh/kWp
PR	0.851	0.771	0.822

and summer days, days with clear sky and days with varying irradiance, and all other cases of weather conditions. This is why the annual shading loss due to far shading is high.

The importance of horizon profile in the simulation model of course depends on the location. In some cases the horizon will lead to late rise of the sun and early sunset. In this cases the far shading losses is likely to have a greater impact on the energy production. The measuring of horizon can be done in several ways. There exist tools which may be used, as mentioned in Section 3.2.5. If these are not available, Google Earth together with horizon drawing tools like Meteonorm software can be used. This was the method selected for obtaining the horizon line in this thesis. A study of how the horizon looks like, and what big of an impact it has on the sunrise and sunset, is important for the evaluation of the horizon profile importance to the simulation model.

### 4.1.5 Module Layout

Module layout includes the placement of the 24 strings, in the simulation model. This enables the analysing of electrical effects of partial shading from near objects. The electrical calculation can be performed for each string in the system and the effect can be visualised in a IV-curve.

In Figure 4.6 this visualisation is shown for string #1 in the PV system at Evenstad for 21st December at 16:15, where an electrical effect due to shading from near objects (trees in this case), can be seen. Figure 4.5 shows the shading situation at this point which leads to the resulting IV curve in Figure 4.6. The string in the Figure with red frame represents string #1, consisting of 11 modules. 6 of the modules are fully shaded, one module is approximately 3/4 shaded, one module is approximately 2/3 shaded and one module is approximately 1/3 shaded. The last two modules are not shaded at all. The resulting irradiance loss due to the shading is 57.2 %, and the loss due to the electrical effect is 29.5 % at time time. The total loss results in a power output reduction from a potential of 154 W to 21 W.

The loss due to the electrical effect is a result of the fact that each cell in the modules is not assigned with it's own bypass diode. If this where to be the case, each cell would not be affected by the other shaded cells. The modules used in the PV array at Evenstad are delivered by the manufacturer with three bypass diodes for the 60 cells in the module. Hence, each bypass diode covers 20 cells. Because of this an electrical loss appears due to the partial shading of some modules. The current in the strings of cells where some cells are partially shaded, is limited by the most shaded cells, as explained in Section 2.2.3.

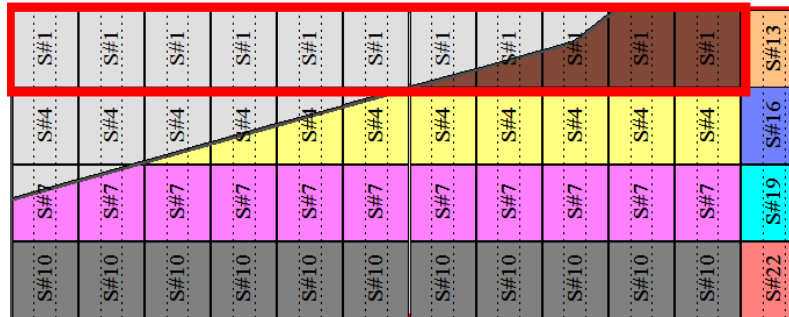


Figure 4.5: Shading of string #1 for 21st December at 16:15.

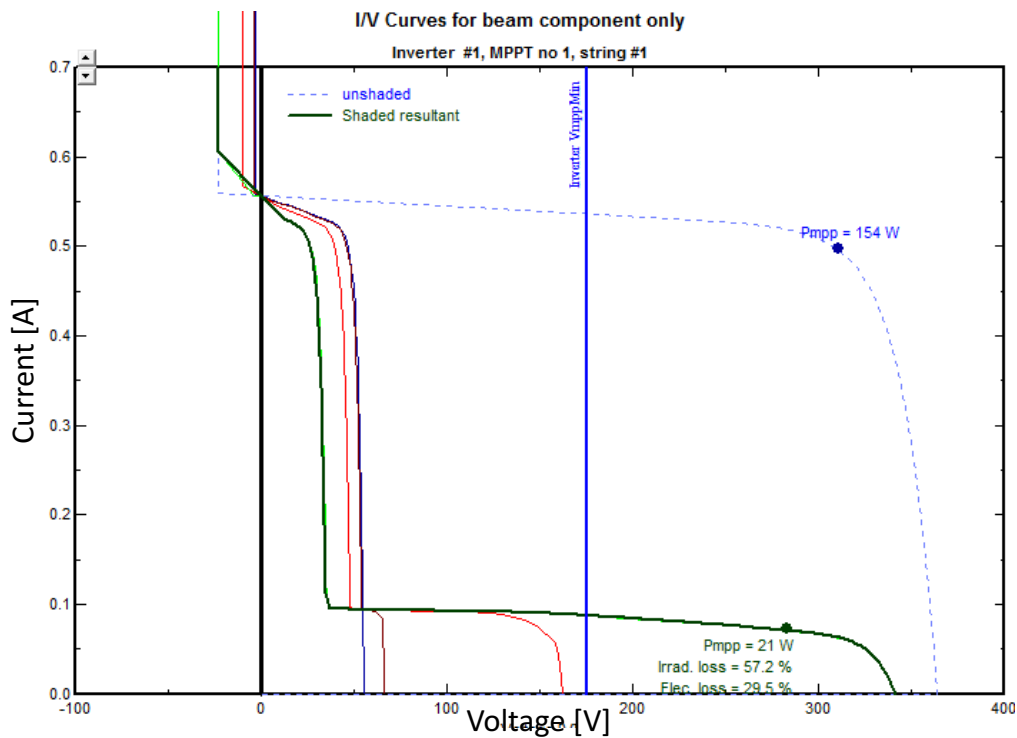


Figure 4.6: IV curve of shaded string #1 for PV system at Evenstad on 21st December at 16:15.

The results of simulations with module layout implemented, are not listed in a table and presented here. This is because the simulations give an annual loss of 0.0 % due to electrical loss detailed module calculations. This means that the result is the same as presented for far shading in Table 4.4.

The electrical shading effect is not an important factor in the simulation model for Evenstad to achieve accurate simulations. For models where there are larger near shading losses, this parameter would have greater impact on the results.

#### 4.1.6 Modified Module (IAM Losses)

Simulations can be performed to see if the match between simulated and measured system performance actually improves after implementing the IAM values presented

in Section 3.2.6. Two simulations are compared, containing first the REC 255PE module included in the PVsyst database, and then the modified REC 255PE module with new IAM values. The values for the first simulation are the same as the result listed in Table 4.4 for far shading. The results from the simulation with the modified module is listed in Table 4.5. When comparing the yield for the three cases of meteo data, an improvement can be seen. The effect of modifying the IAM losses of the module gives a reduction to the IAM factor from 4.2 % to 2 %, which gives a better performance of the system. This increase in performance shows the importance of implementing the correct values for the modules.

**Table 4.5:** Simulation results: IAM losses.

	Year	14-06-2014	18-07-2014
Total yield	61.48 MWh/year	505.3 kWh/day	277.5 kWh/day
Specific yield	873 kWh/kWp	7 kWh/kWp	4 kWh/kWp
PR	0.860	0.776	0.832

## 4.2 Inverter Simulations

In this section simulations of only one inverter in the system is carried out. First a discrepancy analysis of the simulation model with respect to inverter settings including power ratio and power output limit, is presented. Then study of the expected power output per inverter, performance of each inverter in the system and degradation of the inverters is presented and discussed.

### 4.2.1 Power Ratio

In PVsyst the nominal power ratio for the two sub-arrays assumed as a default, that the inverter with 2 MPPT inputs behaves as two identical inverters of half the power. This means that each MPPT has a nominal power of half the total nominal power of the inverter. For the Sunny Boy 5000 TL inverter used for the system at Evenstad, each MPPT gets a nominal power of 2.5 kW. This is usually not the case for real inverters, where the total output nominal power can be shared between the MPPT inputs. The nominal power ratio describes how the inverter is sized according to the PV array. Usually inverter providers recommend a power ratio of 1.0 to 1.1.

When the power ratio is equally distributed, hence 50 % of nominal power,  $P_{nom}$ , per sub-array, the power ratios becomes 1.22 for the sub-array with 11 modules in series and 1.33 for the sub-array with 12 modules in series. 1.33 is not a high power ratio according to PVsyst [15]. To get acceptable values, the power ratio is selected to be equal for the two sub-arrays, and becomes 1.27 and 1.28 for the 11 module strings and 12 module strings, respectively. This gives a specified  $P_{nom}$  for the two MPPT of 2.2 kW and 2.4 kW, which together makes up the full  $P_{nom}$  for the inverter of 2.6 kW. When implementing this change, the result for energy output for the day 14-06-2014 for one inverter increased form 42.33 kWh to 42.41 kWh. This is a small

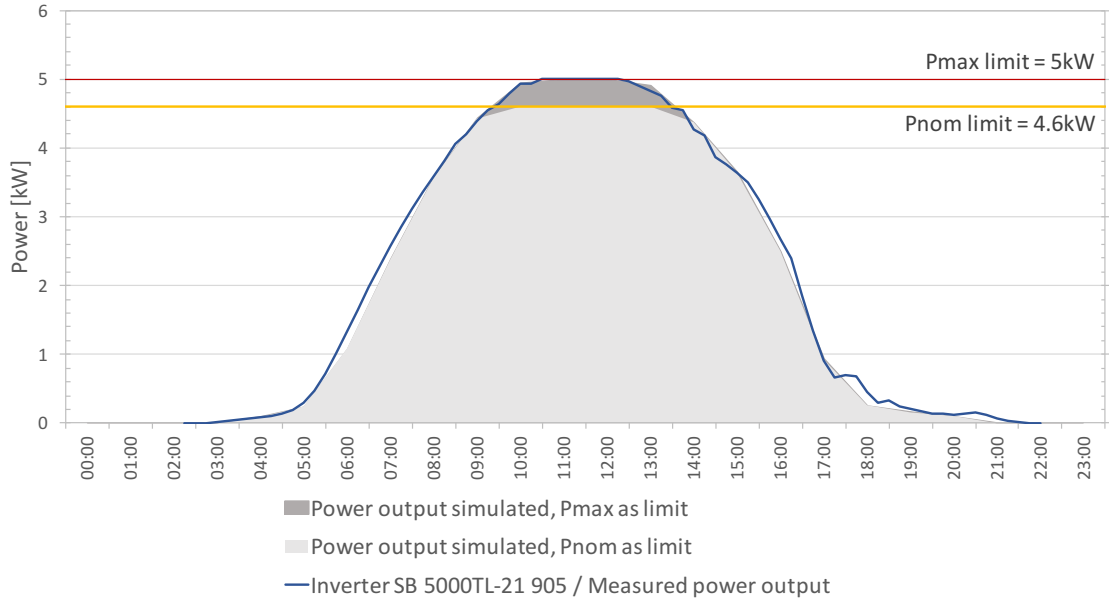


**Figure 4.7:** Inverter power output comparison of real measured power output (blue line) and simulated power output (grey area) for an the inverter with best performance (Inverter SB 5000TL-21 905) on the day 14-06-2014. The red line represents inverter power output limit of 4.6 kW, and the yellow line represents inverter power output limit of 5 kW

increase, but an increase is desired because the simulated energy output is lower than the actual energy output of one inverter of of 44.50 kWh, and makes the model more accurate with respect to the actual values.

## 4.2.2 Power Output Limit

Figure 4.7 represent two simulations done for one inverter consisting of one 12 module string and one 11 module string connected, for date 14-06-2014. This represents one out of 12 inverters in the system at Evenstad. The two simulations include:

1. Inverter nominal power as power output limit:  $P_{out,limit} = 4.6kW$
2. Inverter maximum power as power output limit:  $P_{out,limit} = 5kW$

In PVsyst limitation of the power is the default behaviour at power overcharging, which is when the available PV power at MPP will lead to overcoming the nominal output power,  $P_{nom}$ , of the inverter. This means that when the PV array is producing more power than  $P_{nom}$ , the power output is limited to  $P_{nom}$ . If the system undertakes overpower ( $P_{out} > P_{nom}$ ), power can dissipate and the system can experience overheating which can lead to supplementary aging of the system.

$P_{nom}$  power limit is the case for the first simulation where the resulting power output is illustrated by the light grey field in Figure 4.7. The yellow line indicated

power limitation of  $P_{nom} = 4.6\text{kW}$ , and it can easily be seen that the power output is limited to this value. The result of the simulation is that the power output for the inverter becomes 42.41 kWh. For the best operating inverter (SB 5000TL-21 905) the power output is 44.50 kWh [10]. This is a reduction of 2.38 kWh per inverter. If this were to be the case for all the 12 inverters in the system, it will lead to a total of 28.56 kWh for clear sky days. This limitation will not be a problem for days where the irradiance never reaches a level where the PV array production leads to a power output over  $P_{nom}$ . This is, however, the case for date 14-06-2014 which is a clear sky day.

In Figure 4.7 comparison of actual operation of the inverter in the system at Evenstad with best performance (highest power output) on the day of 14-06-2014, and the operation of the inverter in simulation 1. The finding is that the real operation of the inverters in the system is that they actually don't limit the operation. The power output of the real inverters is limited to the maximum power output of the inverter which is 5 kW. To achieve simulations which correspond to actual operation of the inverters, settings must be changed in PVsyst so that the power output is not limited to  $P_{nom}$ , but to the maximum power output of the inverter. This is done in the second simulation. Under *Grid inverter definition* in PVsyst settings for the allowance of overpower, can be selected. This gives a power output illustrated by the dark grey area in Figure 4.7. By comparing this area to the actual power output of the best operating inverter, it can be seen how the output is quite accurate. The simulated energy output becomes 44.0 kWh with  $P_{max}$  as power limit of the inverter.

### 4.2.3 Temperature Dependence

To see the effect of high module and ambient temperatures on the power output, simulations of two clear sky days with different temperatures throughout the day were performed. The module temperature during the two days selected are displayed in Figure 4.10. The simulated energy output is listed in Table 4.6.

By comparing the loss diagrams for these two simulations, it can be seen that the loss due to temperature is higher for 14-06-2014 than for 08-05-2016. These diagrams can be seen in Figure 4.8 for 14-06-2014 and Figure 4.9 for 08-05-2016.

**Table 4.6:** Results for simulated and measured values for date 14-06-2014 and 08-05-2016 for one inverter.

	14-06-2014		08-05-2016	
	Simulated	Measured	Simulated	Measured
Yield per inverter [kWh]	44.00	44.50	41.56	40.69
Performance ratio (PR)	0.803	0.906	0.827	0.853
Specific yield [kWh/kWp]	7	7.497	7	6.927

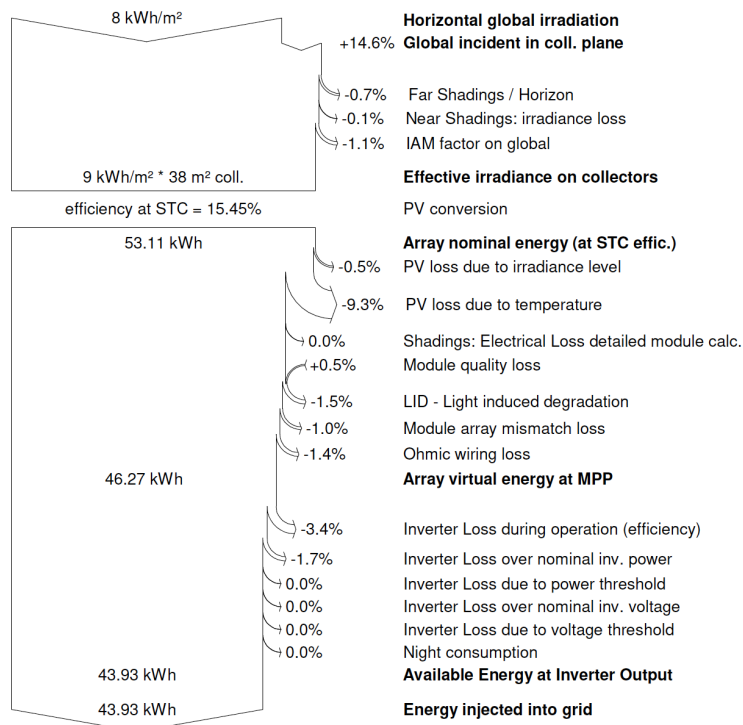


Figure 4.8: Loss diagram for date 14-06-2014 for simulations of one inverter.

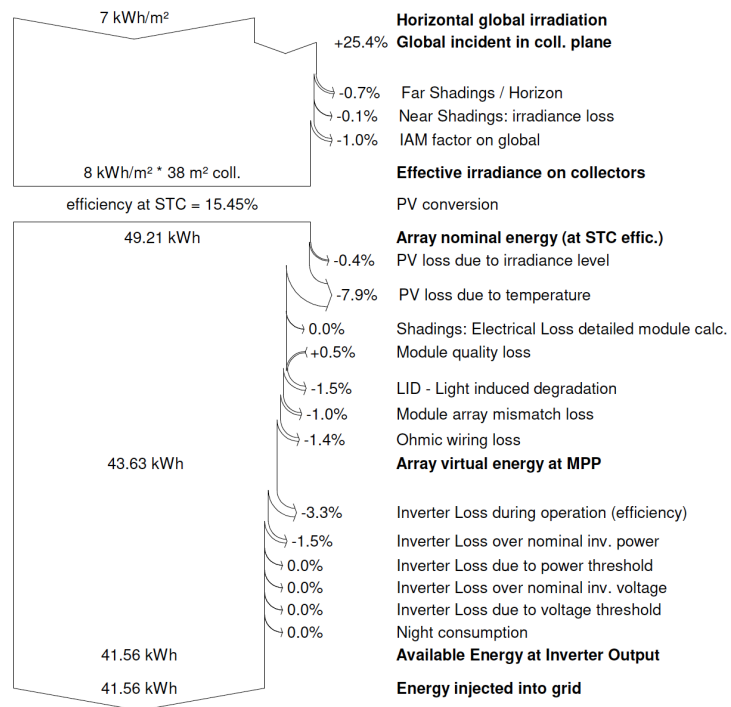
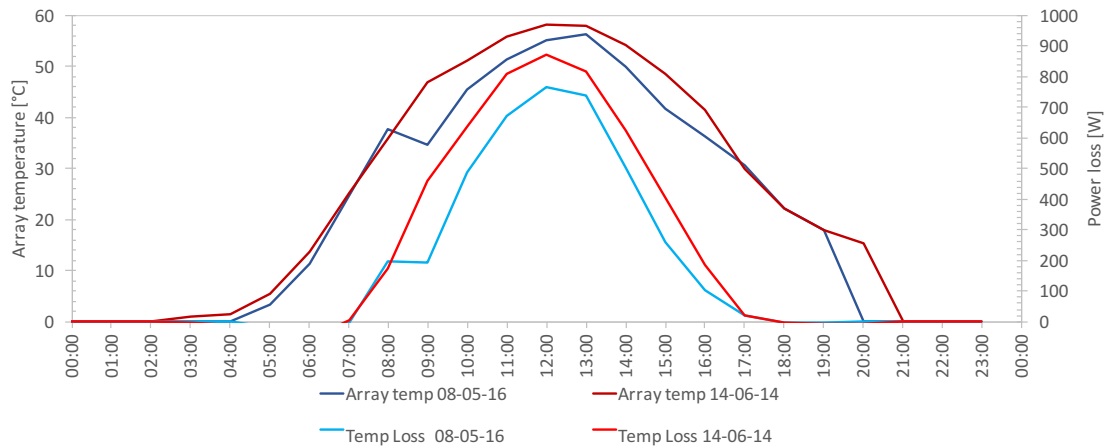


Figure 4.9: Loss diagram for date 08-05-2016 for simulations of one inverter.



**Figure 4.10:** Power loss due to module temperature for 14-06-2014 (dark red) and 08-05-2016 (dark blue), and array temperature for 14-06-2014 (light red) and 08-05-2016 (light blue).

The loss due to temperature is also illustrated in Figure 4.10, where it can be seen how the power loss is increasing with increasing array temperature. This Figure also illustrates well how more power is lost due to temperature for 14-06-2014 than for 08-05-2016. It is known that the power output of modules are reduced with increasing temperature according to Equation 2.12, and in the Figure it can easily be seen how the power loss due to temperature is dependent on array temperature.

Comparison of simulated and measured energy output for the two days, reveal that the the simulated result for 08-05-2016 is higher then the measured. This is not the case for 14-06-2014. The measured values are listed in Table 4.6. It may be that PVsyst simulation overestimate the power loss calculation due to temperature, since the simulated total energy output of the inverter is lower than the actual production for 14-06-2014 and that this is not the case for 08-05-2016 where the temperature is lower.

The final report for these two simulations are included in Appendix B.

#### 4.2.4 Performance of Each Inverter in the System

When looking at measured energy production on a clear sky day for the 12 inverters in the system, it can be seen that every inverter is not performing as the simulated inverter in section 4.2.2. Figure 4.11 shows power output for each inverter in the time slot 09:00 - 17:00 for date 14-06-2014. It can be observed that the inverters are operating differently, especially at mid day where the irradiance and production is highest.

Another interesting observation is that the inverter which has the best performance at clear sky days like in Figure 4.11 doesn't necessarily produce in total over a year the most energy.

As discussed in Section 4.2.2 the power output is limited to the maximum power

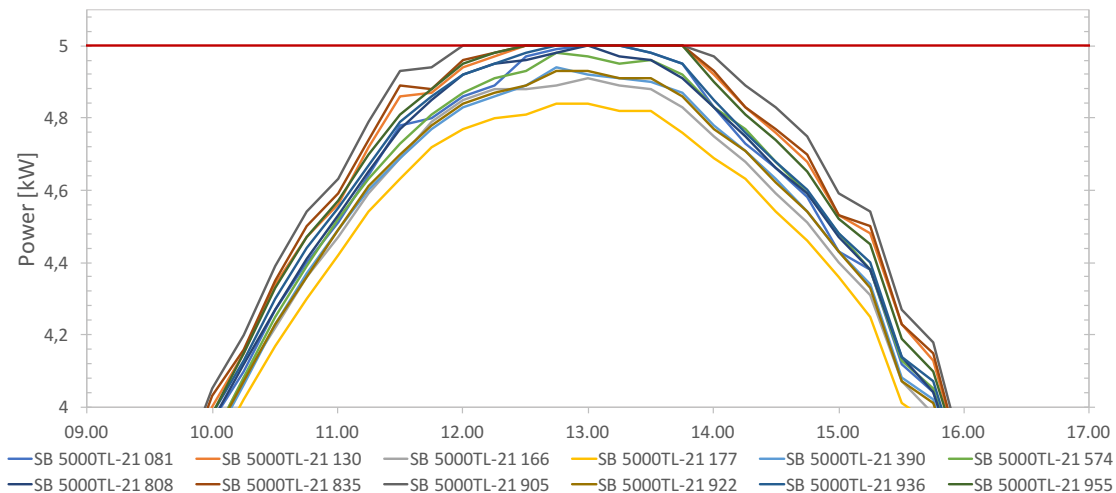


**Figure 4.11:** Power output of all inverters for time period 09:00-17:00 on date 14-06-2014.

of the inverter which is 5 kW. This can be seen in Figure 4.11, and will lead to loss of the excess power produced by the PV array over 5 kW. Which is the case for the inverters with highest power output. The question is: Why isn't the system equipped with inverters with higher power rating?

The sizing of the system is a sum of several parameters, which (sometimes) drag in different directions. First of all, the Sunny Boy 5000TL-21 was the biggest 1-phase inverter available at time of installation [50]. Seeing that the grid is a IT-system, 1-phase inverters has to be used. When designing a PV system, the customers needs have to be considered. The goal for this system was not to collect "the last kW of power", but to cover the desired and expected kWh of electricity generation and to achieve over 55 MWh/year. A key factor was to reach the goal in a cost efficient way. A bigger inverter would be more expensive, and since the days with power production potential over 5 kW per inverter are not many, a larger inverter would probably not be cost efficient. When the system was designed and simulated in advance, the radiation distribution of solar intensity on-site was not known. To keep the design of the system simple was also a factor which was considered to reduce the risk of faults and errors. This included the string configurations, simple mounting and similar components (one type of inverter and one type of module).

All these factors together gave the proposed system consisting of 12 inverters with 5 kW power sizing and 276 PV modules. When looking at the simulations and measured data for produced power for each inverter and the system, two possible conclusions can be made. Either the inverters are undersized with respect to the number of modules, or too many modules was installed.

The Sunny Boy 5000 TL inverter chosen is a suitable inverter with regards to the demands given. It was at times of installation the largest one-phase inverter available. It has fast, simple and professional attachment, which reduces risk for mounting faults. It is well suited for demanding and partially shaded PV systems. A conclusion can be made that more panels was installed than what was needed to



meet the customers demand to energy production.

### 4.2.5 Degradation of Inverters

The system has been operating for 3 years. This gives valuable, long term data to see how the performance of the system is developing along the years. When comparing the annual energy output over the three years for all the inverters, it can be seen that the output is decreasing for each year, for almost all the 12 inverters. Figure 4.12 shows this comparison. Only inverter SB 5000TL-21 081 and SB 5000TL-21 385 are not decreasing in annual energy output between year 2015 and 2016. The trend may imply that the degradation of the system happens almost linearly.

This can be checked by simulation for the three years using measured meteo data. If the system is really degrading like what is presented in the Figure, the simulated yield for each inverter should be higher than the measured yield when compared. Since meteo data for years 2014, 2015 and 2016 were time consuming and difficult to assemble, only data from 1st of January 2017 to 23rd of May 2017 were collected, and used for simulation of one inverter. The simulated yield for the period is 2007 kWh. This is compared to the measured yield for the same period for each inverter, and is displayed in Figure 4.13. None of the inverters for the period in 2017 produced as much energy as what was simulated. This may indicate the linear degradation.

However, the soiling losses is not taken into account for the simulations, and is most likely the reason for the difference in yield for measured and simulated. When only comparing for the month of May where there were no soiling losses due to snow (see Section 4.4 for evaluation of snow days in the period for 2017), two observations is made. First, the simulated and measured yield are almost the same. The difference is calculated to be 2.5 %. The additional difference may be because of other soiling loss, e.g. dust and pollen. There is a lot of pollen in the month of May in Norway [53].

Hence, the degradation it may seem like is happening for the inverters in Figure 4.12, may be disproved by the evaluation of May 2017.

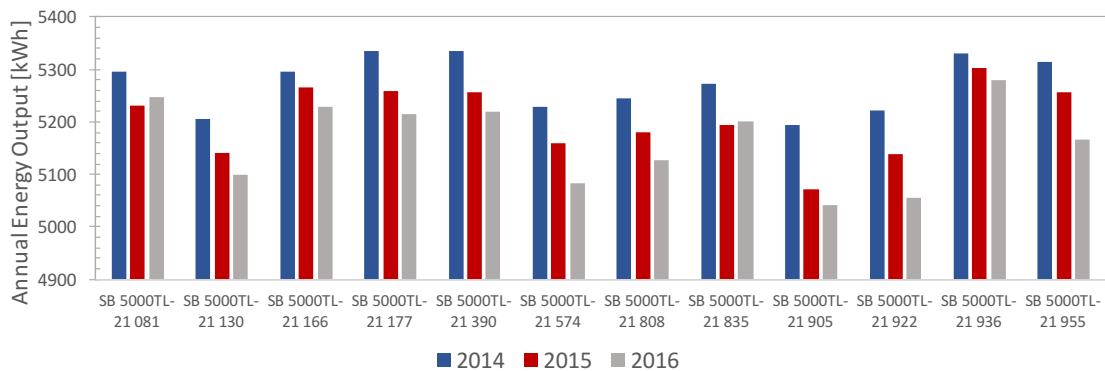


**Figure 4.12:** Annual energy output per inverter for 2014, 2015 and 2016.

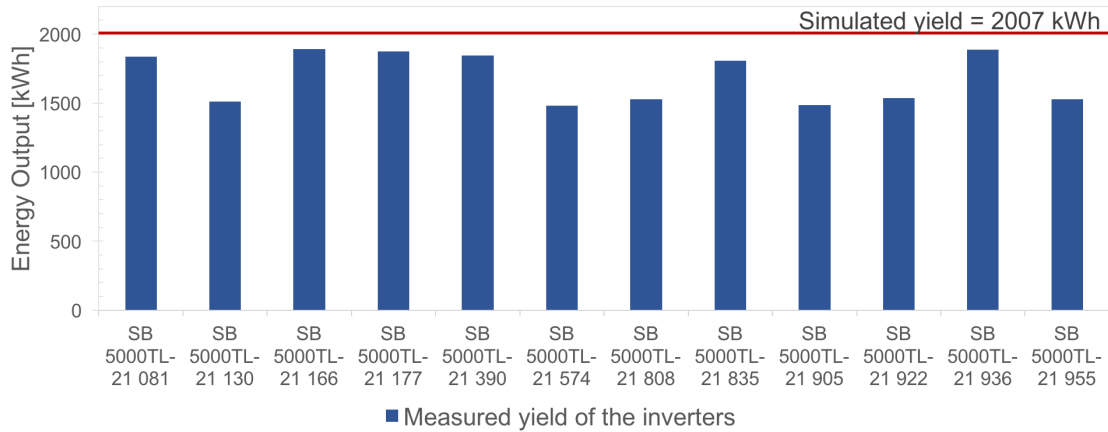


**Figure 4.13:** Yield per inverter for period 1st of January 2017 to 23rd of May 2017, compared to simulated yield for the same period.

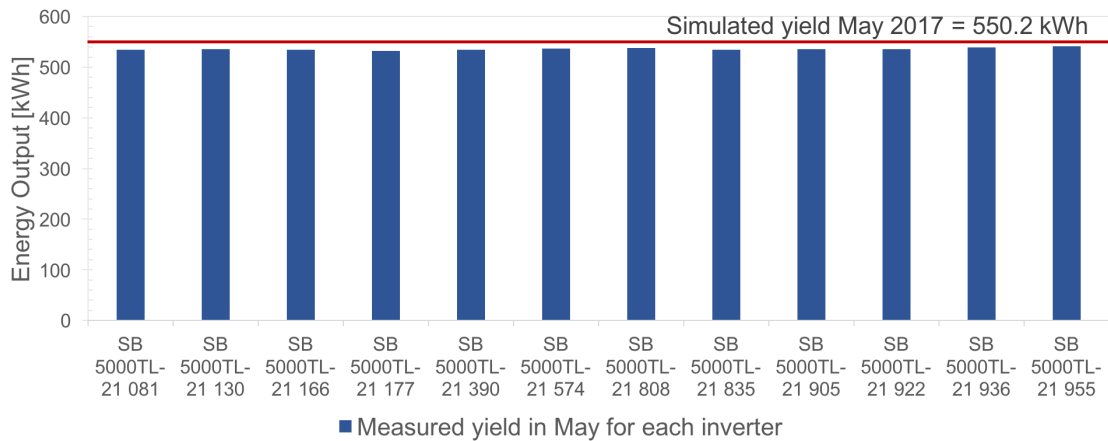


**Figure 4.14:** Yield per inverter for May 2017, compared to simulated yield for the same period.

## 4.2.6 Soiling Loss Due to Snow

When looking at Figures 4.12 and 4.13, it may seem like the inverters are performing somewhat different. A hypothesis is that this difference is due to soiling loss in the form of snow. This can be further investigating by looking at selected months where there is hard shading because of snow. The measured yield for February 2017 is represented in Figure 4.15. In this Figure and when investigating the data for the measured yield, the inverters are divided into two groups. 6 of the inverters are producing some energy in February, and 6 of the inverters are producing nothing. What is causing this difference?

When looking at the system in reality, there are two snow guards. One placed under the strings connected to inverters 4, 5 and 6, and one placed under the strings 10, 11 and 12 (See Figure 3.5). These snow guards prevent the snow from falling off the roof in order to ensure safety. A drawback for performance of the system is that they also prevent the snow to slide off the modules, making them produce no energy. These snow guard is most likely one of the reasons for the difference in yield

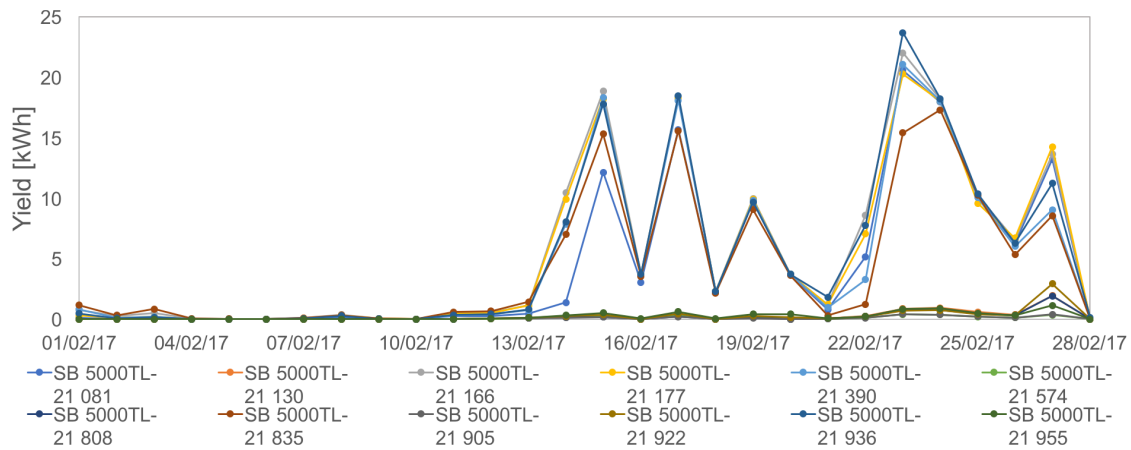


**Figure 4.15:** Measured yield of each inverter in February 2017.

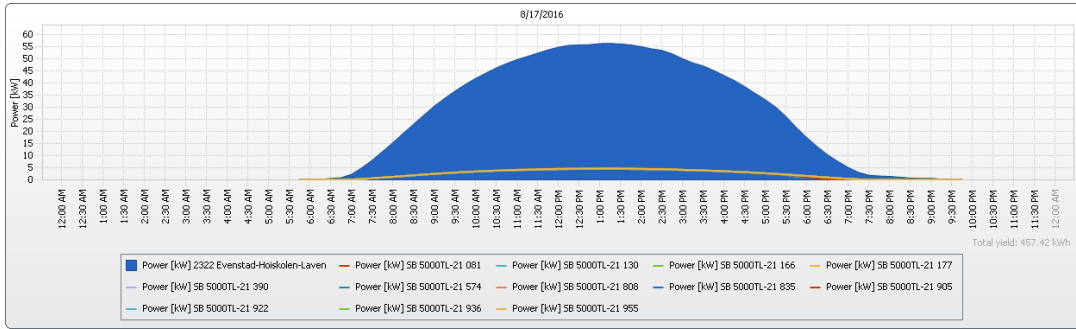
between the inverters. Which inverters according to the labelling of the inverters as shown in Figure 4.15, belongs to the different strings as labelled in Figure 3.5 is not known. The labelling is correspond to the names given to the inverters on-site. A note for future installation of PV systems is to have labelling for measured data which provide necessary information for analysing of the system.

### 4.3 Daily Simulations

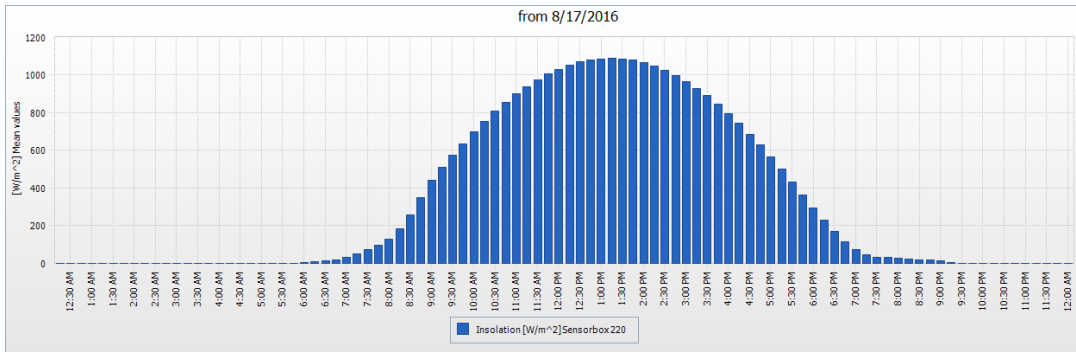
In this section simulations that was performed of some specific days will be presented. The selected days and the related results are listed in Table 4.7.

At Sunny Portal production data for each day of operation for the PV system is available. This data can be used to check if the model constructed in PVsyst is an adequate model. This is done by comparing the production anticipated by simulations in PVsyst to the actual production on a specific day. This comparison can answer questions on the comparison of anticipated and actual production for a hole year.

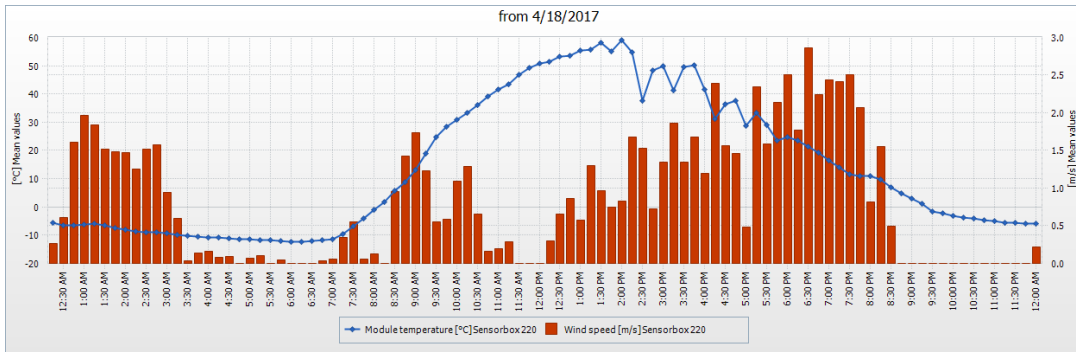
The dates selected for the simulations listed in Table 4.7 are clear sky day with no clouds. Figure 4.16b shows how the irradiance is on a clear sky day, measured four times every hour (every 15th minute). This Figure is for date 17-08-2016. Figure 4.16c shows how the module temperature is increasing with increasing ambient temperature shown in Figure 4.16d. The performance ratio was on this day measured to be 0.999 [10]. The simulated performance ratio for this day was 0.806. Hence, the simulated performance ratio was lower than the actual. The specific yield was measured to be 6.499 kWh/kWp and simulated to be 7 kWh/kWp. In Figure 4.16a the total power production on this day as well as the production through each inverter can be seen.



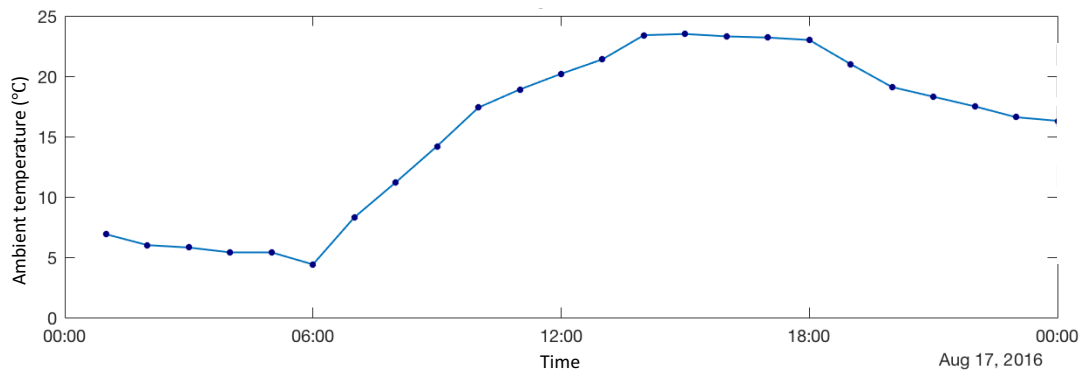
(a) Total power production and power through each 12 inverters. [10]



(b) Irradiance [10].



(c) Module temperature and wind speed [10].



(d) Ambient temperature collected from Matlab script.

**Figure 4.16:** Meteorological conditions and power production at Evenstad for date 17-08-2016.

**Table 4.7:** Results for daily simulations and actual values for selected dates.

	AC Energy Production		Discrepancy from yield	
	Actual	Simulated	$\Delta$ kWh	%
17-08-2016	457.42 kWh	459.9 kWh	13.14 kWh	2.86%
08-05-2016	487.56 kWh	500.7 kWh	13.14 kWh	2.26 %
03-05-2015	513.45 kWh	510.1 kWh	-3.35 kWh	-0.60 %
28-06-2015	519.09 kWh	532.8 kWh	13.71 kWh	2.57 %
14-06-2014	527.64 kWh	528.8 kWh	1.16 kWh	0.22 %

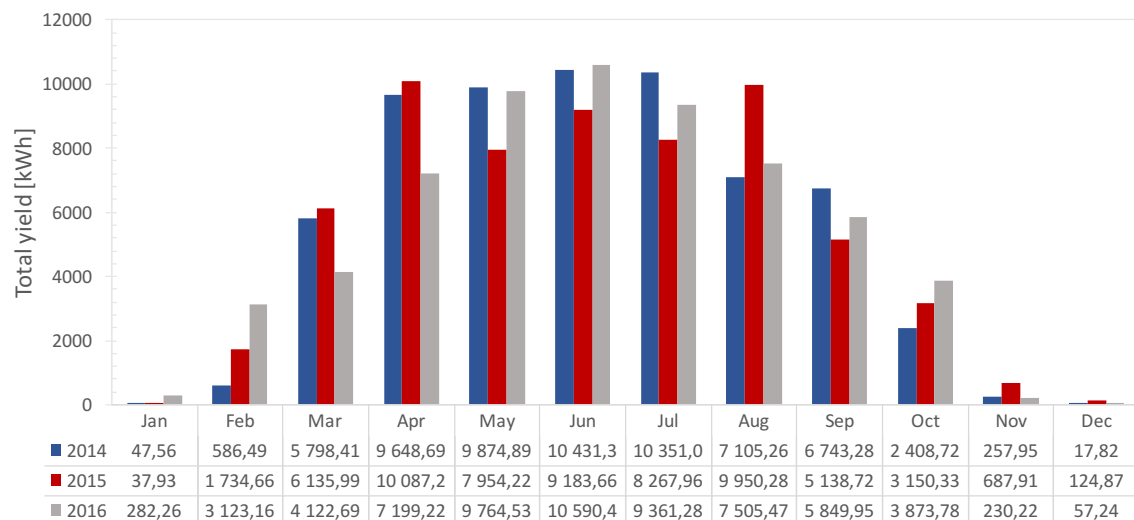
## 4.4 Analysis of Annual Yield and Monthly Simulations

In Section 4.1 and 4.2, simulations for different settings for the simulation model were performed. The daily simulations in previous section gave result with quite accurate power output compared to the actual power output. In this section study of annual yield and performance of the whole system over a year will be presented. In addition, monthly simulations for 2017 will be carried out.

Figure 4.17 shows the total yield for each months for the years 2014, 2015 and 2016. These are the three years where the system have been operating for a full year. The total yield for each year, is listed in Table 4.8.

**Table 4.8:** Total yield for years 2014, 2015 and 2016

Year	Total yield [kWh]	Yearly reduction [kWh]	Yearly reduction [%]
2014	63 271	<i>First operating year</i>	
2015	62 453	817.77	1.292 %
2016	61 960	493.46	0.790 %

**Figure 4.17:** Total yield for each month for years 2014, 2015 and 2016.

Two observations can be made from looking at Figure 4.17 and Table 4.8. First observation, by looking at the Table, is that the total yield for the three years of operation is decreasing for each year. This brings up the question if this is due to degradation of the system or if it is only a case of difference in amount of irradiance and weather conditions. If degradation of the system continues for the following years with same trend as anticipated from looking at the annual yield, expected output for the coming years can be anticipated. A positive observation is that it doesn't seem like the yield is decreasing as much each year, and that the degradation happens exponentially. If this is the case, the yield will stabilise and one can expect equal yield for each year.

The second observation, by looking at the Figure, is that the yield for each month is varying for the different years. This shows that the yield is dependent on meteorological conditions and the difference in amount of irradiance. Hence, the decreasing annual yield is most likely due to difference in weather conditions and amount of irradiance for each year, and not because of degradation of the system. The exponential reduction which it seems to be, can be a coincidence.

There are two methods to check these two observations. One is to collect data for more years of operation and observe if the decrease in yield continuous in the given trend. This though, requires time and can not be used as a method in this thesis. The other method is to do simulations with the measured meteorological data and compare simulated yield to actual yield for a given time period. Because irradiance, module temperature and ambient temperature is measured on-site, accurate simulations can be made. The accuracy of the model was confirmed from the daily simulations presented in previous sections.

Meteorological data for a whole year are available in daily graphs at Sunny Portal. However, a problem is that the downloading of this data, as explained earlier, is quite time consuming. This makes the simulation as mentioned above difficult. Because of this, simulations for 2014, 2015 and 2016 is not carried out in this thesis. However, data for the months January, February, March, April and May until 23rd of May for 2017, was downloaded. With this data simulated monthly yield can be compared to measured monthly yield, and the observations can be checked to some extent. The report of the simulation of 2017 is included in Appendix B.1.

The result from the simulation compared to measured yield is displayed in Figure 4.18. The values and the difference between simulated and measured values are listed in Table 4.9. There is a difference for all the months except May, where the simulated is almost the exact same as the measured. A reasonable explanation for at least the winter months January, February and March, is soiling losses from snow. This may also be the case for April, which can be verified by checking the amount of snow for this month.

The history of snow depth in Norway can be found at the site [Senorge.no](http://Senorge.no) [54]. A so called snow map is provided, where the snow depth at certain days can be displayed. Snow can slide off modules or melt due to heating of the modules or radiation from the sun. This is especially the case for April where the solar radiance is stronger and days are longer. So to see if soiling due to snow is the reason for the yield difference, amount of new snow (nysnø) have to be checked. These are

**Table 4.9:** Results for daily simulations and actual values for selected dates.

Month	Jan.	Feb.	Mar.	Apr.	May
Measured yield [ <i>kWh</i> ]	251	2530	6794	8025	6454
Simulated yield [ <i>kWh</i> ]	51	853	5701	7180	6432
Difference [%]	80 %	66 %	16 %	11 %	0.3 %

days were the snow is most likely to cover the modules. By investigating the map for April at Senorge.no, there was at least nine days with snow which may cover large amount of the array. Though it is not normal with snow in April, even in cold Norway, 2017 was an exception. Snow as late as 25th of April was observed. The days with snow in April 2017, is consistent with the days within April where there is a difference in measured and simulated yield. Measured yield compared to simulated yield for April is shown in Figure 4.19. The days with snow are marked in red, and a difference in measured and simulated yield can be seen for each of these nine days.

The degradation of the system, discussed earlier, does not appear to be the case when comparing the measured and simulated yield for May 2017. This is the fourth year of operation, and the system is producing almost the same energy as expected

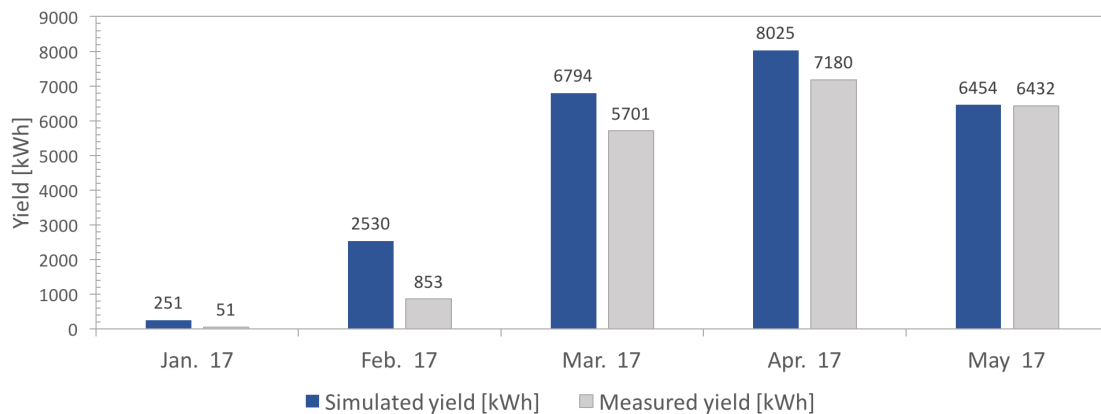


**Figure 4.18:** Monthly comparison of simulated and measured yield for 2017.

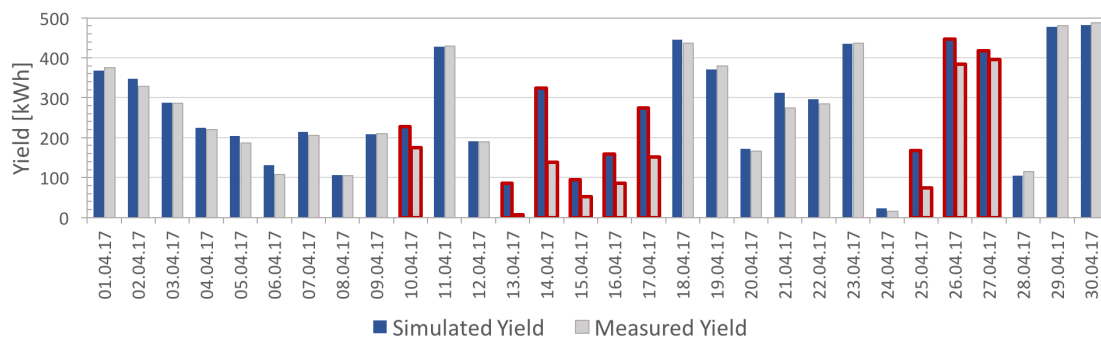


**Figure 4.19:** Days with snow in April (marked in red). These are the days with difference in measured vs. simulated yield.

by simulations. The performance of the system does not seem to degrade. It is desired to test this theory for other months as well, to ensure that this is true. This is not carried out in this thesis because of the lack of available data, as explained earlier.



# Chapter 5

## Conclusion

### Discrepancy analysis of the simulation model

The goal of the discrepancy analysis of the simulation model was to gain knowledge about the effect of implementing the different simulation parameters. In PVsyst a quite accurate model of the PV system can be designed. In some cases the effect of implementing certain parameters in the model can be insignificant. An analysis of parameters of importance to the result of the simulation should be made for each project.

For the PV system at Evenstad this analysis was performed by simulating different variants of the model. Three different variants of meteorological data were used: one year of data from the Meteonorm database, one day of real meteo measurements from a clear sky day, and one day of real meteo measurements from a cloudy day. First a base scenario was implemented, which acts as a default model including the mandatory inputs of a PVsyst model. Next an analysis of the optimal tilt angle for the system at Evenstad was performed. This study resulted in an optimal tilt angle of  $42^\circ$ , with respect to the annual yield. The annual yield with this tilt angle was 62.3 MWh which is higher than the base scenario yield of 61.97 MWh. Even though the optimal tilt angle will give higher yield, it's concluded that this is not a desired tilt angle of the system at Evenstad, because the rooftop where the array is mounted already has an angle of  $35^\circ$ . Additional mounting systems required for obtaining optimal tilt angle will give increased expenses and only a small scale increase in annual yield. Since cost efficiency plays a major role in the decision on whether to install a PV system, optimal tilt angle is not a desired choice for this system.

For the subsequent simulation variants additional parameters and settings were implemented to the model. They provide a more realistic model compared of the real system at Evenstad. First a detailed near shading 3D model was constructed. This included all near objects to the PV array which may cause shading on the modules. The effect of near shading object may have major impact on the power production of the total array, due to the electrical effect caused by partial shading. The result of the analysis was that the objects observed near the array did not cause considerable losses in the yield of the system. Next the horizon line (far shading) was implemented. The loss effect due to the horizon varied with the time frame of

the meteorological data. The shading losses became 1.8 % for a yearly simulation, 0.7 % for the clear day and 1.6 % for the shaded day. The reason for the difference in shading loss is because of the variation in the amount of irradiance in the morning and evening with respect to the total irradiance. For the yearly simulation and the cloudy day, a larger part of the irradiance is lost due to shading by the horizon in the morning and evening.

In the simulation variant where the module layout is implemented, the electrical effect of partial shading from the near shading objects can be analysed. The shading case for 21st of December at 16.15, gave an irradiance loss of 57 %, and an additional electrical loss of 29.5 %. This electrical loss is due to the fact that not each cell in every module has a bypass diode. The modules are delivered by the manufacturer with three bypass diodes, which each covers 20 cells of the module. Hence, some cells which are not fully shaded, or not shaded at all, still produce less than their potential. This is because the current through them is limited by the current in the most shaded cell.

The manufacturer of the modules used at Evenstad, REC, provides data related to the cell loss due to reflection on the PV cell surface [48]. Values for the IAM losses according to REC data were implemented to the simulation model to see the effect on the performance and energy output. The result was an annual reduction in the IAM losses of 2.2 %.

### **Inverter simulations**

In the simulations done for one inverter in the system at Evenstad, two settings in PVsyst were found to be important to implement correctly with respect to the real operation of the inverters. These settings were the power ratio and the power output limit. The resulting energy output of the simulations was compared to the actual energy output of one inverter to find what settings gave the most realistic model. The power ratio should be equally distributed for the two sub-arrays, such that the power ratio is at acceptable values according to PVsyst.

As a default in PVsyst, the power limit of the inverter is set to the nominal power of the inverter. When analysing the energy output measurement of the inverters at Evenstad, this does not seem to be the operating condition of the inverters in reality. The inverters produce power up to the maximum limit of the inverter at 5 kW. Hence, the setting in the simulation model of the inverter power limit should be set to  $P_{max}$ . When implementing these settings the simulated energy output of one inverter becomes 44.0 kWh, which is 0.5 kWh lower than the measured output of 44.5 kWh.

Results of simulations with meteorological data from two different clear sky days with difference in measured module temperature, revealed the dependence on temperature for power output. It also revealed that PVsyst simulations may overestimate the power loss calculation due to high module temperatures.

## System performance

Is the PV system at Evenstad performing as expected, or is there a degradation in the system which will continue to decrease the system performance for the coming years of operation? Several simulations and investigations that were carried out in this thesis can give some answers to this question.

First, by looking at the measured yield for each year for the whole system and for each inverter, it may look like there is a small degradation of the system performance. A well carried out investigation of the degradation is difficult without meteo data from all the years of operation. The data from 2017 which were made available gives some indications. When comparing the simulated yield using the measured meteo data from 2017 in the simulations, to the measured yield for each inverter for the same period, it may look like there is a degradation of the system. None of the inverters are performing as well as the simulation indicates. But it is concluded that this is because of soiling losses as a consequence of snow in the months January, February, March and April. May didn't have any snow, and were used to further investigate the degradation of the system. When comparing the measured yield to the simulated yield for each inverter as well as the whole system, the difference was found as low as 0.3 % for the period 1st to 23rd of May. This indicates that the system is still performing well, almost exactly as anticipated, and the decrease in annual yield from 2014 to 2016, is most likely because of weather conditions and not because of significant degradation of the system performance.

When investigating the performance of the inverters, some conclusions about the design of the system at Evenstad were made. The reasons for choosing the selected Sunny Boy inverter was because it was the biggest 1-phase inverter available in Norway at time of installation. The goal when designing the system was not to collect "the last kW of power", but to produce over 55 MWh/year, and the goal was to be reached in a cost efficient way. These factors gave the proposal of a system of 276 modules and 12 inverters of power rating 5 kWp. The analysis carried out in this thesis revealed that the system may consist of too many modules than what is needed to meet the customers demand of a yield of 55 MWh/year. Because of the composition of the number of modules and the inverter of the selected size, power is lost when the strings connected to the inverter produce more than 5 kW. The inverter is undersized with regards to the maximum power that can be produced by the modules.



# Chapter 6

## Further Work

This thesis should be considered as a preliminary analysis of the PV system at Evenstad. The assessment of system performance carried out in this thesis can be considered as a supplement to the insight to PV system operation in Norway. Further and more detailed analysis of this system will give more information about the performance and also general information about PV system performance in Norway.

As a first note to further investigation of performance of the system at Evenstad, additional simulations using measured meteorological data should be performed. Measured meteo data for all years of operation in hourly time steps should be downloaded and imported to PVsyst. Other simulation software packages can also be used if preferred, but PVsyst is shown in this thesis to give accurate simulation results when compared to real measured data. The simulation results should be compared to measured production data to further analyse the system performance. A study of the system after more years of operation can be of great value. The system at Evenstad was one of the first large PV power plants installed in Norway, and the biggest one when installed in 2013 [55]. As the downloading of meteo data were considered as quite time consuming, this is acknowledged as the biggest limitation to this thesis. For further study this should be looked into. Adequate values for system loss due to soiling loss from snow can also be found with several years of comparisons.

With regards to the economics an analysis of the system design can be of interest. Can a different selection of inverters, modules or other components in the system give lower installation cost? Since a conclusion was made that the system was installed with too many modules in order to meet the customer's condition of at least 55 MWh of annual production, a different design proposal with fewer modules would give additional information about PV system design. An economic evaluation of additional mounting to obtain optimal tilt angle would also be of interest. This can give information about the additional cost of obtaining the higher yield when having an optimal tilt angle for the system.

A more detailed collection of data about the system implemented in the simulation model can be done for further development of the simulation model of the real system. This would include horizon measurement and gathering of information

about near shading objects on-site. The data about horizon line and dimension and placement of near shading objects implemented in the model established in this thesis were collected by the use of Google Earth and drawing tools like Meteonorm software. They are only estimations and can not be considered as accurate values. Information about which strings are connected to the different inverters shown in measured production data can enable further study of the performance of each inverter.

Study of the customer energy demand and how the PV system are fulfilling this, can also be of interest. Load data can be imported to PVsyst and compared to the PV production. In hourly time steps, power demand throughout the day can be compared to the power production of the PV system.

# Bibliography

- [1] J. L. Sawin (Lead Author), “Renewables 2016 - global status report,” vol. ISBN 978-3-9818107-0-7, 2016. Read more at: <http://www.ren21.net/status-of-renewables/global-status-report/>.
- [2] D. Babovic, R. Andersen, and F. Larsen, “Utnytt solenergien.” [www.tek17.no/utnytt-solenergien/](http://www.tek17.no/utnytt-solenergien/). Accessed: 2017-02-16.
- [3] D. Nugent and B. K. Sovacool, “Assessing the lifecycle greenhouse gas emissions from solar pv and wind energy: A critical meta-survey,” *Energy Policy*, vol. 65, pp. 229–244, 2014.
- [4] D. Spilde, “Elektrisitetsbruk i norge mot 2030.” [www.nve.no/energibruk-og-effektivisering/energibruk-i-norge/elektrisitetsbruk-i-norge-mot-2030/](http://www.nve.no/energibruk-og-effektivisering/energibruk-i-norge/elektrisitetsbruk-i-norge-mot-2030/), June 2016. Norges vassdrags- og energidierktorat, Accessed: 2017-02-14.
- [5] IEA - International Energy Agency, “Trends 2016 in photovoltaic application,” *Report IEA PVPS T1-30:2016*, vol. 21st, 2016.
- [6] SSB, “Electricity 2015.” [www.ssb.no/energi-og-industri/statistikker/elektrisitet/aar](http://www.ssb.no/energi-og-industri/statistikker/elektrisitet/aar). Published: 2016-11-30, Accessed: 2017-02-28.
- [7] Norsk solenergiforening, “Om Solenergi - Statistikk.” <http://solenergi.no/statistikk/>. Accessed: 2017-02-14.
- [8] Accenture and WWF (World Wide Fund for Nature), “Solkraft i norge – fremtidige muligheter for verdiskaping,” 2016.
- [9] D. C. Jordan and S. R. Kurtz, “Photovoltaic degradation rates—an analytical review,” *Progress in photovoltaics: Research and Applications*, vol. 21, no. 1, pp. 12–29, 2013.
- [10] Sunny Portal, “PV System profile for 2322 Evenstad-Hoiskolen-Laven.” [www.sunnyportal.com/Templates/PublicPageOverview.aspx?page=998f37a6-50bd-4d84-837e-183c9336c88b&plant=225ab166-58fb-4816-8fa0-9e34e7377b3d&splang=en-US#](http://www.sunnyportal.com/Templates/PublicPageOverview.aspx?page=998f37a6-50bd-4d84-837e-183c9336c88b&plant=225ab166-58fb-4816-8fa0-9e34e7377b3d&splang=en-US#). Accessed: 2017-04-19.
- [11] T. B. Åsheim, “Grid connected photovoltaic systems with smartgrid functionality,” *Norwegian University of Science and Technology (NTNU)*,

- Desember 2016. Department of Electric Power Engineering, Project work, Supervisor: Prof. Lars Norum.
- [12] G. M. Masters, *Renewable and efficient electric power systems*. John Wiley & Sons, 2nd ed., 2013.
- [13] C. Honsberg and S. Bowden, “Pv education.” <http://pveducation.org/>. Accessed: 2017-03-02, Chapter 2.4 - Air mass.
- [14] J. Kleissl, *Solar energy forecasting and resource assessment*. Academic Press, 2013.
- [15] PV Syst, “PV Syst help [Online].” <http://files.pvsyst.com/help/>. Accessed: 2017-04-18.
- [16] Norsk solenergiforening, “Solinnstrålingen i Norge.” <http://solenergi.no/om-solenergi/solinnstraling/>. Accessed: 2017-05-27.
- [17] K. vindteknikk, “Resource mapping of solar energy an overview of available data in norway,” 2013.
- [18] R. A. Messenger and J. Ventre, *Photovoltaic Systems Engineering*. Hoboken: CRC Press, 3rd ed., 2010.
- [19] K. Mertens, *Photovoltaics: Fundamentals, Technology and Practice*. Wiley, 2014.
- [20] MathWorks, “Pv array.” <https://se.mathworks.com/help/physmod/sps/powersys/ref/pvarray.html>. Accessed: 2016-11-20.
- [21] J. L. Crozier, “Characterization of cell mismatch in photovoltaic modules using electroluminescence and associated electro-optic techniques,” Master’s thesis, Nelson Mandela Metropolitan University, Faculty of Science, January 2012. Supervisor: Prof E.E. van Dyk.
- [22] The MathWorks, Inc., “Example: Partial shading of a pv module.” <https://se.mathworks.com/help/physmod/sps/examples/partial-shading-of-a-pv-module.html?searchHighlight=partial%20shading>. Accessed: 2016-11-19.
- [23] Solar Electric Supply, Inc., “Rec solar rec255pe-(us) blk solar panel - specifications.” <https://www.solarelectricsupply.com/rec-solar-rec255pe-blk-solar-panels>. Accessed: 2017-05-05.
- [24] REC Solar ASA, “Degradation in rec panels ensuring long-lasting high performance of rec panels,” *NE-11-05-05 Rev.A*, September 2014.
- [25] G. Publishing, “Solar angle calculator.” *The Solar Electricity Handbook*, <http://solarelectricityhandbook.com/solar-angle-calculator.html>. Accessed: 2017-05-26.



- [26] V. Sharma and S. Chandel, "Performance and degradation analysis for long term reliability of solar photovoltaic systems: a review," *Renewable and Sustainable Energy Reviews*, vol. 27, pp. 753–767, 2013.
- [27] P. Suresh and J. Thomas, "Performance analysis of stand-alone pv systems under non-uniform operating conditions using pvsyst," vol. 1, pp. 19–25, 2014. Advanced Research in Electrical and Electronic Engineering.
- [28] SMA Solar Technology AG, "PV Inverters - Basic Facts for Planning PV Systems." [www.sma.de/en/partners/knowledgebase/pv-inverters-basic-facts-for-planning-pv-systems.html](http://www.sma.de/en/partners/knowledgebase/pv-inverters-basic-facts-for-planning-pv-systems.html), June 2010. Accessed: 2017-03-09.
- [29] Northern Arizona Wind and Sun, "Inverter basics and selecting the right model." [www.solar-electric.com/inverter-basics-selection.html](http://www.solar-electric.com/inverter-basics-selection.html). Accessed: 2017-03-13.
- [30] S. Z. M. Noor, A. M. Omar, N. N. Mahzan, and I. R. Ibrahim, "A review of single-phase single stage inverter topologies for photovoltaic system," *2013 IEEE 4th Control and System Graduate Research Colloquium*, August 2013.
- [31] Everything about solar energy, "Differences between self-commutated and line-commutated inverters." <http://energyprofessionalsymposium.com/?p=9899>. Posted: August 2010, Accessed: 2016-11-04.
- [32] J. C. Sivertsen and P. Søyland, "Design and installation of a grid-connected pv system," Master's thesis, University of Agder, Faculty of Engineering and Science, Department of Engineering Sciences, June 2014. Supervisor: Georgi Hristov Yordanov.
- [33] M. Calais, J. Myrzik, T. Spooner, and V. G. Agelidis, "Inverters for single-phase grid connected photovoltaic systems-an overview," *PESC Record - IEEE Annual Power Electronics Specialists Conference*, vol. 4, pp. 1995–2000, 2002.
- [34] S. B. Kjaer, J. K. Pedersen, and F. Blaabjerg, "A review of single-phase grid-connected inverters for photovoltaic modules," *IEEE Transactions on Industry Applications*, vol. 41, September/October 2005.
- [35] J. Myrzik and M. Calais, "String and module integrated inverters for single-phase grid connected photovoltaic systems - a review," *2003 IEEE Bologna Power Tech Conference Proceedings*, vol. 2, p. 8, 2003.
- [36] R. Hudson, M. Behnke, R. West, S. Gonzalez, and J. Ginn, "Design considerations for three-phase grid connected photovoltaic inverters," *Conference Record of the Twenty-Ninth IEEE Photovoltaic Specialists Conference, 2002*, pp. 1396–1401, 2002.
- [37] K. Aikawa, H. Magoroku, H. Miyata, H. Ikarashi, and C. Nagaoka, "Highly efficient power conditioning system for large photovoltaic generation systems," *Hitachi Review*, vol. 62(1), 2013.

- [38] IEEE 929-2000, “929-2000, IEEE Recommended Practice for Utility Interface of Photovoltaic (PV) Systems,” *IEEE-SASB Coordinating Committees*, 2000.
- [39] T. S. Basso and R. DeBlasio, “IEEE 1547 series of standards: interconnection issues,” *IEEE Transactions on Power Electronics*, vol. 19, no. 5, pp. 1159–1162, 2004.
- [40] A. Mermoud and B. Wittmer, *PV Syst User’s manual, PVsyst6*. PVsyst SA, Route du Bois-de-Bay 107 - 1242 Satigny - Switzerland, January 2014.
- [41] Solmetric, Inc, “Solmetric suneye.” [www.solmetric.com/](http://www.solmetric.com/). Accessed: 2017-04-19.
- [42] By Hunter Research and Technology, LLC, “Theodolite in app store.” <https://itunes.apple.com/us/app/theodolite/id339393884?mt=8>. Accessed: 2017-04-19.
- [43] A. D. Pettersen, “Simulation and experimental study of power losses due to shading and soiling on photovoltaic (pv) module,” Master’s thesis, Norwegian University of Life Sciences (NMBU), Faculty of Environmental Science and Technology, February 2015.
- [44] A. Mermoud, “What is the accuracy of the pvsyst simulation results ?” <http://forum.pvsyst.com/viewtopic.php?f=30&t=1649>. Published: 2014-04-22, Accessed: 2017-05-05.
- [45] P. J. Axaopoulos, E. D. Fylladitakis, and K. Gkarakis, “Accuracy analysis of software for the estimation and planning of photovoltaic installations,” *International Journal of Energy and Environmental Engineering*, vol. 5, no. 1, p. 1, 2014.
- [46] NASA, “Albedo.” [https://neo.sci.gsfc.nasa.gov/view.php?datasetId=MCD43C3\\_M\\_BSA](https://neo.sci.gsfc.nasa.gov/view.php?datasetId=MCD43C3_M_BSA). Accessed: 2017-06-07.
- [47] Meteorologisk Institutt, “Vaeret som var evenstad, stor-elvdal (hedmark).” <https://www.yr.no/sted/Norge/Hedmark/Stor-Elvdal/Evenstad~156275/statistikk.html>. Accessed: 2017-05-10.
- [48] REC Solar ASA, “Assessing reflection from rec peak energy series panels,” *NE-18-09*, January 2014.
- [49] SMA Solar Technology AG, “Measurement accuracy - energy values and efficiency for pv inverter sunny boy and sunny mini central.” <http://files.sma.de/dl/7418/Messgenau-UEN092520.pdf>. Accessed: 2017-05-10, Number: Messgenau-UEN092520, Version: 2.0, Type: Technical information.
- [50] Thor Christian Tuv, FUSen, “Conversation and e-mail correspondence.” 2017-05-16.
- [51] SMA Solar Technology AG, “Sunny webbox.” <http://files.sma.de/dl/2585/WEBBOX-DEN102530.pdf>. Accessed: 2017-05-25.

- 
- [52] SMA Solar Technology AG, “Sunny sensorbox.” [http://napelem.net/napelem\\_arak/adatlap/SMA\\_SENSORBOX\\_EN.pdf](http://napelem.net/napelem_arak/adatlap/SMA_SENSORBOX_EN.pdf). Accessed: 2017-05-02.
- [53] Norges Astma- og Allergiforbund, “Pollenkalender 2017.” <http://pollenvarslingen.no/Pollenkalender.aspx>. Accessed: 2017-06-12.
- [54] NVE, met.no and Kartverket, “Senorge: Snow map.” [www.senorge.no/](http://www.senorge.no/). Accessed: 2017-06-06.
- [55] J. Seehusen, “Solcelleprosjekt på høgskolen i hedmark: Statsbygg snart klar med norges største solcelleanlegg.” <https://www.tu.no/artikler/statsbygg-snart-klar-med-norges-storste-solcelleanlegg/235080>. Teknisk Ukeblad, Accessed: 2017-06-15.



# List of Figures

1.1	Average annual growth of renewable energy capacity, 2014 to 2015 . . .	2
1.2	Accumulated installed PV capacity in Norway from 2004 to 2016 . . .	3
1.3	Geograohical location of PV system at Evenstad . . . . .	4
1.4	Picture of the PV system at Evenstad . . . . .	4
2.1	Extraterrestrial solar spectrum compared to 5800 K blackbody . . . .	8
2.2	Definition of air mass . . . . .	9
2.3	Components of sunlight . . . . .	9
2.4	Definition of solar angles . . . . .	10
2.5	Flow diagram of a grid connected system. . . . .	12
2.6	PV cell when hit by photons that are absorbed, and connected to a load . . . . .	13
2.7	Simple equivalent circuit for a irradiated PV cell . . . . .	14
2.8	IV-characteristics and power output of a PV cell . . . . .	15
2.9	A more complex and accurate circuit equivalent of a PV cell . . . . .	15
2.10	I-V and P-V characteristics for a PV array . . . . .	17
2.11	Effect of shading of one cell in a module of $n$ cells. . . . .	18
2.12	Three bypass diodes, each covering one third of the cells. . . . .	18
2.13	Shaded PV module with three bypass-diodes . . . . .	19
2.14	PV cell, PV module, PV string and PV array . . . . .	20
2.15	IV characteristics of a PV array with three modules in series and two strings in parallel. . . . .	21
2.16	Illustration of effect of module tilt angle . . . . .	22
2.17	Module wiring topologies . . . . .	27
3.1	Screen shot of user interface in PVsyst. [40] . . . . .	32
3.2	Screen dialog of Project design. [40] . . . . .	33
3.3	PVsyst excerpt of best clear day quality check of imported meteo data	38
3.4	Tilt and azimuth angle selection in PV Syst . . . . .	41
3.5	Sketch of the PV plant at Evenstad . . . . .	42
3.6	3D model of PV array and its surroundings for near shading analysis	43
3.7	Snapshot of the horizon at Evenstad . . . . .	44
3.8	Sun path diagram and horizon profile . . . . .	44
3.9	Graph for Incident angle modifier . . . . .	45
3.10	Module layout for PV System at Evenstad. . . . .	45
3.11	Inverter efficiency vs. DC input power . . . . .	46
3.12	Hours of total irradiation for different irradiance values for Evenstad .	47
3.13	Meteorological conditions at Evenstad for date 18-04-2017 . . . . .	50
3.14	Measured irradiance and hourly values generated by PVsyst . . . . .	52

4.3	Tilt angle range for iterations . . . . .	61
4.4	Shading factor diagram of Evenstad. . . . .	62
4.5	Shading of string #1 for 21st December at 16:15. . . . .	64
4.6	IV curve of shaded string #1 for PV system at Evenstad on 21st December at 16:15. . . . .	64
4.7	Inverter power output comparison of real measured and simulated power output . . . . .	66
4.8	Loss diagram for date 14-06-2014 for simulations of one inverter. . . . .	68
4.9	Loss diagram for date 08-05-2016 for simulations of one inverter. . . . .	68
4.10	Power loss due to module temperature and array temperature . . . . .	69
4.11	Power output of all inverters for time period 09:00-17:00 on date 14-06-2014. . . . .	70
4.12	Annual energy output per inverter for 2014, 2015 and 2016. . . . .	71
4.13	Yield per inverter for period 1st of January 2017 to 23rd of May 2017, compared to simulated yield for the same period. . . . .	72
4.14	Yield per inverter for May 2017, compared to simulated yield for the same period. . . . .	72
4.15	Measured yield of each inverter in February 2017. . . . .	73
4.17	Total yield for each month for years 2014, 2015 and 2016. . . . .	75
4.18	Monthly comparison of simulated and measured yield for 2017. . . . .	77
4.19	Days with snow in April (marked in red). These are the days with difference in measured vs. simulated yield. . . . .	77
A.1	Inverter characteristics . . . . .	99

# List of Tables

2.1	Solar Angles . . . . .	10
2.2	Standard Test Conditions (STC). . . . .	15
2.3	Optimum tilt angle of solar modules by month for Oslo, Norway [25].	22
3.1	The geographical location of the PV system at Evenstad . . . . .	40
3.2	Orientation parameters selected in PVsyst for Evenstad. . . . .	40
3.3	PV Array characteristics. . . . .	42
3.4	Technical data of sub-arrays. . . . .	42
3.5	IAM values for non-treated and AR treated glass for REC modules. [48] . . . . .	45
4.1	System overview: base scenario. . . . .	59
4.2	Simulation results: Base scenario. . . . .	59
4.3	Simulation results: near shading. . . . .	62
4.4	Simulation results: Far shading. . . . .	63
4.5	Simulation results: IAM losses. . . . .	65
4.6	Results for simulated and measured values for one inverter . . . . .	67
4.7	Results for daily simulations and actual values for selected dates. . . .	75
4.8	Total yield for years 2014, 2015 and 2016 . . . . .	75
4.9	Results for daily simulations and actual values for selected dates. . . .	77
A.1	Information and data about PV system at Evenstad . . . . .	97
A.1	Information and data about PV system at Evenstad . . . . .	98
A.2	IAM values for non-treated and AR treated glass for REC modules. [48] . . . . .	98
A.3	Horixon line points, azimuth and height values in degrees [°]. . . . .	98
A.4	3D model dimensions. . . . .	98





# Appendices



# Appendix A

## Simulation Data

### A.1 Simulation Data

In this appendix data about the PV system at Evenstad, which is used to establish a simulation model in PVsyst, are listed. The different tables contains data of different parameters and settings.

**Table A.1:** Information and data about PV system at Evenstad. Used for the simulation model in PVsyst.

<b>Simulation parameters</b>			
<b>Orientation</b>			
Tilt angle:	35°		
Azimuth angle:	−10°		
Field type:	Fixed tilted plane		
<b>System parameters</b>			
Total system power	70.380 kWp		
Total nb. of modules	276	Total strings	24
Module area	455 m <sup>2</sup>	Cell area	403 m <sup>2</sup>
<u>Sub-array #1:</u>			
Number of modules	132	Modules per string	11
Nb. of MPPT inputs	12	Nb. of strings	12
Module type	REC 255PE BLK		
Module manufacturer	REC Solar AS		
Unit nominal power	255 W	Total power	33.7 kWp
<u>Sub-array: #2</u>			
Number of modules	144	Modules per string	12
Nb. of MPPT inputs	12	Nb. of strings	12
Module type	REC 255PE BLK		
Module manufacturer	REC Solar AS		
Unit nominal power	255 W	Total power	36.7 kWp

**Table A.1:** Information and data about PV system at Evenstad. Used for the simulation model in PVsyst.

<b>Simulation parameters</b>			
<u>Inverter:</u>			
Number of inverters	12		
Inverter type	Sunny Boy 5000TL-21		
Inverter manufacturer	SMA		
Operating voltage	175 – 500 V		
Unit nominal power	4.60 kWac	Total nominal power	55 kWac

**Table A.2:** IAM values for non-treated and AR treated glass for REC modules. [48]

Angle	10°	30°	50°	60°	70°	75°	80°
IAM non-treated glass (%)	100.0	99.9	98.5	95.3	87.0	79.0	67.7
IAM AR treated glass (%)	100.0	100.1	99.4	97.4	91.1	84.1	72.2

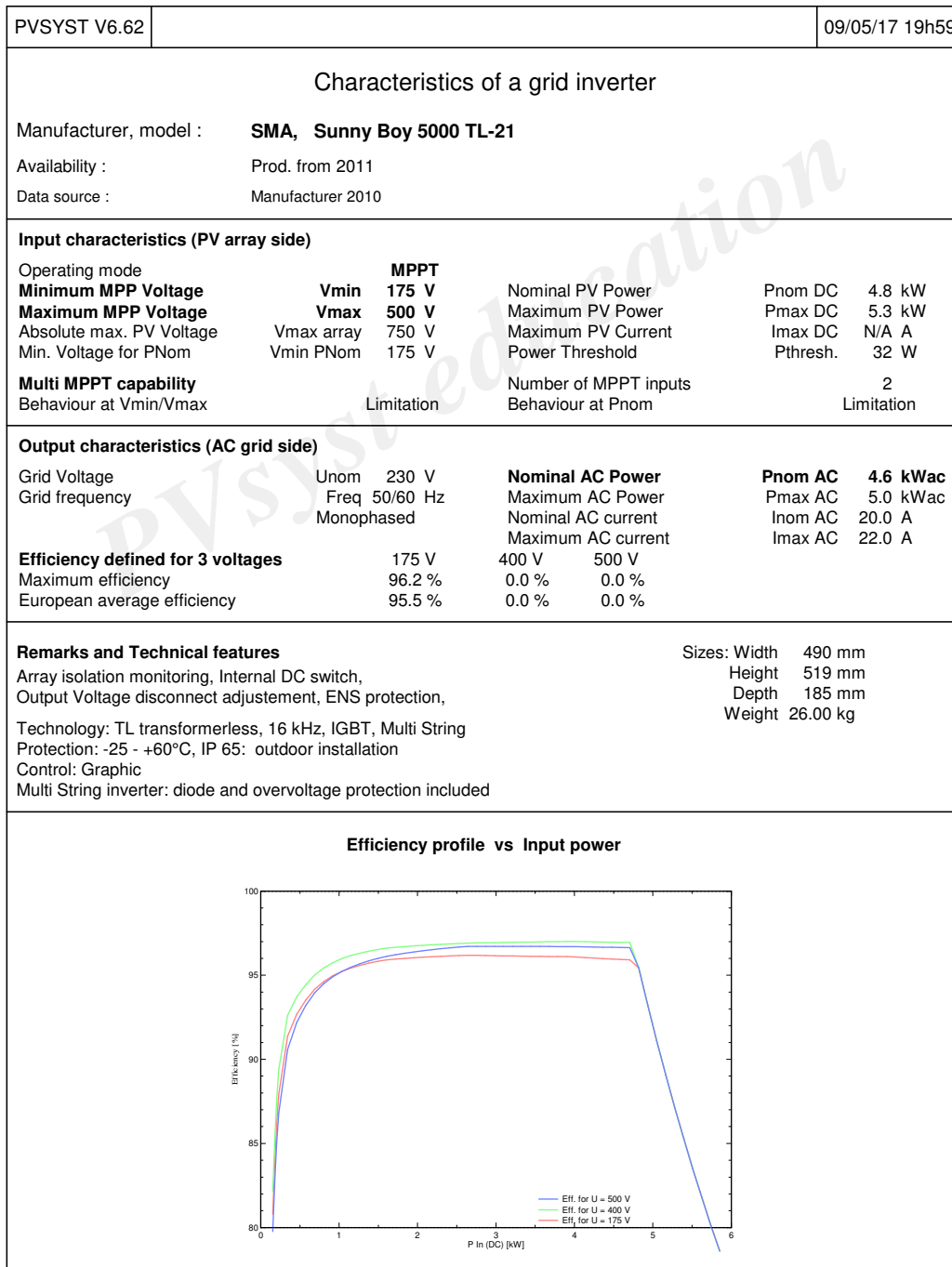
**Table A.3:** Horixon line points, azimuth and height values in degrees [°].

Average height	9.5°								
Azimuth	[°]	-180.0	-173.2	-167.9	-159.6	-151.3	-144.5	-139.2	-133.2
Height	[°]	19.4	18.2	17.1	15.9	14.3	12.8	10.8	10.4
Azimuth	[°]	-123.0	-96.0	-90.0	-80.0	-61.0	-49.0	-31.0	-11.0
Height	[°]	10.0	10.0	9.6	9.0	2.0	2.0	2.0	4.0
Azimuth	[°]	0.0	10.0	31.0	45.0	54.0	72.0	90.0	95.0
Height	[°]	7.6	10.0	11.0	11.6	12.0	10.0	7.4	7.0
Azimuth	[°]	116.0	135.0	138.0	162.0	179.0	180.0		
Height	[°]	9.0	9.9	10.0	15.0	15.0	15.0		

**Table A.4:** 3D model dimensions.

<b>Main building:</b>			
Length:	68 m	Width:	11 m
		Height:	10.3 m
<b>Main building roof:</b>			
Width:	12.6 m	Tilt angle:	35°
<b>Small building:</b>			
Length:	14 m	Width:	8 m
Roof tilt angle:	30°	Gable eaves:	0.5 m
		Lateral eaves:	0.5 m
<b>Tree heights:</b>			
Tree #1:	9.5 m	Tree #2:	10.5 m
Tree #2:	14.0 m	Tree #2:	14.0 m

## A.2 Inverter Characteristics



PV Syst Education License, Norwegian University of Science and Technology NTNU (Norway)

Figure A.1: Inverter characteristics



# Appendix B

## Simulation Reports

In this appendix some relevant simulation reports is included which is generated after simulation in PVsyst. Number of pages and what information is included in the report generated by PVsyst varies depending on the input data of the simulation model.

Page one include information about the meteo file chosen by the user, location coordinates and name, and chosen simulation variant and name. This page also include the simulation parameters implemented in the model.

Page two consist of the horizon definition. The values implemented which makes up the horizon line and the sun path diagram with horizon line implemented are included.

Page three consist of the near shading definition. Here a picture of the 3D model shall be included, but it some problems concerning this occurred after an update of PVsyst, such that the figure no longer were included. This is why the page is blank for the following reports. The figure which should have been included can be seen in Figure 3.6

Page four consist of the main results from the simulation. This include the system production for the set period, two graphs of normalized production and PR, as well as a table including balances and main results.

Page five consist of the loss diagram for the system.

## **B.1 Report Simulation for Whole system: January 1st to May 23rd 2017**



### Grid-Connected System: Simulation parameters

<b>Project :</b>		<b>Evenstad</b>		
<b>Geographical Site</b>	<b>Evenstad</b>	<b>Country</b>	<b>Norway</b>	
<b>Situation</b>	Latitude	61.42° N	Longitude	11.08° E
Time defined as	Legal Time	Time zone UT+1	Altitude	259 m
	Albedo	0.20		
<b>Meteo data:</b>	<b>Evenstad</b>	ASCII file - Imported		

<b>Simulation variant :</b>	<b>Simulation IAM scenario</b>
	Simulation date 06/06/17 14h24

<b>Simulation parameters</b>			
<b>Collector Plane Orientation</b>	Tilt	35°	Azimuth -10°
<b>Models used</b>	Transposition	Perez	Diffuse Perez, Meteororm
<b>Horizon</b>	Average Height	4.9°	
<b>Near Shadings</b>	Detailed electrical calculation	(acc. to module layout)	
<b>PV Arrays Characteristics (2 kinds of array defined)</b>			
<b>PV module</b>	Si-poly	Model	<b>REC 255PE / PE-BLK</b>
Custom parameters definition		Manufacturer	REC
<b>Sub-array "Sub-array #1"</b>			
Number of PV modules	In series	11 modules	In parallel 12 strings
Total number of PV modules	Nb. modules	132	Unit Nom. Power 255 Wp
Array global power	Nominal (STC)	<b>33.7 kWp</b>	At operating cond. 30.3 kWp (50°C)
Array operating characteristics (50°C)	U mpp	302 V	I mpp 100 A
<b>Sub-array "Sub-array #2"</b>			
Number of PV modules	In series	12 modules	In parallel 12 strings
Total number of PV modules	Nb. modules	144	Unit Nom. Power 255 Wp
Array global power	Nominal (STC)	<b>36.7 kWp</b>	At operating cond. 33.0 kWp (50°C)
Array operating characteristics (50°C)	U mpp	329 V	I mpp 100 A
<b>Total</b>	Arrays global power	Nominal (STC)	<b>70 kWp</b>
		Module area	<b>455 m<sup>2</sup></b>
		Total	276 modules
		Cell area	403 m <sup>2</sup>
<b>Inverter</b>			
Original PVSyst database	Model	<b>Sunny Boy 5000 TL-21</b>	
Characteristics	Manufacturer	SMA	
	Operating Voltage	175-500 V	Unit Nom. Power 4.60 kWac
<b>Sub-array "Sub-array #1"</b>	Nb. of inverters	12 * MPPT 50 %	Total Power 28 kWac
<b>Sub-array "Sub-array #2"</b>	Nb. of inverters	12 * MPPT 50 %	Total Power 28 kWac
<b>Total</b>	Nb. of inverters	12	Total Power 55 kWac
<b>PV Array loss factors</b>			
Thermal Loss factor	Uc (const)	20.0 W/m <sup>2</sup> K	Uv (wind) 0.0 W/m <sup>2</sup> K / m/s
Wiring Ohmic Loss	Array#1	50 mOhm	Loss Fraction 1.5 % at STC
	Array#2	54 mOhm	Loss Fraction 1.5 % at STC
	Global		Loss Fraction 1.5 % at STC
LID - Light Induced Degradation			Loss Fraction 1.5 %
Module Quality Loss			Loss Fraction -0.5 %
Module Mismatch Losses			Loss Fraction 1.0 % at MPP

## Grid-Connected System: Simulation parameters (continued)

Incidence effect (IAM): User defined IAM profile

10°	30°	50°	60°	70°	75°	80°	85°	90°
1.000	1.000	0.994	0.974	0.911	0.841	0.722	0.476	0.000

**User's needs :**

Unlimited load (grid)

### Grid-Connected System: Horizon definition

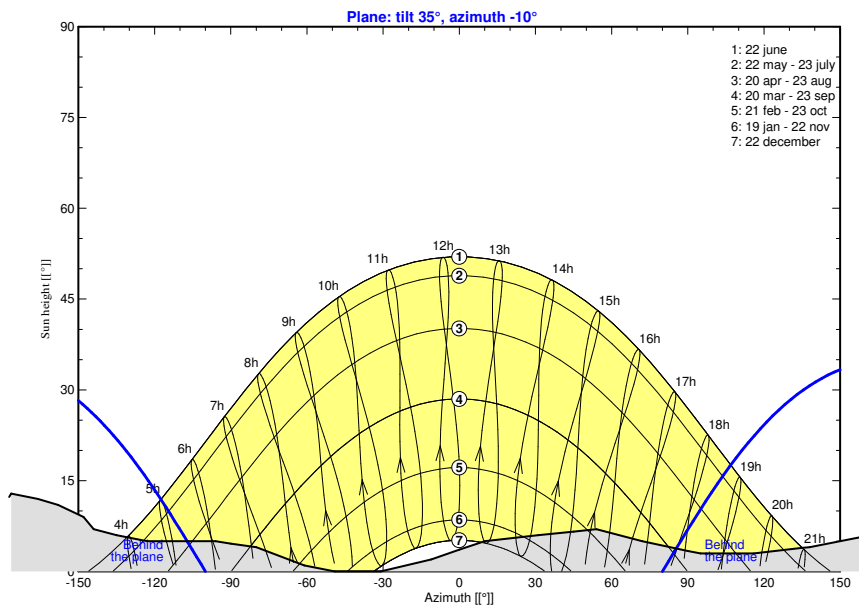
**Project :** Evenstad  
**Simulation variant :** Simulation IAM scenario

<b>Main system parameters</b>		System type	<b>Grid-Connected</b>	
<b>Horizon</b>		Average Height	4.9°	
<b>Near Shadings</b>		Detailed electrical calculation (acc. to module layout)		
PV Field Orientation		tilt	35°	azimuth -10°
PV modules		Model	REC 255PE / PE-BLK	Pnom 255 Wp
PV Array		Nb. of modules	276	Pnom total <b>70.4 kWp</b>
Inverter		Model	Sunny Boy 5000 TL-21	Pnom 4600 W ac
Inverter pack		Nb. of units	12.0	Pnom total <b>55.2 kW ac</b>
User's needs		Unlimited load (grid)		

<b>Horizon</b>	Average Height	4.9°	Diffuse Factor	0.98
	Albedo Factor	100 %	Albedo Fraction	0.86

Height [°]	11.0	11.0	13.0	12.0	11.0	9.0	7.0	6.0	5.0	5.0
Azimuth [°]	-180	-179	-178	-166	-158	-148	-144	-135	-123	-96
Height [°]	4.6	4.0	1.0	0.0	0.0	2.0	3.6	5.0	6.0	6.6
Azimuth [°]	-90	-80	-61	-49	-31	-11	0	10	31	45
Height [°]	7.0	5.0	3.4	3.0	3.0	3.9	4.0	6.0	11.0	11.0
Azimuth [°]	54	72	90	95	116	135	138	162	179	180

**Meteonorm horizon for, Lat. = 61.424°, Long. = 11.079°**



**Grid-Connected System: Near shading definition**

**Project :** Evenstad  
**Simulation variant :** Simulation IAM scenario

<b>Main system parameters</b>	System type	<b>Grid-Connected</b>
<b>Horizon</b>	Average Height	4.9°
<b>Near Shadings</b>	Detailed electrical calculation	(acc. to module layout)
PV Field Orientation	tilt	35° azimuth -10°
PV modules	Model	REC 255PE / PE-BLK Pnom 255 Wp
PV Array	Nb. of modules	276 Pnom total <b>70.4 kWp</b>
Inverter	Model	Sunny Boy 5000 TL-21 Pnom 4600 W ac
Inverter pack	Nb. of units	12.0 Pnom total <b>55.2 kW ac</b>
User's needs	Unlimited load (grid)	

**Perspective of the PV-field and surrounding shading scene**

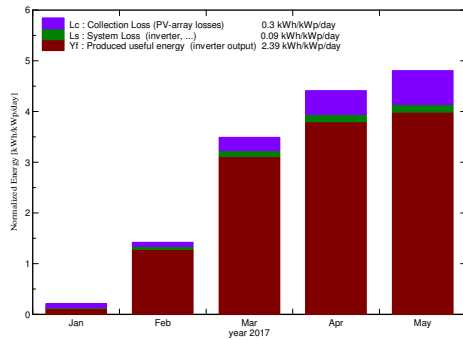
### Grid-Connected System: Main results

**Project :** Evenstad  
**Simulation variant :** Simulation IAM scenario

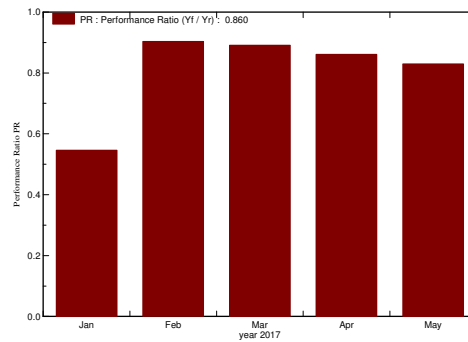
<b>Main system parameters</b>		System type	<b>Grid-Connected</b>	
<b>Horizon</b>		Average Height	4.9°	
<b>Near Shadings</b>		Detailed electrical calculation (acc. to module layout)		
PV Field Orientation		tilt	35°	azimuth -10°
PV modules		Model	REC 255PE / PE-BLK	Pnom 255 Wp
PV Array		Nb. of modules	276	Pnom total <b>70.4 kWp</b>
Inverter		Model	Sunny Boy 5000 TL-21	Pnom 4600 W ac
Inverter pack		Nb. of units	12.0	Pnom total <b>55.2 kW ac</b>
User's needs		Unlimited load (grid)		

<b>Main simulation results</b>	<b>Produced Energy</b>	<b>24.05 MWh</b>	Specific prod.	342 kWh/kWp
System Production	Performance Ratio PR	85.97 %		

**Normalized productions (per installed kWp): Nominal power 70.4 kWp**



**Performance Ratio PR**



**Simulation IAM scenario**  
Balances and main results

	GlobHor	DiffHor	T Amb	GlobInc	GlobEff	EArray	E_Grid	PR
	kWh/m²	kWh/m²	°C	kWh/m²	kWh/m²	MWh	MWh	
Jan. 17	5.9	5.58	-8.79	6.5	4.3	0.287	0.251	0.546
Feb. 17	22.8	15.27	-6.04	39.8	37.3	2.642	2.530	0.903
Mar. 17	69.5	34.68	-1.47	108.3	104.6	7.046	6.794	0.891
Apr. 17	104.2	51.24	2.21	132.4	128.1	8.324	8.025	0.861
May 17	96.7	47.51	7.55	110.5	106.9	6.705	6.454	0.830
Period	299.2	154.28	-1.74	397.6	381.2	25.005	24.055	0.860

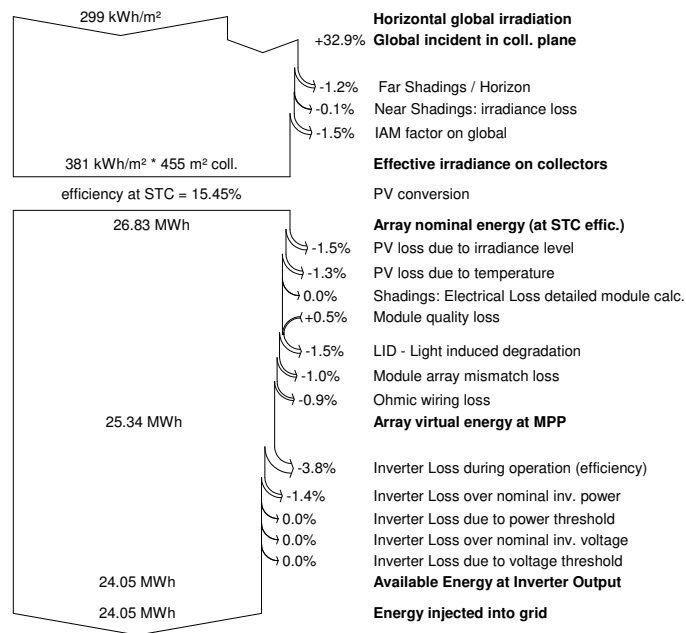
Legends: GlobHor Horizontal global irradiation      GlobEff Effective Global, corr. for IAM and shadings  
 DiffHor Horizontal diffuse irradiation      EArray Effective energy at the output of the array  
 T Amb Ambient Temperature      E\_Grid Energy injected into grid  
 GlobInc Global incident in coll. plane      PR Performance Ratio

### Grid-Connected System: Loss diagram

**Project :** Evenstad  
**Simulation variant :** Simulation IAM scenario

<b>Main system parameters</b>	System type	<b>Grid-Connected</b>
<b>Horizon</b>	Average Height	4.9°
<b>Near Shadings</b>	Detailed electrical calculation	(acc. to module layout)
PV Field Orientation	tilt	35° azimuth -10°
PV modules	Model	REC 255PE / PE-BLK Pnom 255 Wp
PV Array	Nb. of modules	276 Pnom total <b>70.4 kWp</b>
Inverter	Model	Sunny Boy 5000 TL-21 Pnom 4600 W ac
Inverter pack	Nb. of units	12.0 Pnom total <b>55.2 kW ac</b>
User's needs	Unlimited load (grid)	

#### Loss diagram over the whole year



## **B.2 Report Simulation for One Inverter: 14-06-2014**

### Grid-Connected System: Simulation parameters

**Project :** **Evenstad one inverter one day**

**Geographical Site** **Evenstad** **Country** **Norway**

**Situation** Latitude 61.42° N Longitude 11.08° E  
 Time defined as Legal Time Time zone UT+1 Altitude 259 m  
 Albedo 0.20

**Meteo data:** **Evenstad** ASCII file - Imported

**Simulation variant :** **Simulation one inverter 140614 module temp**

Simulation date 15/05/17 14h01

**Simulation parameters**

**Collector Plane Orientation** Tilt 35° Azimuth -10°

**Models used** Transposition Perez Diffuse Perez, Meteororm

**Horizon** Average Height 4.9°

**Near Shadings** Detailed electrical calculation (acc. to module layout)

**PV Arrays Characteristics (2 kinds of array defined)**

<b>PV module</b>	Si-poly	Model	<b>REC 255PE / PE-BLK</b>	
Custom parameters definition		Manufacturer	REC	
<b>Sub-array "Sub-array #1"</b>				
Number of PV modules	In series	11 modules	In parallel	1 strings
Total number of PV modules	Nb. modules	11	Unit Nom. Power	255 Wp
Array global power	Nominal (STC)	<b>2805 Wp</b>	At operating cond.	2524 Wp (50°C)
Array operating characteristics (50°C)	U mpp	302 V	I mpp	8.4 A
<b>Sub-array "Sub-array #2"</b>				
Number of PV modules	In series	12 modules	In parallel	1 strings
Total number of PV modules	Nb. modules	12	Unit Nom. Power	255 Wp
Array global power	Nominal (STC)	<b>3060 Wp</b>	At operating cond.	2754 Wp (50°C)
Array operating characteristics (50°C)	U mpp	329 V	I mpp	8.4 A
<b>Total</b> Arrays global power	Nominal (STC)	<b>6 kWp</b>	Total	23 modules
	Module area	<b>38.0 m<sup>2</sup></b>	Cell area	33.6 m <sup>2</sup>

**Inverter** Model **Sunny Boy 5000 TL-21**

Custom parameters definition Manufacturer SMA

Characteristics Operating Voltage 175-500 V Unit Nom. Power 4.60 kWac  
 Max. power (=>25°C) 5.00 kWac

<b>Sub-array "Sub-array #1"</b>	Nb. of inverters	1 * MPPT 48 %	Total Power	2.2 kWac
<b>Sub-array "Sub-array #2"</b>	Nb. of inverters	1 * MPPT 52 %	Total Power	2.4 kWac
<b>Total</b>	Nb. of inverters	1	Total Power	5 kWac

**PV Array loss factors**

Module temperature Values read on the meteo file

Wiring Ohmic Loss	Array#1	598 mOhm	Loss Fraction	1.5 % at STC
	Array#2	652 mOhm	Loss Fraction	1.5 % at STC
	Global		Loss Fraction	1.5 % at STC



## Grid-Connected System: Simulation parameters (continued)

LID - Light Induced Degradation

Loss Fraction 1.5 %

Module Quality Loss

Loss Fraction -0.5 %

Module Mismatch Losses

Loss Fraction 1.0 % at MPP

Incidence effect (IAM): User defined IAM profile

10°	30°	50°	60°	70°	75°	80°	85°	90°
1.000	1.000	0.994	0.974	0.911	0.841	0.722	0.476	0.000

**User's needs :**

Unlimited load (grid)

### Grid-Connected System: Horizon definition

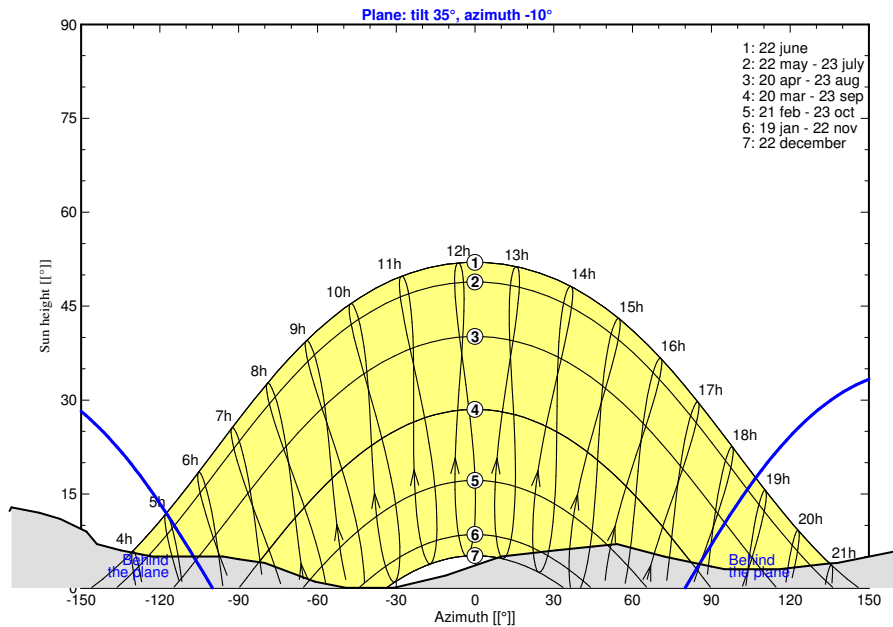
**Project :** Evenstad one inverter one day  
**Simulation variant :** Simulation one inverter 140614 module temp

<b>Main system parameters</b>	System type	Grid-Connected
<b>Horizon</b>	Average Height	4.9°
<b>Near Shadings</b>	Detailed electrical calculation	(acc. to module layout)
PV Field Orientation	tilt	35° azimuth -10°
PV modules	Model	REC 255PE / PE-BLK Pnom 255 Wp
PV Array	Nb. of modules	23 Pnom total <b>5.87 kWp</b>
Inverter	Model	Sunny Boy 5000 TL-21 Pnom 4600 W ac
User's needs	Unlimited load (grid)	

<b>Horizon</b>	Average Height	4.9°
	Albedo Factor	100 %
	Diffuse Factor	0.98
	Albedo Fraction	0.86

Height [°]	11.0	11.0	13.0	12.0	11.0	9.0	7.0	6.0	5.0	5.0
Azimuth [°]	-180	-179	-178	-166	-158	-148	-144	-135	-123	-96
Height [°]	4.6	4.0	1.0	0.0	0.0	2.0	3.6	5.0	6.0	6.6
Azimuth [°]	-90	-80	-61	-49	-31	-11	0	10	31	45
Height [°]	7.0	5.0	3.4	3.0	3.0	3.9	4.0	6.0	11.0	11.0
Azimuth [°]	54	72	90	95	116	135	138	162	179	180

**Meteonorm horizon for, Lat. = 61.424°, Long. = 11.079°**



**Grid-Connected System: Near shading definition**

**Project :** Evenstad one inverter one day

**Simulation variant :** Simulation one inverter 140614 module temp

<b>Main system parameters</b>	System type	<b>Grid-Connected</b>		
<b>Horizon</b>	Average Height	4.9°		
<b>Near Shadings</b>	Detailed electrical calculation	(acc. to module layout)		
PV Field Orientation	tilt	35°	azimuth	-10°
PV modules	Model	REC 255PE / PE-BLK	Pnom	255 Wp
PV Array	Nb. of modules	23	Pnom total	<b>5.87 kWp</b>
Inverter	Model	Sunny Boy 5000 TL-21	Pnom	4600 W ac
User's needs	Unlimited load (grid)			

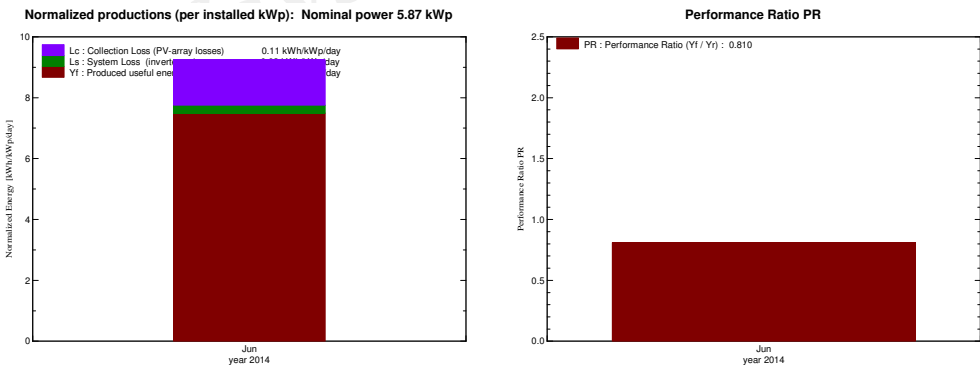
**Perspective of the PV-field and surrounding shading scene**

### Grid-Connected System: Main results

**Project :** Evenstad one inverter one day  
**Simulation variant :** Simulation one inverter 140614 module temp

<b>Main system parameters</b>	System type <b>Grid-Connected</b>	
<b>Horizon</b>	Average Height 4.9°	
<b>Near Shadings</b>	Detailed electrical calculation (acc. to module layout)	
PV Field Orientation	tilt 35°	azimuth -10°
PV modules	Model REC 255PE / PE-BLK	Pnom 255 Wp
PV Array	Nb. of modules 23	Pnom total <b>5.87 kWp</b>
Inverter	Model Sunny Boy 5000 TL-21	Pnom 4600 W ac
User's needs	Unlimited load (grid)	

<b>Main simulation results</b>	<b>System Production</b>	<b>Produced Energy 43.93 kWh</b>	Specific prod. 7 kWh/kWp
	<b>Performance Ratio PR</b>	<b>81.02 %</b>	



**Simulation one inverter 140614 module temp**  
Balances and main results

	GlobHor kWh/m <sup>2</sup>	DiffHor kWh/m <sup>2</sup>	T Amb °C	GlobInc kWh/m <sup>2</sup>	GlobEff kWh/m <sup>2</sup>	EArray kWh	E_Grid kWh	PR
<b>June 14</b>	8.065	1.908	13.43	9.245	9.056	45.51	43.93	0.810
Period	8.065	1.908	13.43	9.245	9.056	45.51	43.93	0.810

Legends: GlobHor Horizontal global irradiation      GlobEff Effective Global, corr. for IAM and shadings  
 DiffHor Horizontal diffuse irradiation      EArray Effective energy at the output of the array  
 T Amb Ambient Temperature      E\_Grid Energy injected into grid  
 GlobInc Global incident in coll. plane      PR Performance Ratio

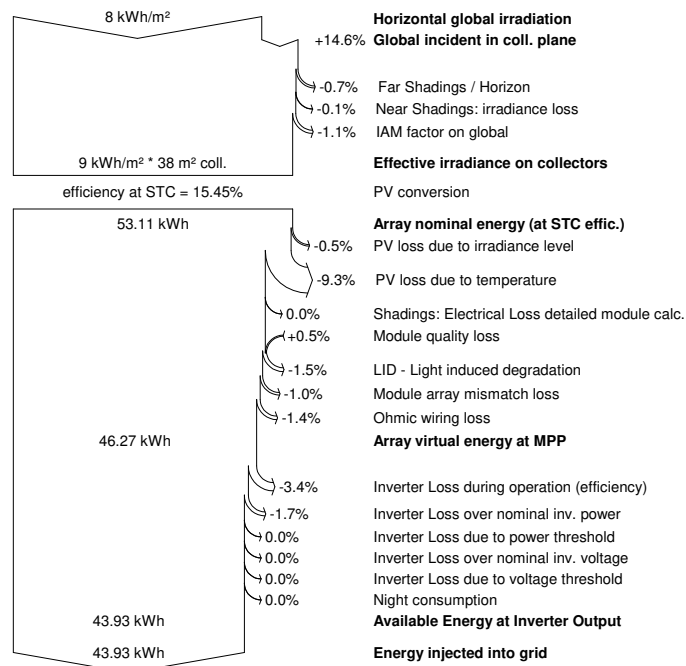
### Grid-Connected System: Loss diagram

**Project :** Evenstad one inverter one day

**Simulation variant :** Simulation one inverter 140614 module temp

<b>Main system parameters</b>	System type	<b>Grid-Connected</b>
<b>Horizon</b>	Average Height	4.9°
<b>Near Shadings</b>	Detailed electrical calculation	(acc. to module layout)
PV Field Orientation	tilt	35° azimuth -10°
PV modules	Model	REC 255PE / PE-BLK Pnom 255 Wp
PV Array	Nb. of modules	23 Pnom total <b>5.87 kWp</b>
Inverter	Model	Sunny Boy 5000 TL-21 Pnom 4600 W ac
User's needs	Unlimited load (grid)	

#### Loss diagram over the whole year



### **B.3 Report Simulation for One Inverter: 08-05-2016**

### Grid-Connected System: Simulation parameters

**Project :** **Evenstad one inverter one day**

**Geographical Site** **Evenstad** **Country** **Norway**

**Situation** Latitude 61.42° N Longitude 11.08° E  
 Time defined as Legal Time Time zone UT+1 Altitude 259 m  
 Albedo 0.20

**Meteo data:** **Evenstad** ASCII file - Imported

**Simulation variant :** **Simulation one inverter 080516**  
 Simulation date 15/05/17 13h53

**Simulation parameters**

**Collector Plane Orientation** Tilt 35° Azimuth -10°

**Models used** Transposition Perez Diffuse Perez, Meteororm

**Horizon** Average Height 4.9°

**Near Shadings** Detailed electrical calculation (acc. to module layout)

**PV Arrays Characteristics (2 kinds of array defined)**

<b>PV module</b>	Si-poly	Model	<b>REC 255PE / PE-BLK</b>	
Custom parameters definition		Manufacturer	REC	
<b>Sub-array "Sub-array #1"</b>				
Number of PV modules	In series	11 modules	In parallel	1 strings
Total number of PV modules	Nb. modules	11	Unit Nom. Power	255 Wp
Array global power	Nominal (STC)	<b>2805 Wp</b>	At operating cond.	2524 Wp (50°C)
Array operating characteristics (50°C)	U mpp	302 V	I mpp	8.4 A
<b>Sub-array "Sub-array #2"</b>				
Number of PV modules	In series	12 modules	In parallel	1 strings
Total number of PV modules	Nb. modules	12	Unit Nom. Power	255 Wp
Array global power	Nominal (STC)	<b>3060 Wp</b>	At operating cond.	2754 Wp (50°C)
Array operating characteristics (50°C)	U mpp	329 V	I mpp	8.4 A
<b>Total</b> Arrays global power	Nominal (STC)	<b>6 kWp</b>	Total	23 modules
	Module area	<b>38.0 m<sup>2</sup></b>	Cell area	33.6 m <sup>2</sup>

**Inverter** Model **Sunny Boy 5000 TL-21**

Custom parameters definition Manufacturer SMA

Characteristics Operating Voltage 175-500 V Unit Nom. Power 4.60 kWac  
 Max. power (=>25°C) 5.00 kWac

<b>Sub-array "Sub-array #1"</b>	Nb. of inverters	1 * MPPT 48 %	Total Power	2.2 kWac
<b>Sub-array "Sub-array #2"</b>	Nb. of inverters	1 * MPPT 52 %	Total Power	2.4 kWac
<b>Total</b>	Nb. of inverters	1	Total Power	5 kWac

**PV Array loss factors**

Module temperature Values read on the meteo file

Wiring Ohmic Loss	Array#1	598 mOhm	Loss Fraction	1.5 % at STC
	Array#2	652 mOhm	Loss Fraction	1.5 % at STC
	Global		Loss Fraction	1.5 % at STC

## Grid-Connected System: Simulation parameters (continued)

LID - Light Induced Degradation

Loss Fraction 1.5 %

Module Quality Loss

Loss Fraction -0.5 %

Module Mismatch Losses

Loss Fraction 1.0 % at MPP

Incidence effect (IAM): User defined IAM profile

10°	30°	50°	60°	70°	75°	80°	85°	90°
1.000	1.000	0.994	0.974	0.911	0.841	0.722	0.476	0.000

User's needs :

Unlimited load (grid)



### Grid-Connected System: Horizon definition

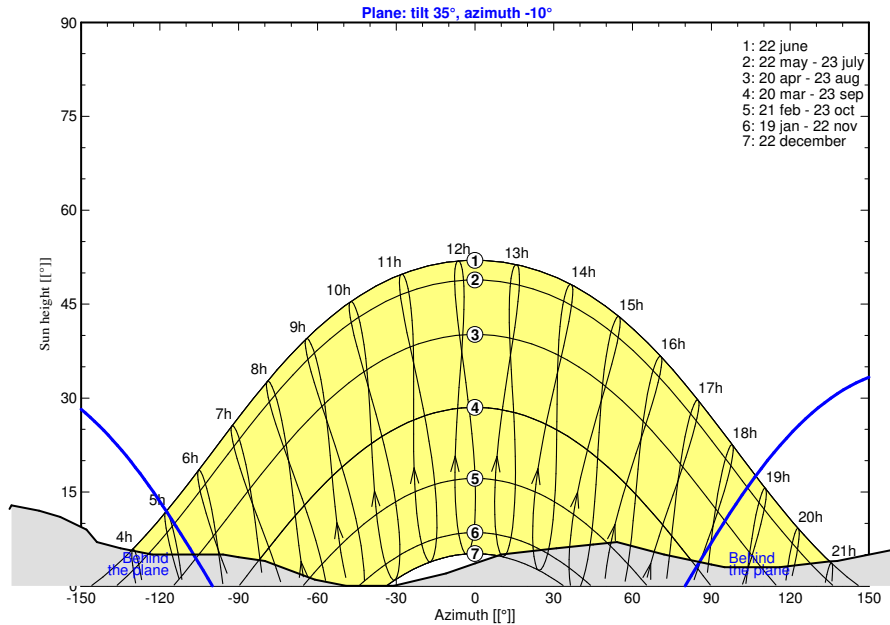
**Project :** Evenstad one inverter one day  
**Simulation variant :** Simulation one inverter 080516

<b>Main system parameters</b>	System type	<b>Grid-Connected</b>		
<b>Horizon</b>	Average Height	4.9°		
<b>Near Shadings</b>	Detailed electrical calculation	(acc. to module layout)		
PV Field Orientation	tilt	35°	azimuth	-10°
PV modules	Model	REC 255PE / PE-BLK	Pnom	255 Wp
PV Array	Nb. of modules	23	Pnom total	<b>5.87 kWp</b>
Inverter	Model	Sunny Boy 5000 TL-21	Pnom	4600 W ac
User's needs	Unlimited load (grid)			

<b>Horizon</b>	Average Height	4.9°	Diffuse Factor	0.98
	Albedo Factor	100 %	Albedo Fraction	0.86

Height [°]	11.0	11.0	13.0	12.0	11.0	9.0	7.0	6.0	5.0	5.0
Azimuth [°]	-180	-179	-178	-166	-158	-148	-144	-135	-123	-96
Height [°]	4.6	4.0	1.0	0.0	0.0	2.0	3.6	5.0	6.0	6.6
Azimuth [°]	-90	-80	-61	-49	-31	-11	0	10	31	45
Height [°]	7.0	5.0	3.4	3.0	3.0	3.9	4.0	6.0	11.0	11.0
Azimuth [°]	54	72	90	95	116	135	138	162	179	180

**Meteonorm horizon for, Lat. = 61.424°, Long. = 11.079°**



**Grid-Connected System: Near shading definition**

**Project :** Evenstad one inverter one day  
**Simulation variant :** Simulation one inverter 080516

<b>Main system parameters</b>	System type	<b>Grid-Connected</b>	
<b>Horizon</b>	Average Height	4.9°	
<b>Near Shadings</b>	Detailed electrical calculation	(acc. to module layout)	
PV Field Orientation	tilt	35°	azimuth -10°
PV modules	Model	REC 255PE / PE-BLK	Pnom 255 Wp
PV Array	Nb. of modules	23	Pnom total <b>5.87 kWp</b>
Inverter	Model	Sunny Boy 5000 TL-21	Pnom 4600 W ac
User's needs	Unlimited load (grid)		

**Perspective of the PV-field and surrounding shading scene**

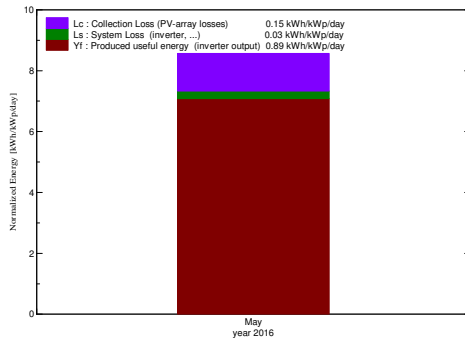
### Grid-Connected System: Main results

**Project :** Evenstad one inverter one day  
**Simulation variant :** Simulation one inverter 080516

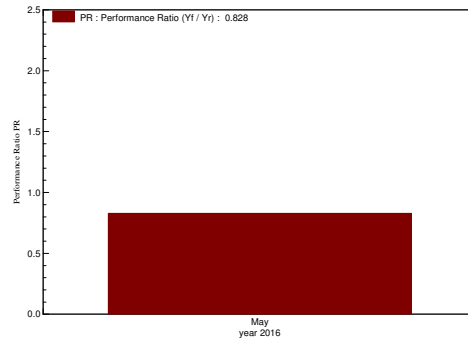
<b>Main system parameters</b>	System type	<b>Grid-Connected</b>		
<b>Horizon</b>	Average Height	4.9°		
<b>Near Shadings</b>	Detailed electrical calculation	(acc. to module layout)		
PV Field Orientation	tilt	35°	azimuth	-10°
PV modules	Model	REC 255PE / PE-BLK	Pnom	255 Wp
PV Array	Nb. of modules	23	Pnom total	<b>5.87 kWp</b>
Inverter	Model	Sunny Boy 5000 TL-21	Pnom	4600 W ac
User's needs	Unlimited load (grid)			

<b>Main simulation results</b>			
System Production	<b>Produced Energy</b>	<b>41.56 kWh</b>	Specific prod. 7 kWh/kWp
	Performance Ratio PR	82.75 %	

**Normalized productions (per installed kWp): Nominal power 5.87 kWp**



**Performance Ratio PR**



**Simulation one inverter 080516**  
Balances and main results

	GlobHor	DiffHor	T Amb	GlobInc	GlobEff	EArray	E_Grid	PR
	kWh/m²	kWh/m²	°C	kWh/m²	kWh/m²	kWh	kWh	
<b>May 16</b>	6.827	1.623	11.74	8.564	8.391	43.00	41.56	0.828
Period	6.827	1.623	11.74	8.564	8.391	43.00	41.56	0.828

Legends: GlobHor Horizontal global irradiation      GlobEff Effective Global, corr. for IAM and shadings  
 DiffHor Horizontal diffuse irradiation      EArray Effective energy at the output of the array  
 T Amb Ambient Temperature      E\_Grid Energy injected into grid  
 GlobInc Global incident in coll. plane      PR Performance Ratio

### Grid-Connected System: Loss diagram

**Project :** Evenstad one inverter one day  
**Simulation variant :** Simulation one inverter 080516

<b>Main system parameters</b>	System type	<b>Grid-Connected</b>
<b>Horizon</b>	Average Height	4.9°
<b>Near Shadings</b>	Detailed electrical calculation	(acc. to module layout)
PV Field Orientation	tilt	35° azimuth -10°
PV modules	Model	REC 255PE / PE-BLK Pnom 255 Wp
PV Array	Nb. of modules	23 Pnom total <b>5.87 kWp</b>
Inverter	Model	Sunny Boy 5000 TL-21 Pnom 4600 W ac
User's needs	Unlimited load (grid)	

#### Loss diagram over the whole year

